JNC TY9400 2002-016

Study on Pb/Bi Corrosion of Structural and Fuel Cladding Materials for Nuclear Applications

- Part1:Corrosion investigation of steels after 800 and 2,000 h exposure to stagnant liquid Pb/Bi at elevated temperatures

June 2002

Japan Nuclear Cycle Development Institute
Forschungszentrum Karlsruhe GmbH

JNC TY9400 2002-016
June, 2 0 0 2

Study on Pb/Bi Corrosion of Structural and Fuel Cladding Materials for Nuclear Applications

Part 1: Corrosion investigation of steels after 800 and 2,000 h exposure to stagnant liquid Pb/Bi at elevated temperatures

Georg Müller*, Gustav Schumacher*, Alfons Weisenburger*, Annette Heinzel*, Frank Zimmermann*, Tomohiro Furukawa** and Kazumi Aoto**

Abstract

One of the main problems in the development of advanced heavy metal cooled reactor systems is the compatibility of structural and fuel cladding materials with potential coolants. Lead alloys are foreseen as coolant which attack steel by dissolving its components at the temperatures that occur in a reactor loops.

In order to investigate the corrosion phenomena of three Japanese original materials (316FR, P122 and ODS) in the original state and after Al alloying into the surface by GESA in lead-bismuth eutectic (LBE) at elevated temperature, corrosion tests were carried out in stagnant LBE for 800h and 2,000h under oxygen control at 10^{-6}wt%.

The major results are as follows;

(1) For three original materials, protective oxide layers were formed on the surface of the specimens exposed to 500°C and 550°C.

(2) Above 600°C the oxidation behavior of the original materials changed, the oxide scales got very thin. There were attacks of LBE on singular spots at the surface of three materials. The phenomena were observed after 800h exposure for 316FR and ODS, and after 2,000h for P122.

(3) The three GESA alloyed materials show good corrosion resistance without any attack at all temperatures. Although, a few structural defects were observed on the surface, no dissolution attack occurred. The defect spots (small cracks) were closed with a Cr-Al spinel compound and sealed by this process.

* Institut für Hochleistungsimpuls- und Mikrowellentechnik (Institute for Pulsed Power and Microwave Technology) , Forschungszentrum Karlsruhe GmbH

** Advanced Material Research Group, Advanced Technology Division, O-arai Engineering Center, Japan Nuclear Cycle Development Institute

JNC TY9400 2002-016
2 0 0 2 年 6 月

原子炉構造及び燃料材料の鉛ビスマス中腐食に関する研究

第1報：高温停留鉛ビスマス中800及び2,000時間浸漬材の腐食評価

Georg Müller*, Gustav Schumacher*, Alfons Weisenburger*,
Annette Heinzel*, Frank Zimmermann*, 古川智弘**,
青砥紀身**

要旨

重金属冷却炉の開発の中の主要課題の一つは、原子炉構造および燃料材料と冷却材との共存性である。冷却材として適用が検討されている鉛合金は、原子炉内の冷却材循環温度下で鋼材の成分溶出によって鋼材を腐食させる。

国産3鋼種オリジナル材料（316FR、P122およびODS）およびGESA処理と称するそれらにアルミニウム溶射を施した材料の高温鉛ビスマス（LBE）中での腐食挙動を評価するために、10^{-6}wt%の酸素濃度制御下で800hおよび2,000hの停留LBE中腐食試験を実施した。

本研究により得られた結果は以下のとおり。

(1) 500°Cおよび550°CのLBEに浸漬したオリジナル材3鋼種の表面には、保護酸化皮膜が形成されていた。

(2) 600℃以上のLBEに浸漬したこれら3鋼種の酸化挙動には変化が認められ、皮膜が非常に薄くなっていた。そして、接液表面にLBEによる腐食が観察された。その状況は316FRおよびODSでは800h浸漬試験材から認められ、P122では2,000h浸漬で認められた。

(3) GESA処理材は、全温度において腐食が観察されず、良い耐食性を示していた。Al溶射部にいくつかの微小き裂が観察されたが、オリジナル材で認められたような腐食は観察されなかった。この微小き裂はCr-Alスピネル型化合物で満たされていた。

---

* Institut für Hochleistungsimpuls- und Mikrowellentechnik, Forschungszentrum Karlsruhe GmbH（独・カールスルーエ研究所 Institute for Pulsed Power and Microwave Technology)

** 核燃料サイクル開発機構 大洗工学センター 要素技術開発部 新材料研究グループ

Content

Lists of Tables and Figures

1 Introduction

For the development of advanced heavy metal cooled reactor systems where lead alloys are foreseen as coolant durability of structural materials must be considered because one of the main problem is the corrosion of structural materials in high temperature lead alloys.

In October 2001 a research agreement come into force between Japan Nuclear Cycle Development Institute (JNC) and Forschungszentrum Karlsruhe GmbH (FZK) entitled: "Cooperation regarding Study on Lead-Bismuth Corrosion Studies of the Structural and the Fuel Cladding Materials for Nuclear Application".

One part of this cooperation is dealing with long term screening corrosion investigations in oxygen controlled stagnant liquid Pb/Bi. The table below shows the full set of parameters and the steels to be investigated.

This report is the first one and describes the results after 800 and 2000 h of exposure in stagnant Pb/Bi with an oxygen content of 10^{-6} wt% (grey columns in the table).

Material (amount)	T [°C]	O_2 content 10^{-4} w[%]				O_2 content 10^{-6} w[%]				O_2 content 10^{-7} - 10^{-8} w[%]*			
		800h	2000h	5000h	10000h	800h	2000h	5000h	10000h	800h	2000h	5000h	10000h
316FR original (15'')	500					X	X	X	X				
	550	X	X	X		X	X	X	X	X	X	X	
	600					X	X	X	X				
316FR GESA (3)	500					X	X	X	X				
	550					X	X	X	X				
	600					X	X	X	X				
P122 Original (15'')	500					X	X	X	X				
	550	X	X	X		X	X	X	X	X	X	X	
	600					X	X	X	X				
P122 GESA (3)	500					X	X	X	X				
	550					X	X	X	X				
	600					X	X	X	X				
ODS Original (18''')	500					X	X	X	X				
	550					X	X	X	X				
	600					X	X	X	X				
	650	X	X	X		X	X	X	X	X	X	X	
ODS GESA (6)	500					X	X	X	X				
	550					X	X	X	X				
	600					X	X	X	X				
	650	X	X	X		X	X	X	X	X	X	X	

Parameter set for corrosion investigation in COSTA

2 Problems in liquid Pb/Bi – steel compatibility

Unprotected steel undergoes severe attack by liquid lead and lead/bismuth alloy by dissolution of metal components in the liquid metal.

The highest solubility in lead is that of Ni for which the phase diagram [1] shows a value of 2 at% at 550°C. The respective phase diagrams for Cr and Fe give reasonable values only for temperatures above 1000 °C. Values of 1 at% Cr and 0.15 at% Fe can be obtained for 1200 °C [1]. Model calculations provide solubilities of about 0.2 at% Cr and 10^{-3} at% Fe at 600 °C [2]. Contradictory values are given for the solubilities of Cr and Fe by [3] that amount to $6 \cdot 10^{-4}$ and $8 \cdot 10^{-4}$ at%, respectively, at 700 °C. Since all the solubilities vary with temperature, transport processes will take place which live from the higher solubility at high temperatures and precipitation at low temperatures. A temperature difference of 150 °C is about typical for liquid metal cooling loops. Therefore already small solubilities can lead to heavy corrosion effects with high flow velocities, in the range of 1 m/s, and long exposure times.

Especially because of the high solubility of Ni in the liquid metal, severe intergranular attack was observed for AISI 316 steel in liquid lead. Corrosion effects in the 100 µm range occurred in ferritic Fe-Cr steels between 575 and 750 °C after 3250 h of exposure [4].

During the last years not much was known about possibilities to improve the compatibility of steel with liquid Pb and Pb/Bi. Some compatibility tests with ferritic steels were reported which revealed corrosion attack can be minimized if an oxide layer exists on the steel surface [3,5]. However for long application of steel in liquid metal loops it is necessary to stabilize the oxide layer on the steel to prevent decomposition by solution of oxygen in the liquid metal. Gromov et. al. [5] and Markov [6] stabilized the oxide layer by maintaining an oxygen concentration of 10^{-6} at% in liquid Pb or Pb-Bi with an oxygen control system.

An overview on the corrosion behavior of two different austenitic steels in a loop with liquid lead at 550 °C as a function of oxygen concentration after 3000 h of exposure is presented in Fig. 1 [6]. At oxygen concentrations below 10^{-7} at% in lead, corrosion is determined by solution of alloy components in steel. It increases strongly with decreasing oxygen content. Above 10^{-6} at% oxygen concentration corrosion is caused by oxidation of the surface that on the other hand protects the steel from dissolution of alloying components. No clear statement about the corrosion behavior can be

given for the transition zone between 10^{-6} and 10^{-7} at% oxygen, in which dissolution as well as oxidation could be possible. We think that the part of the curves between the data points at $5 \cdot 10^{-5}$ wt% and 10^{-5} wt% can not be predicted realistically. However, from the discussion about the influence of oxygen concentration it becomes obvious that it is necessary to measure and control the oxygen concentration exactly, to keep the conditions of the liquid lead in a range of low corrosion effects. After a certain time period, oxygen in Pb or Pb-Bi will be depleted by oxide formation on the surface of the structural steel and thus the conditions will shift to the region with low oxygen concentration and hence strong corrosion effects, if there would be no oxygen control.

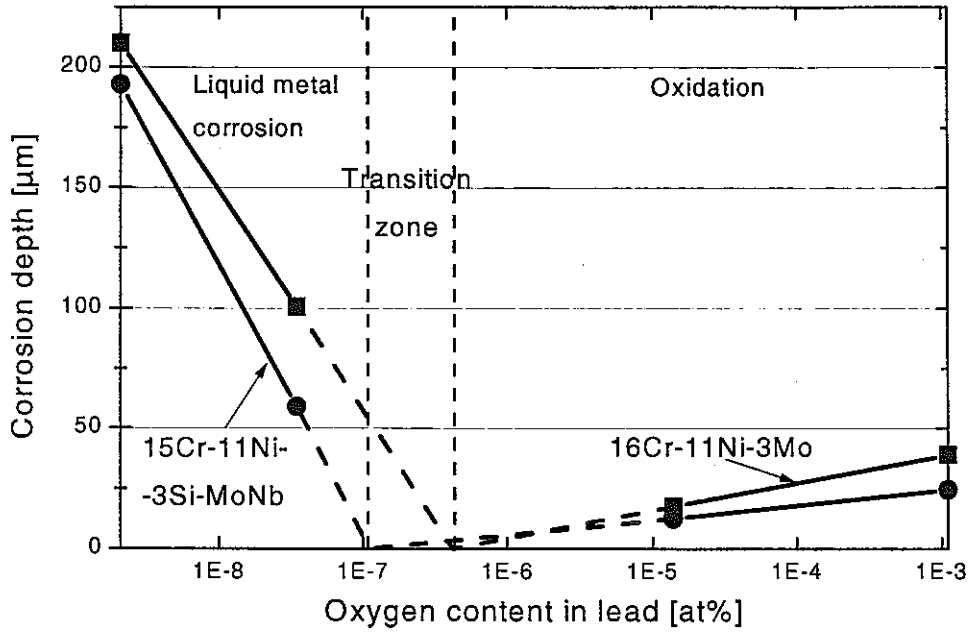

Fig. 1: Corrosion behavior of steels in flowing lead after 3000 h at 550 °C, from [10]. Oxide layer is Me_3O_4 type.

Another way to slow down corrosion of metals in liquid Pb would be to use metals with no or very low solubility in lead. Those metals are W with a solubility of <0.0056 at% and Mo with <0.011 at% at 1200 °C [7]. Molybdenum was reported to be highly resistant, even at 1000 °C [3]. Good results were obtained also with Fe-Cr alloys containing 8 at% Al that allow formation of a protective alumina scale also at low oxygen potentials [3]. Other experiments [8] employing an Fe aluminide layer on MANET steel, which was oxidized before the experiment, resulted in no corrosion attack in liquid Pb-17Li after 10000 h at 450 °C. Thermodynamic investigations of Al-Fe alloys [9] showed the possibility that a self-healing of the alumina scale can take place if the kinetics of the process is high enough. The procedure to alloy Al into the steel sur-

face by the GESA process was employed recently [10]. This procedure has the advantage that in the region of the melt depth an almost constant Al concentration exists and not a diffusion profile. No corrosion effects could be observed with this treatment also after 2000 h exposure in a Pb/Bi-loop at 600 °C [11]. Recent, not yet published examinations after 7000 h in the same loop showed also no corrosion attack.

3 Principles of oxygen control

Our procedure is the control of the oxygen concentration in the liquid metal bath by an atmosphere with a definite oxygen partial pressure that determines the chemical potential of oxygen within the liquid metal bath. To prevent PbO precipitation and to support Fe_3O_4 formation, the following conditions must be established:

$$2\Delta_f G^0_{PbO} > RT \ln p_{O_2} > 0.5\Delta_f G^0_{Fe_3O_4} \qquad (1)$$

The standard values ΔG^0 of the Gibbs energies of formation are known for the oxides in question and with these values the equilibrium oxygen partial pressure region that retains the stable conditions can be determined. The easiest way to do this is to draw a diagram that contains oxygen potentials of the relevant oxides PbO, NiO, Fe_3O_4 and Cr_2O_3 and the lines for constant oxygen partial pressures and constant p_{H_2} / p_{H_2O} ratios as a function of temperature. The latter will be used to control the oxygen potential as follows:

$$p_{O_2} = \frac{p^2_{H_2O}}{p^2_{H_2}} \exp \frac{2\Delta_f G^0_{H_2O}}{RT} \qquad (2)$$

The diagram in Fig. 2 demonstrates in which region the stable conditions exist and how they can be established. The ordinate shows the chemical potential of oxygen, the abscissa the temperature. Dashed lines in the diagram represent the isobars of the oxygen partial pressure and the lines of constant p_{H_2} / p_{H_2O} ratios in the gas atmosphere above the oxidizing species or above the liquid lead or lead-bismuth that dissolved oxygen, respectively. The important region in the diagram is the one between the lines of the oxygen potential for PbO and Fe_3O_4 in the temperature regime of 400 - 650 °C.

For working conditions with reduced corrosion we have to select a field of oxygen

partial pressures, the lines of which would not cross the PbO- and Fe_3O_4-lines within the temperature regime of 400-650°C. Lines of constant p_{H_2} / p_{H_2O} ratios within the borders of this field show the ratios that must be established to maintain the appropriate oxygen partial pressures.

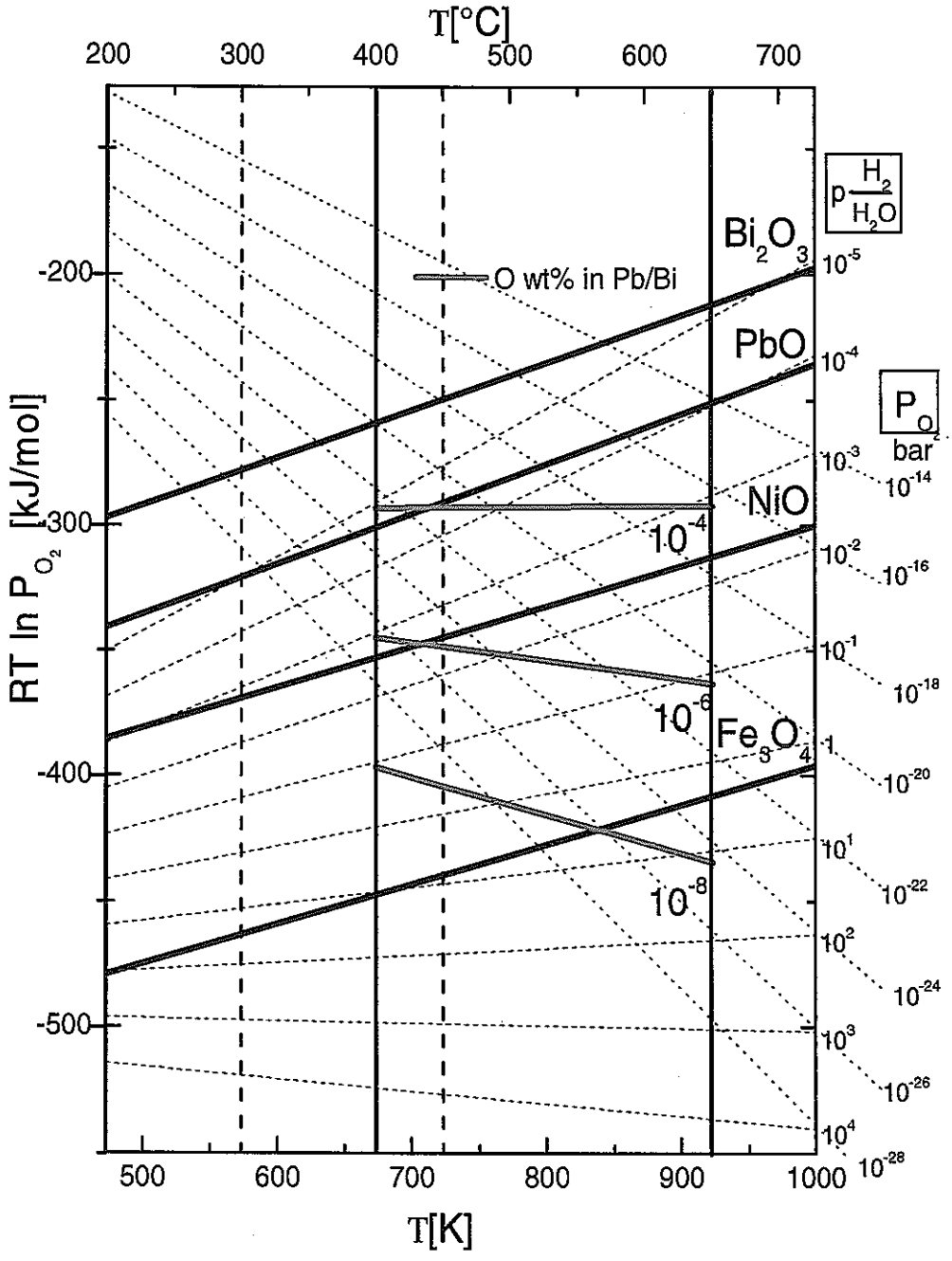

Fig. 2: Oxygen potential-diagram with PbO, Fe_3O_4 and other oxides of interest containing lines of constant oxygen partial pressures and H_2/H_2O ratios. Lines of constant oxygen concentration are drawn for 10^{-8}, 10^{-6} and 10^{-4} wt% oxygen in Pb/Bi.

If we choose a p_{H_2} / p_{H_2O} ratio of 0.4 we will attain $p_{O_2} \approx 10^{-21}$ at 650 °C and $p_{O_2} \approx 10^{-29}$ at 400 °C. At both temperatures we still form iron oxide and no PbO in the case of stagnant Pb or Pb/Bi. If we consider a liquid metal loop, there will be no equilibration across the temperature region via the p_{H_2} / p_{H_2O} ratio but through the oxygen dissolved in Pb or Pb/Bi. In this case we have to consider the variation of the oxygen potential for a constant oxygen concentration throughout the considered temperature region between 400 and 650 °C.

Let us consider first the case of liquid lead.

For calculation of the oxygen concentration c_O related to an oxygen partial pressure p_{O_2} we need to know the activity coefficient γ_0 at the phase boundary to PbO, which we get from the following relation for the oxygen activity a_O in lead:

$$a_O = \gamma_0 c_O = \frac{c_O}{c_{O,s}} = \left(\frac{p_{O_2}}{p_{O_2,s}} \right)^{\frac{1}{2}} \tag{3}$$

The suffix (s) indicates the values that correspond to saturation conditions at which the activity becomes unity.

For calculations in the region between the phase boundary PbO and the potential for oxidation of steel to Fe_3O_4 we have to assume the activity coefficient γ_0 to be constant and equal to $1/C_{O,S}$. This assumption is probably good enough, but experiments are under way to confirm it.

We turn now to the calculations for the Pb/Bi eutectic alloy.

The first problem is to obtain values of $C_{O,S}$ for the Pb/Bi alloy. The only measurements that are known are those for unalloyed Pb and Bi which furthermore scatter about by a factor of 3 and sometimes more. We use the value given by Massalski [1] for Pb and those by Griffith [12] for Bi. There is only one relation that gives the dependence of $C_{O,S}$ for eutectic Pb/Bi by Orlov [13], however, there exists no indication whether this relation is obtained by measurement or calculation from the Pb and Bi data.

Instead of using the $C_{O,S}$ data for Pb/Bi from Orlov [13] we calculated data by using Alcocks approximation for the partial molar free energy of oxygen, ΔG_{O_2}, in alloys [14]:

$$\Delta G_{O_2}(Pb/Bi[O]) = x_{Pb}\Delta G_{O_2}(Pb[O]) + x_{Bi}\Delta G_{O_2}(Bi[O]) - 2\Delta G_M^{x,s} \tag{4}$$

where Pb[O] and Bi[O] relates to oxygen dissolved in Pb and Bi respectively, $\Delta G_M^{x,s}$ ist the excess free enthalpy of mixing liquid Pb/Bi and x_{Pb}, x_{Bi} are the respective molar fractions. We see the difference to the pure lead alloy. Besides the different oxygen potentials in Pb and Bi the interaction of Pb and Bi in the metal alloy has to be taken into account also. For calculation of $c_{O,S}$ (Pb/Bi) we replace

$$\Delta G_{O_2}(Pb[O]) = 2RT \ln \frac{C_O(Pb/Bi)}{C_{O,S}(Pb)} + 2\Delta G(PbO) \tag{5}$$

$$\Delta G_{O_2}(Bi[O]) = 2RT \ln \frac{C_O(Pb/Bi)}{C_{O,S}(Bi)} + \frac{2}{3}\Delta G(Bi_2O_3) \tag{6}$$

and for the saturated state because PbO precipitates at first

$$\Delta G_{O_2}(Pb/Bi[O]_S) = 2\Delta G(PbO)\,. \tag{7}$$

Now we have Eq. (4) related to oxygen concentrations and obtain for the saturated state in Pb/Bi

$$C_O(Pb/Bi) = C_{O,S}(Pb)^{X_{Pb}} \cdot C_{O,S}(Bi)^{X_{Bi}} \exp \frac{x_{Bi}(2\Delta G(PbO) - \frac{2}{3}\Delta G(Bi_2O_3)) + 2\Delta G_M^{X,S}}{2RT} \tag{8}$$

Per definition with (7) is now C_O(Pb/Bi)=$C_{O,S}$(Pb/Bi), the quantity we wanted to find. Eq. (7) contains only known thermodynamic quantities, the standard free formation energies of the oxides, the excess free energy of mixing and the saturation concentrations of Pb and Bi listed in Tab. 1 for the temperatures of interest.

T [°C]	$C_{O,S}$ (Pb) [wt%O] [1]	$C_{O,S}$ (Bi) [wt%O] [12]	$C_{O,S}$(Pb/Bi) [wt%O] Eq. (8)
400	$5.0 \cdot 10^{-4}$	$2.68 \cdot 10^{-4}$	$6.76 \cdot 10^{-5}$
450	$1.11 \cdot 10^{-3}$	$5.99 \cdot 10^{-4}$	$1.62 \cdot 10^{-4}$
500	$2.1 \cdot 10^{-3}$	$1.21 \cdot 10^{-3}$	$3.45 \cdot 10^{-4}$
550	$3.35 \cdot 10^{-3}$	$2.23 \cdot 10^{-3}$	$6.71 \cdot 10^{-4}$
600	$4.75 \cdot 10^{-3}$	$3.85 \cdot 10^{-3}$	$1.2 \cdot 10^{-3}$
650	$6.75 \cdot 10^{-3}$	$6.26 \cdot 10^{-3}$	$2.03 \cdot 10^{-3}$

Tab. 1: Saturation concentrations for eutectic Pb/Bi

The results of the calculation of $C_{O,S}$(Pb/Bi) are shown also in Tab. 1. Fig. 3 shows the used saturation values of Pb and Bi together with those obtained for Pb/Bi by Orlov [13] and those calculated by us as a function of temperature. We see that our values deviate by about a factor of 2 to lower ones compared to those of Orlov.

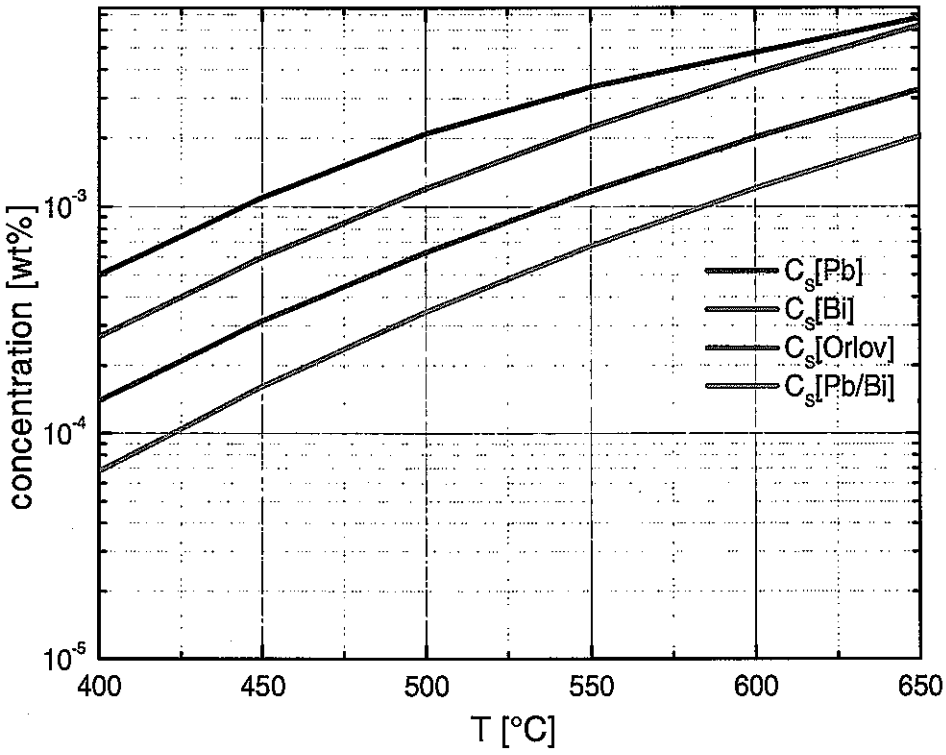

Fig. 3: Comparison of saturation values

For calculation of the relation between the partial molar free energy of oxygen and the oxygen concentration we just use the Gibb equation with $\Delta G_{O_2}(\mathrm{PbO})$ as a standard state, which corresponds to the saturation concentration.

$$\Delta G_{O_2}(Pb/Bi[O]) = 2RT \ln \frac{C_O(Pb/Bi)}{C_{O,S}(Pb/Bi)} + 2\Delta G(PbO) - 2\Delta G_M^{X,S} \qquad (9)$$

With this equation we are now able to calculate the oxygen concentration lines for the Ellingham diagram in Fig. 2. We see the line for 10^{-6} wt% oxygen stays well above the line for magnetite formation, while the one for 10^{-8} wt% crosses this line at 550 °C. Thus, with 10^{-6} wt% we are comfortable in the middle of the safe region while for 10^{-4} wt% we cross the line for PbO. For 10^{-4} wt% we have to stay, therefore, above 500 °C with the lowest temperature of a loop.

The partial pressure of oxygen in the gas in equilibrium with the oxygen concentration in Pb/Bi can be calculated from Eq. (9) to be

$$P_{O_2} = \exp \frac{\Delta G_{O_2}(Pb/Bi[O])}{RT} \qquad (10)$$

Since the furnaces among each other and also the oxygen meter cell in experimental devices will have different temperatures and the oxygen partial pressure varies strongly with temperature, we have to calculate the partial pressure at each one of

the furnace temperatures from the value obtained from the oxygen meter cell which usually measures at 750 °C. Because the H_2/H_2O ratio in the gas supplied to the furnace keeps constant also at the temperature of the meter cell, the partial pressures can be calculated via the H_2/H_2O equilibrium. From Eq. (2) we get for two different temperatures and constant P_{H_2O}/P_{H_2} ratio:

$$\frac{P_{O_2}(T_f)}{P_{O_2}(T_m)} = \exp 2\left(\frac{\Delta_f G_{H_2O}(T_f)}{RT_f} - \frac{\Delta_f G_{H_2O}(T_m)}{RT_m}\right) \tag{11}$$

Herein $P_{O_2}(T_f)$ is the partial pressure in the furnace at T_f to be calculated and $P_{O_2}(T_m)$ the partial pressure measured by the oxygen meter at temperature T_m.

With the changed concentration dependence of the Gibbs function in Eq. (9) the relation between oxygen concentration in Pb/Bi and oxygen partial pressure in the gas phase in Eq. (3) is not valid any more. The subtraction of $2\Delta G_M^{XS}$ on the right side of Eq. (9) requires recalculation of this relation. We do this by setting

$$\Delta G_{O_2}(Pb/Bi[O]) - 2\Delta G(PbO) = RT \ln \frac{P_{O_2}}{P_{O_2,s}} \tag{12}$$

and arrive at:

$$\frac{C_O}{C_{O,s}} \cdot \exp -\frac{\Delta G_m^{x,s}}{RT} = \sqrt{\frac{P_{O_2}}{P_{O_2,s}}} \tag{13}$$

This allows us now to calculate the oxygen partial pressures above the liquid Pb/Bi from the oxygen concentrations in Pb/Bi and vice versa.

4 The COSTA experiment

4.1 New COSTA device

The new COSTA device comprises in its present state 4 furnaces (GERO Type SR 100-1000/11) with gas supplies that provide the 4 different oxygen partial pressures, resp. H_2/H_2O ratios, which are destined for each one of them. Fig. 4 shows the furnaces before connecting the cover gas supply pipes. Therefore, the quartz glass tubes of the furnaces are still open.

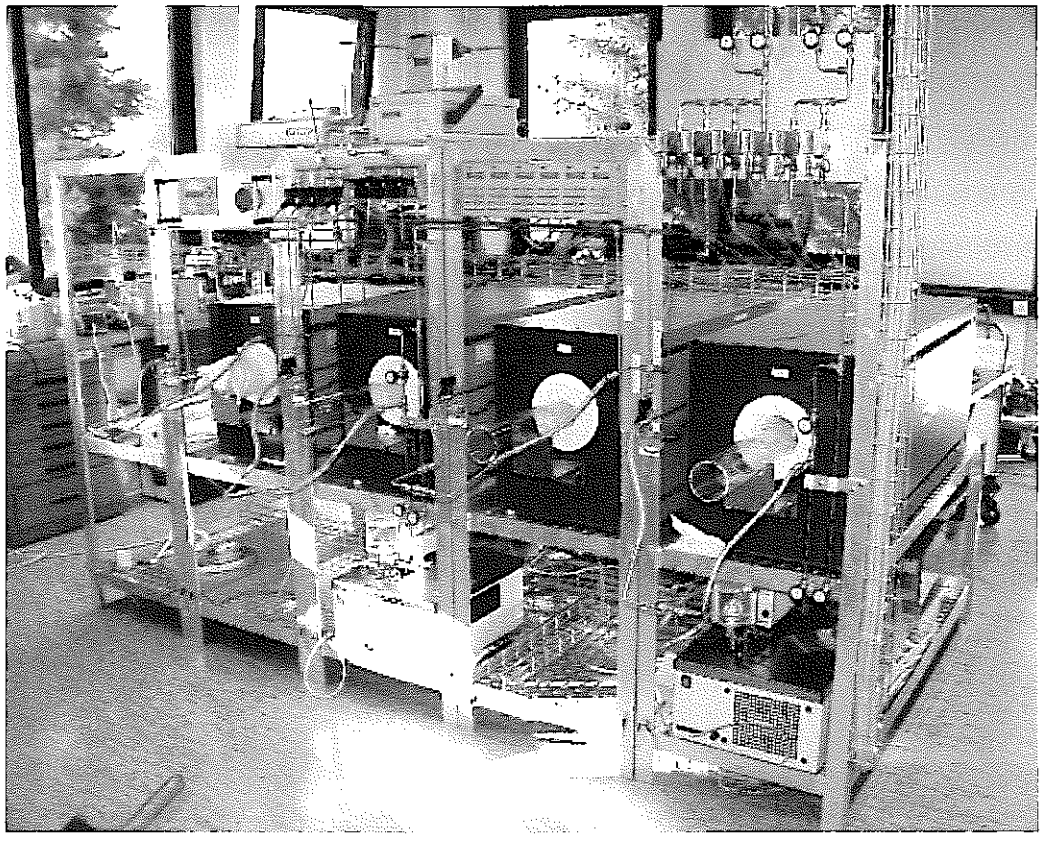

Fig. 4: Furnaces before connecting the cover gas supply tubes

Each one of the furnaces is placed in a rack. In the upper part of the racks are the gas flow and mixing controllers. On top of the rack are the oxygen partial pressure meter and the moisture analyser. The lower part of 2 racks contains a water thermostat for adding a definite amount of water vapour to the cover gas. The mounting of connection tubes of stainless steel is already finished for the gas flow meters and controllers but not jet for the quartz glass tubes which are not covered by lids in this state of construction. The tubular furnaces are heated by Kanthal wires and have a heated length of 1.20 m and a constant (± 5°C) temperature zone of about 85 cm length which is also the length of 4 of the crucible carries containing 6 crucibles each. The measured temperature profiles of the 4 furnaces are shown in Fig. 5 together with the 4 crucible carries below the curves in comparable dimensions.

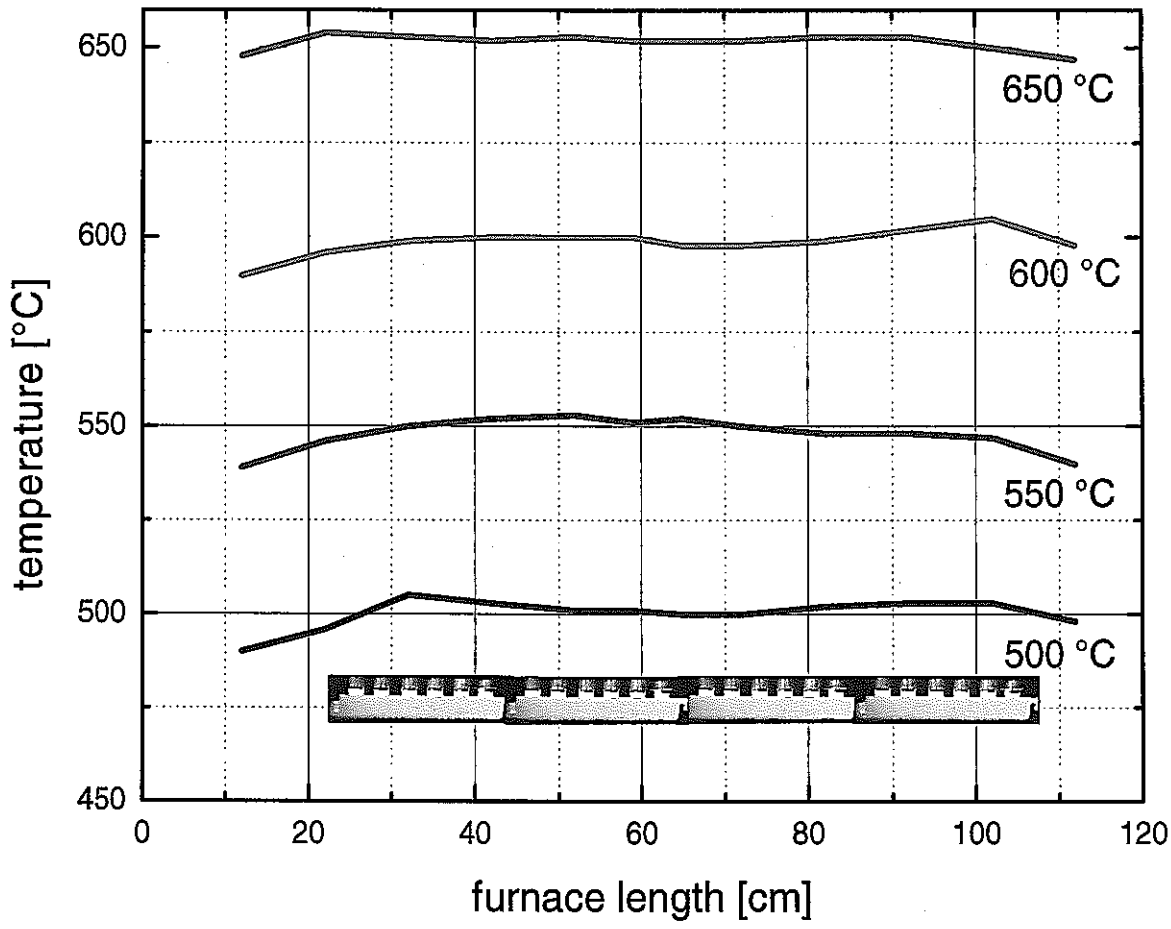

Fig. 5: Measured temperature profiles

The temperatures are controlled by PID controllers. The specimens are contained in ceramic crucibles inside the quartz glass tubes. Both ends of the quartz glass tubes are sealed by lids which contain feed throughs for the cover gas. The lids are sealed inside of the quartz tubes like it is usual for glove box feed throughs. This allows a gas tight connection of the tubes to a little glove box containing the same cover gas for taking out of samples or changing them.

The connection of the gas supply pipes to the gas feed throughs on the quartz tube lids is made by quick lock systems which allow disconnection without air inlet. The last end of the pipes is flexible on a length of 30 cm, thus, the pipes do not hinder the connection of the quartz tube to the specimen exchange box.

4.2 Loading and unloading of specimens

Specimens have to be taken out for examination and eventually new specimens have to be inserted while the whole device is still running. Therefore, an exchange glove box, Fig. 6, was build which connects to one end of the quartz tube of the furnace and allows to take out the crucible carriers and manipulate the specimens immersed in liquid metal contained in the crucibles without freezing it and with no contact to air.

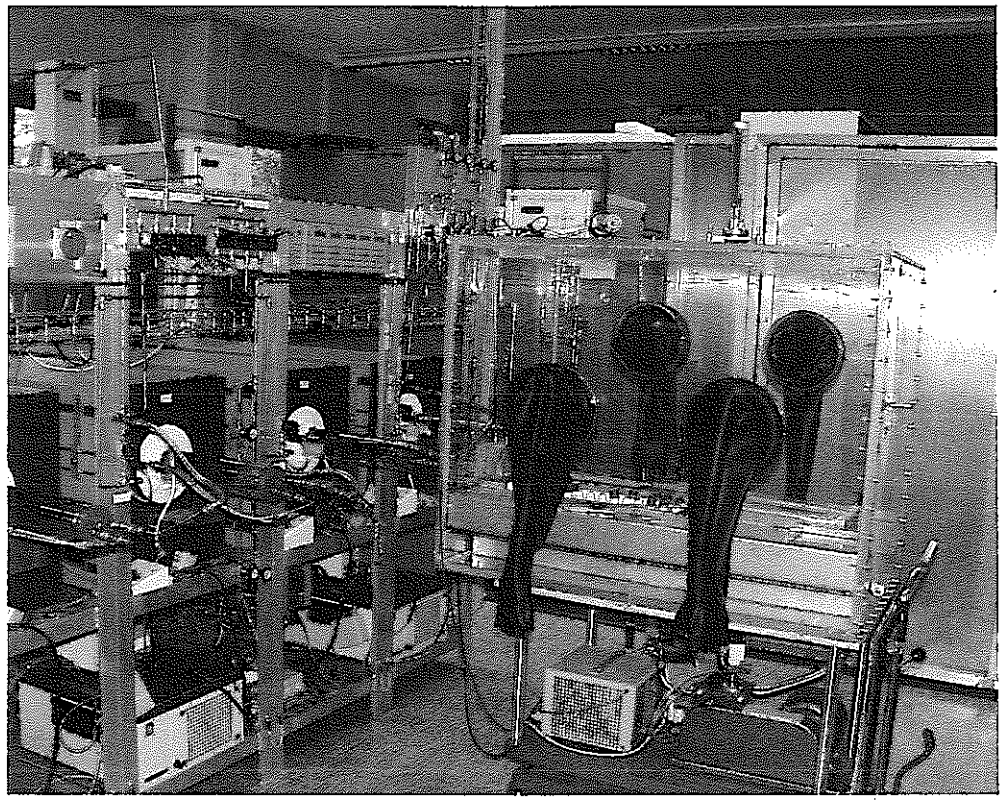

Fig. 6: Exchange glove box

It is important for the whole COSTA device to avoid infiltration of even small amounts of air into the gas circuit during the exchange process because it would cause a sudden increase in the oxygen partial pressure. This would lead to oxidation of the liquid metal surfaces in the crucibles. An oxide film consists of PbO crystals which are not easily dissolved and need a long time to be reduced by the gas atmosphere because solid state diffusion processes are involved. Special care is, therefore, taken to avoid air infiltration during coupling the quartz tubes of the furnaces to the exchange glove box. After disconnection of the flexible gas pipes from the feed throughts of the quartz tube lids the quartz tube is introduced into the tube lock of the exchange box. It slides through a O-ring seal into the outer part of the tube lock. The gas look is then

evacuated and flood with pure argon. After this the lock lid inside the box is opened and the quartz tube lid removed. Now, the crucible carrier can be removed out of the furnace by means of a stable metal wire which is hooked to the first carrier. All carriers in the furnace are hooked together and may be drawn to the open end of the quartz tube from where they can be taken out to the glove box. Fig. 7 shows the glove box connected to the quartz tube of the furnace in the background. Inside the box we see 6 ceramic crucibles containing the specimens immersed in liquid Pb/Bi. They are placed on a ceramic carrier which was moved out of the furnace to the exchange base that is heated at 250 °C to prevent the melt from freezing of the liquid Pb/Bi.

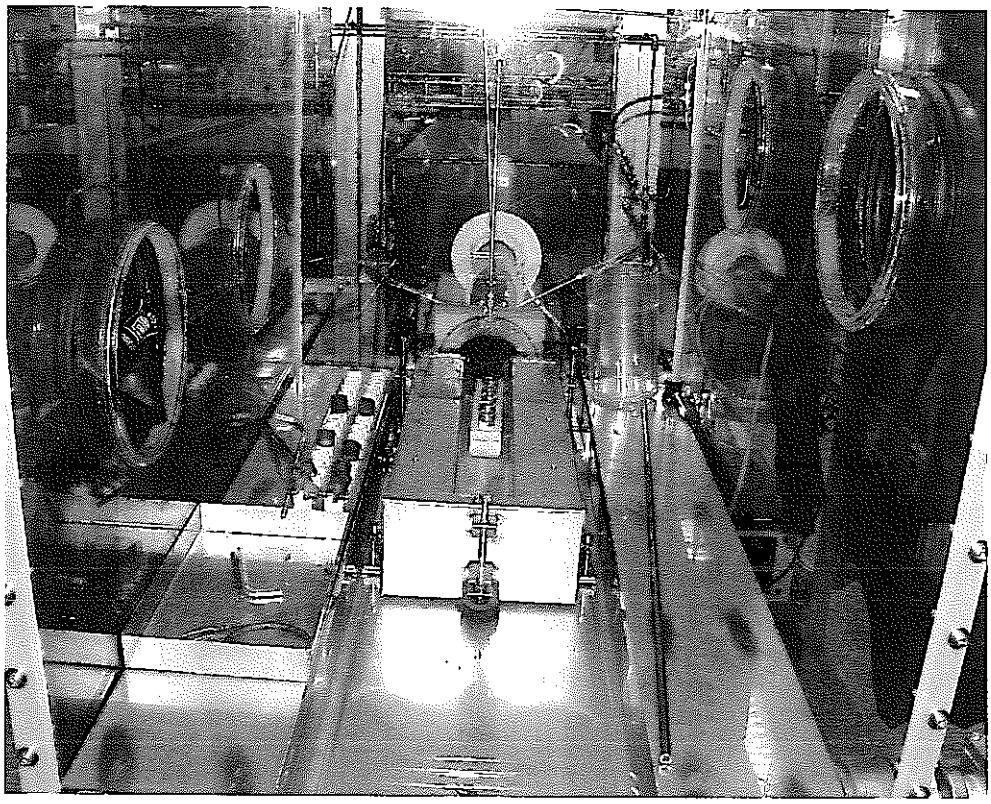

Fig. 7: Ceramic crucibles inside the glove box

4.3 Oxygen control system

The oxygen control system was build on the basis of the thermodynamical considerations described in chapter 2. The principal of the system is drawn in Fig. 8.

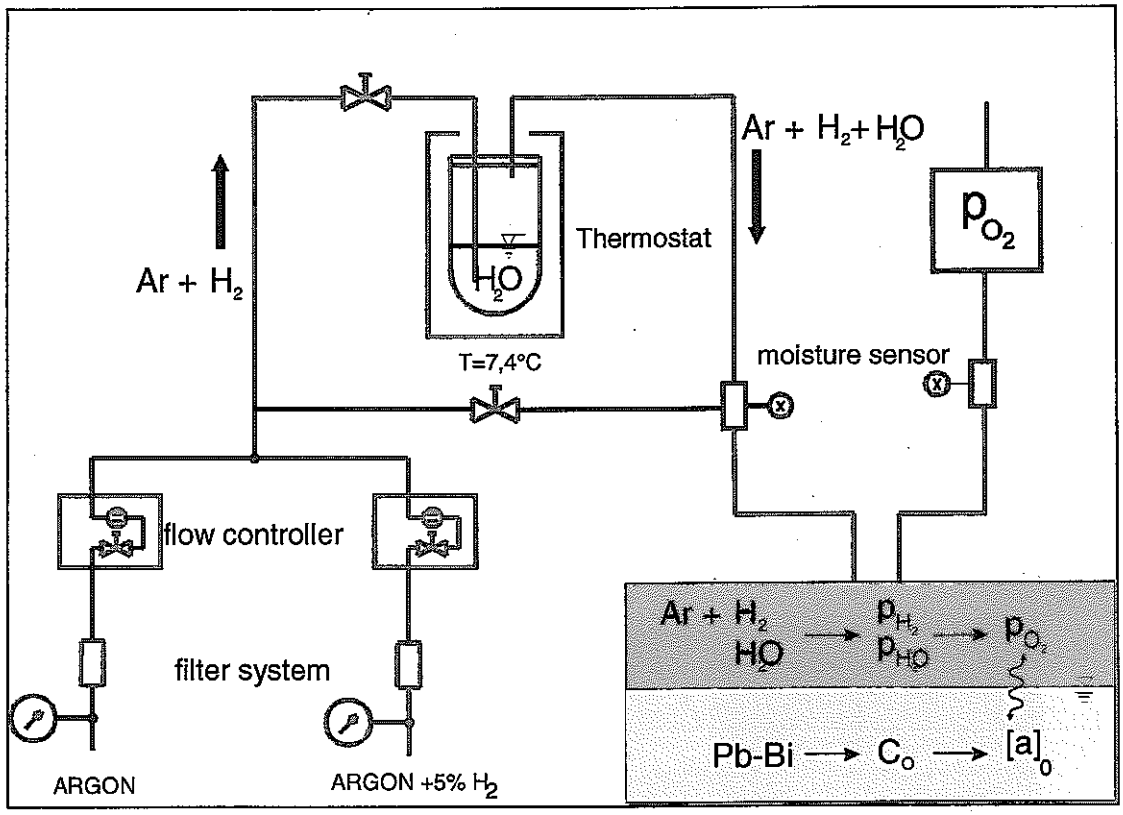

Fig. 8: Oxygen control system

The gas supply consists of one argon and one argon + 5% H_2 bottle of 50 l content with 200 and 150 bar. After reduction of the pressure to 1.5 bar the gases pass a filter system and a flow controller, each after which they get mixed. The gas that contains now the desired hydrogen concentration enters a water bottle inside a thermostat. A automatic fill unit ensures that the level of distilled water keeps always constant. After bubbling through the water the gas diffuses through a glass wool layer to ensure that no water drops reach to the outgoing gas pipe and to give the gas an additional opportunity to equilibrate with the water pressure that corresponds to the thermostat temperature. In this example it is 7.4 °C which corresponds to a vapour pressure of 10 mbar. Thus, it is easy to establish exactly the H_2/H_2O ratio calculated for the required oxygen partial pressure of the experiment. After passing the reaction furnace and equilibration between gas and liquid metal the moisture content and oxygen partial pressure are measured for registration and to ensure the required values are present. There is no measurable change in the H_2/H_2O ratio during equilibration of the gas with the liquid metal to be expected. This should be shown by a little calculation for the case of 10^{-7} wt% oxygen in Pb/Bi which corresponds to an oxygen partial pressure of about 10^{-25} bar that is provided by a gas with $P_{H_2} / P_{H_2O} = 0.4$. Using

this ratio it is easy to replace the oxygen that may be necessary to provide oxygen for the progressing oxidation of the steel in Pb/Bi with 10^{-7} wt% oxygen. With a gas flow of 100 cm^3/min, it is possible to provide 5 cm^3 O_2/min which corresponds to about 500 cm^2 of a Cr_2O_3 layer of 1µm thickness. With the same gas flow, delivery of the oxygen amount necessary for solution of 10^{-7} at% oxygen in 1000 cm^3 Pb takes about 0.1 s. A scheme of the technical realization of the oxygen control for the 4 furnaces of the new COSTA device is drawn in Fig. 9.

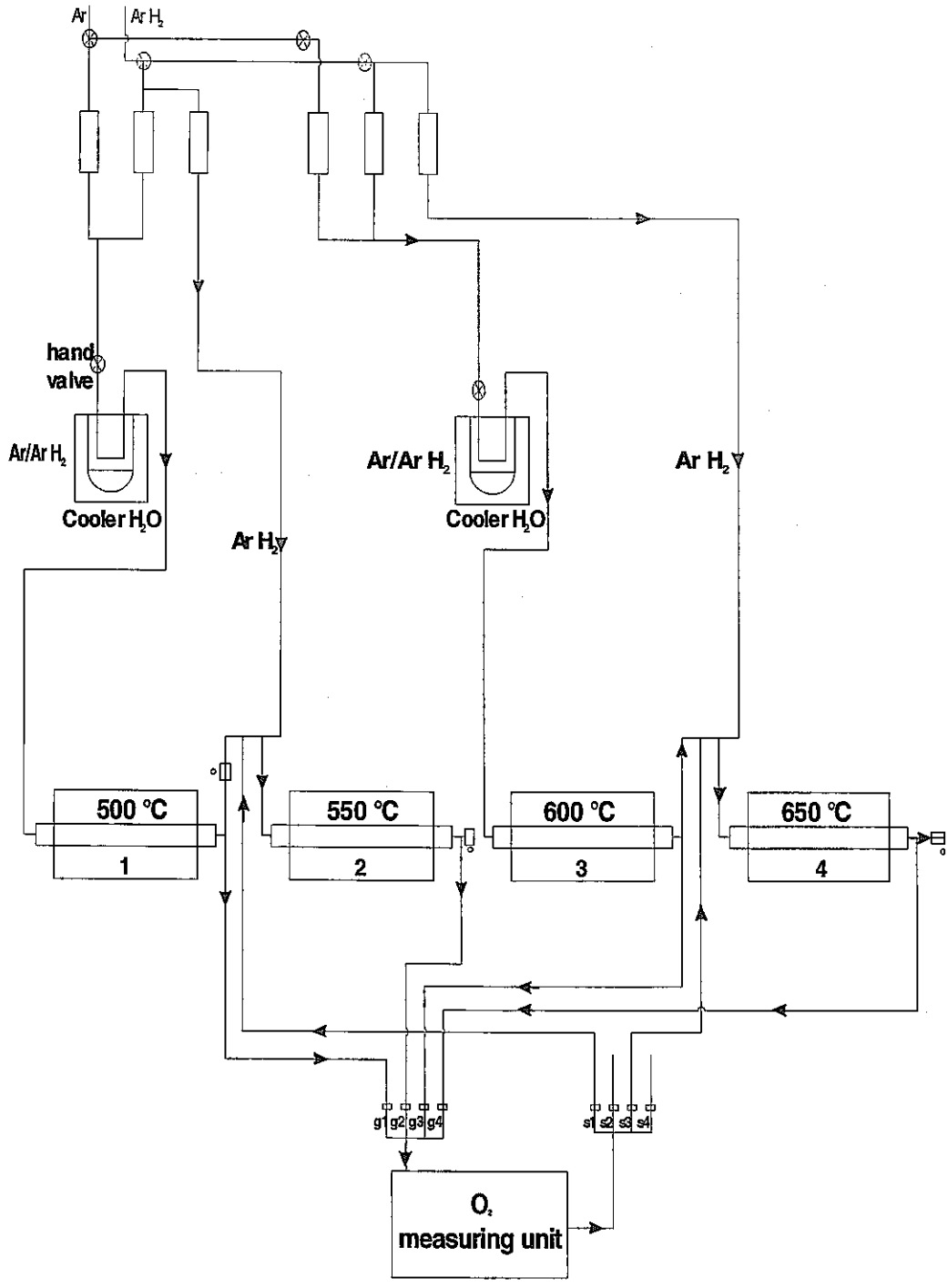

Fig. 9: Scheme of the technical realization of the oxygen control for the 4 furnaces

Also here, one Ar and one Ar 5% H_2 bottle (50 l, 200 bar) provide the gas for the experiment. The gas mixing system is designed such that 2 thermostats are sufficient for the gas conditioning. The gas mixture in the first line passes the thermostat and feeds into furnace 1 with 500 °C to keep the oxygen concentration at 10^{-6} wt%. After it left the furnace just a little more H_2 has to be added to reach this condition for the higher temperature, 550 °C, in furnace 2. From there it is released to the atmosphere. We remember, the oxygen concentration curves have a negative slope with temperature in the Ellingham diagram. Therefore, we need a higher H_2/H_2O ratio for the constant concentration at higher temperatures. The next 2 furnaces No. 3 and 4 are served in the same way.

We did not consider the connections to the oxygen and moisture meter yet for reasons of simplifying. Each furnace exit is connected one after another for ½ h to the measurement station. When gas of furnace 1 is to be measured, the automatic valve at its exit is shut and the ones signed g1 and also s1 (Fig. 9) at the station are opened. Now the gas passes the measurement station before it comes back to the position behind the valve at the exit of furnace 1. From there the gas enters furnace 2. After ½ h of measurement the exit valve at furnace 1 is opened and valves g1 and s1 at he measurement station are shut while g2 and s2 are opened and the exit valve at furnace 2 is closed. Now the gas leaving furnace 2 is measured. After another ½ h g2 and s2 are shut and exit valve 2 opened. Now the same procedure as before starts for furnace 3 and 4. Note, that during measuring the gas of furnace 2 and 4 the gas is released after passing the measurement station to the atmosphere via valves s2 and s4, respectively.

Now the only question not answered is about the function of the hand valves in the flow meter region and before the thermostats. These valves are used to sweep dry Ar 5% H_2 through the system for cleaning of the pipes or reduction of the liquid metal if necessary.

In the first series of experiments the specimens were exposed to Pb/Bi containing 10^{-6} wt% of oxygen at 500, 550, 600 and 650 °C in furnace 1 – 4. Table 2 shows what should be the H_2/H_2O ratios and the oxygen partial pressures in this furnaces and what would be the reading of the oxygen meter.

furnace	1	2	3	4
Temperature [°C]	500	550	600	650
H_2/H_2O ratio	$1.6 \cdot 10^{-2}$	$4.0 \cdot 10^{-2}$	$8.8 \cdot 10^{-2}$	$1.9 \cdot 10^{-2}$
P_{O_2} [bar]	$1.18 \cdot 10^{-24}$	$1.96 \cdot 10^{-23}$	$2.38 \cdot 10^{-22}$	$2.1 \cdot 10^{-21}$
P_{O_2} [bar], oxygen meter at 750 °C	$1.38 \cdot 10^{-16}$	$2.23 \cdot 10^{-17}$	$4.47 \cdot 10^{-18}$	$1.0 \cdot 10^{-18}$

Tab. 2: Data's of furnace 1 – 4.

The actual readings of the oxygen meter and the calculated oxygen partial pressures for the temperatures in furnace 1-4 during the first 2500 h of the experiment are depicted in Fig. 10 and 11. We see that the curves representing the oxygen partial pressures are very close to those required in Tab. 2. If we calculate the oxygen concentrations in Pb/Bi from the measurements presented in Fig. 10, we obtain Fig. 12 which shows that the required value of 10^{-6} wt% is reached with good approximation.

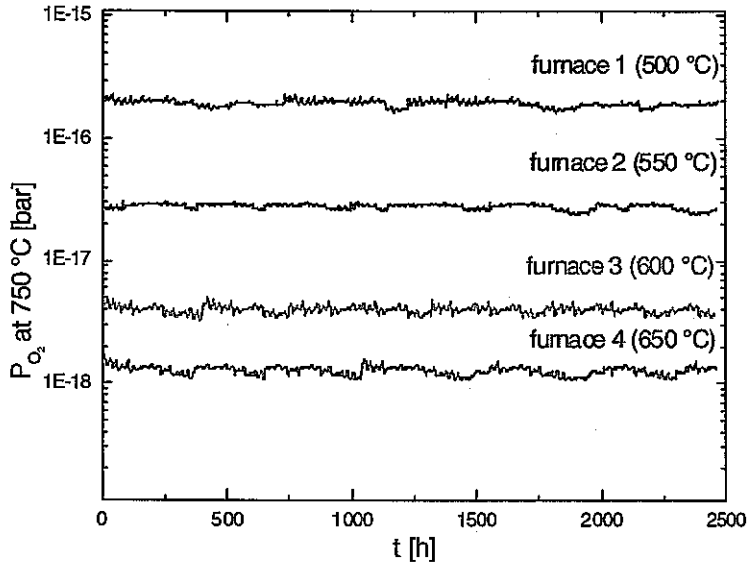

Fig. 10: Oxygen partial pressure at 750 °C measured by P_{O_2}-meter

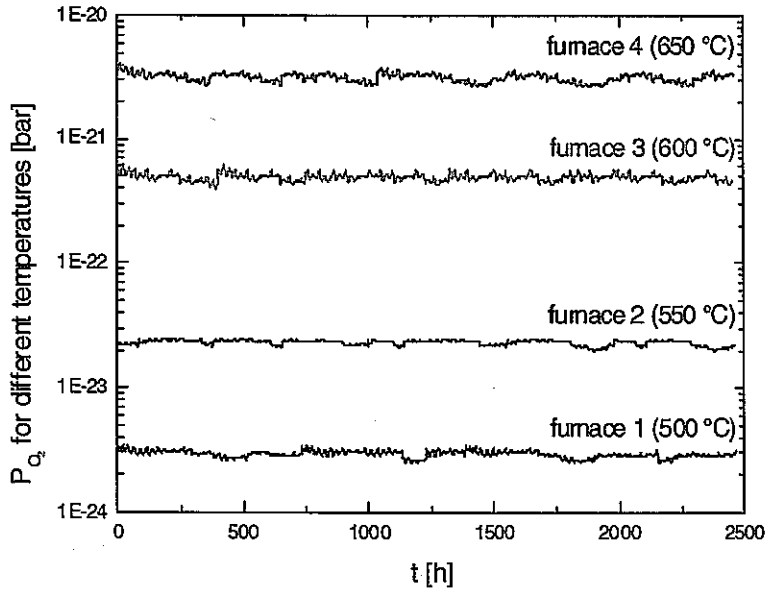

Fig. 11: Oxygen partial pressure inside the furnaces calculated from values at Fig. 10

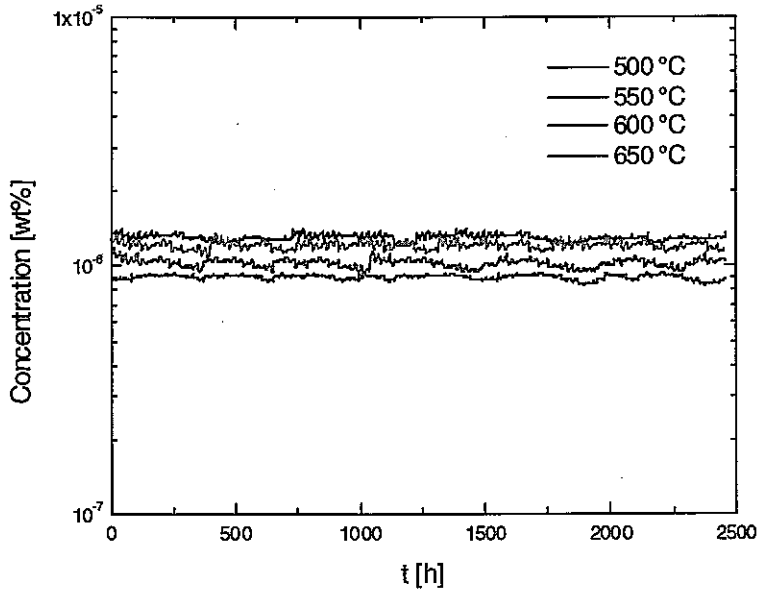

Fig. 12: Oxygen concentration in liquid lead contained in the furnaces with different temperatures

4.4 Specimen preparation and testing

4.4.1 The GESA facility

The surface treatment of the steel specimens employed for the corrosion tests in liquid Pb/Bi was carried out with the GESA (gepulste Elektronenstrahlanlage) facility [15]. The treatment consists of alloying Al into a surface layer of 10 to 15 µm depth. For this purpose, a 18 µm Al-foil is placed on the steel surface. It melts and mixes with the molten steel surface layer. A great part of the Al evaporates during this process, but the remainder, about 25%, is alloyed into the steel.

GESA is a pulsed electron beam facility that consists of a high voltage generator with a pulse duration control unit, a multipoint explosive emission cathode, a controlling grid and an anode which form a triode scheme. The scheme of the GESA facility is shown in Fig. 13.

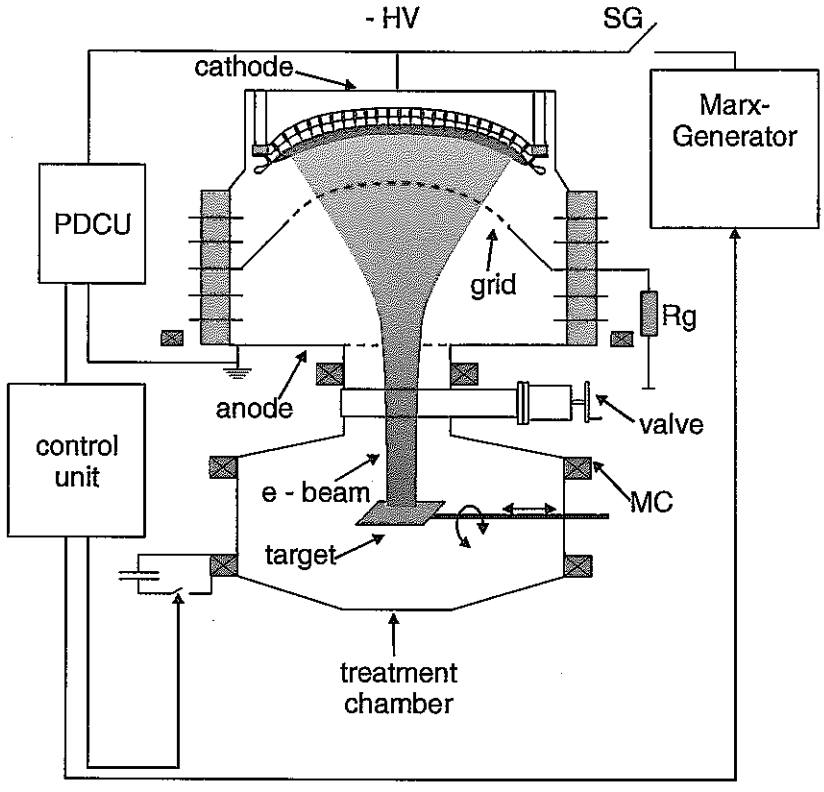

Fig. 13: Scheme of the GESA facility.

The high voltage generator is made according to the Marx scheme. A multipoint explosive emission cathode with an area of 700 cm^2 is used as an electron emitter. The magnetic focusing system which consists of 6 coils guides the electron beam through a 50 cm long transport channel to the target and allows variation of the beam diameter in the range of 6 - 10 cm. A pulse duration control unit (PDCU) allows adjustment of the pulse duration between 5 and 40 µs.

The kinetic energy of the beam electrons can be varied in the range of 50 - 150 keV, with a beam power density up to 2 MW/cm^2 at the target and a pulse duration up to 40 µs. The important parameters for the melting process like electron energy, power density and pulse duration can be chosen independent from each other. The energy density absorption at the target is up to 80 J/cm^2, which is sufficient to melt metallic materials adiabatically up to a depth of 10 - 40 µm. The beam diameter is 6 - 10 cm and this is the area of surface melting by applying one single pulse. Due to the high cooling rate in the order of 10^7 K/s, fine grained structures develop during solidification of the molten surface layer.

An overall view of the GESA facility at FZK is shown in Fig. 14.

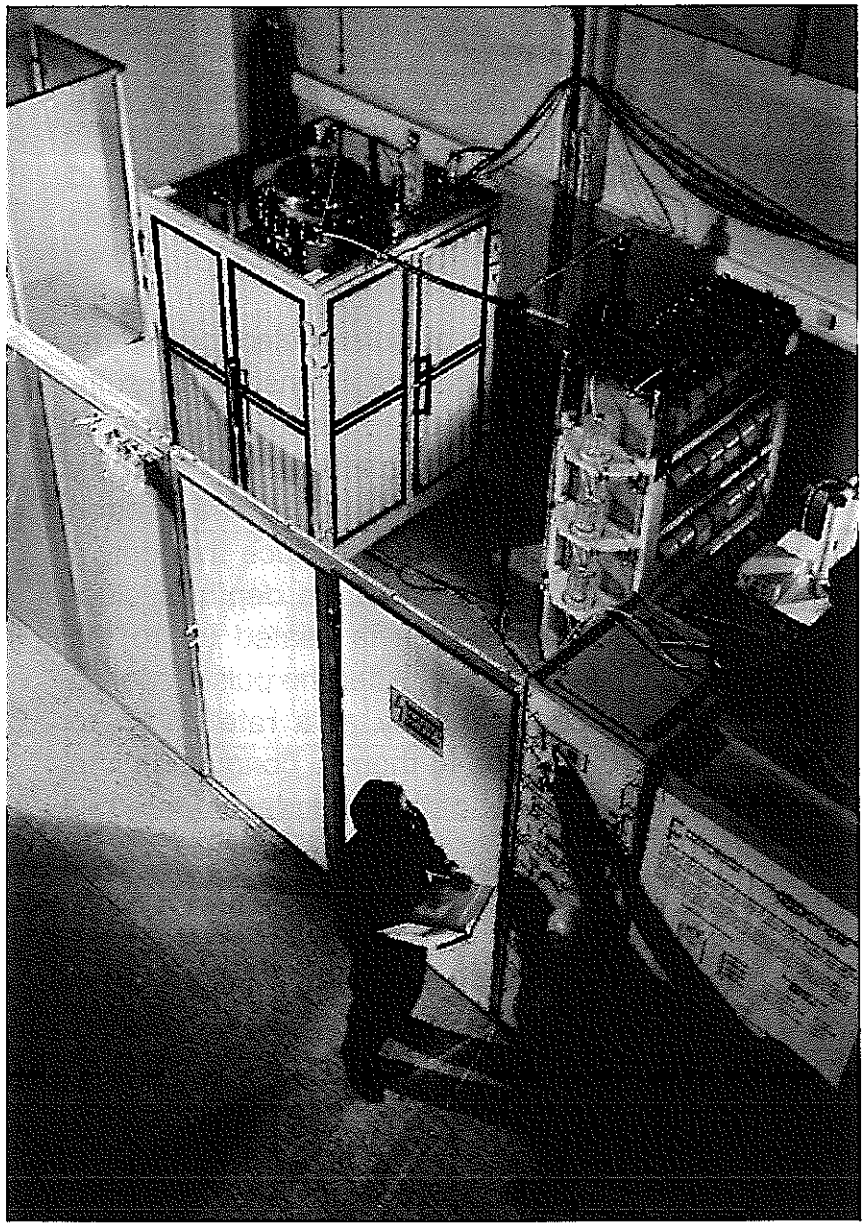

Fig. 14: Overall view of the GESA I facility at FZK

4.4.2 Specimens

The specimens of 27 x 6 x 2 mm dimension had to be cut from massive blocks of the steels P 122, ODS and 316FR delivered by JNC. Chemical compositions of the materials are shown in Tab. 3 to 5. This work was done by electro erosion. At first, bars of 27 x 200 x 2 mm were cut which were then divided into pieces of 6 mm width. Two boreholes were drilled of Ø 1,5 mm into each one of the specimens to allow fixing of the specimens in the liquid metal crucibles. Fig. 15 shows the drawing of a specimen.

	C	Si	Mn	P	S	Cr	Ni	Mo	Co	N	C+N
Heat	0.010	0.47	1.05	0.026	0.001	17.58	12.31	2.46	0.06	0.10	0.11
Product	0.012	0.47	1.04	0.024	0.001	17.61	12.25	2.48	0.06	0.10	0.11

Tab. 3: Chemical Composition of 316FR

	C	Si	Mn	P	S	Cu	Ni	Cr
Heat	0.11	0.27	0.64	0.016	0.002	1.00	0.33	10.54

W	Mo	V	Nb	Sol Al	N	B
1.76	0.34	0.19	0.048	0.001	0.071	0.034

Note; Heat Treatment (NT): 1070'Cx100min (AC) , Tempered: 770Cx440min

Tab. 4: Chemical Composition of P122

	C	Si	Mn	P	S	Ni	Cr
Product	0.13	<0.005	<0.01	0.001	0.003	0.01	8.85

W	Ti	Y	O	N	Ar
1.94	0.20	0.27	0.17	0.011	0.005

Note; Heat Treatment: 1050'Cx1h (AC), 800'Cx1h (AC)

Tab. 5: Chemical composition of ODS

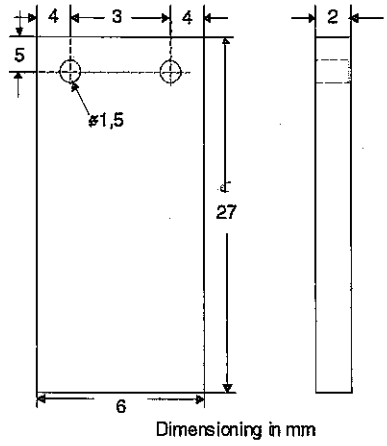

Fig. 15: Technical drawing of a specimen

In a last step the surface of the specimens was polished by grinding. Part of the specimens were treated by alloying Al into the surface using the GESA process.

Table 6 shows the number of specimens of the different steels and their surface preparation.

steel	P122	ODS	316FR
Surface polished	41	50	41
Surface alloying by GESA	12	22	12
Total number of specimens	53	72	53

Tab. 6: Number of specimens prepared

It took almost 2 months to prepare such a high number of specimens by cutting surface grinding, GESA Al-alloying and drilling of the bore holes. Only 2 specimens are mounted in one crucible for the experiments to avoid interaction between the sur-

faces of the specimen inside the liquid metal crucible. Fig. 16 shows the arrangement of the specimens in a crucible which was cut axially to allow a look into the interior.

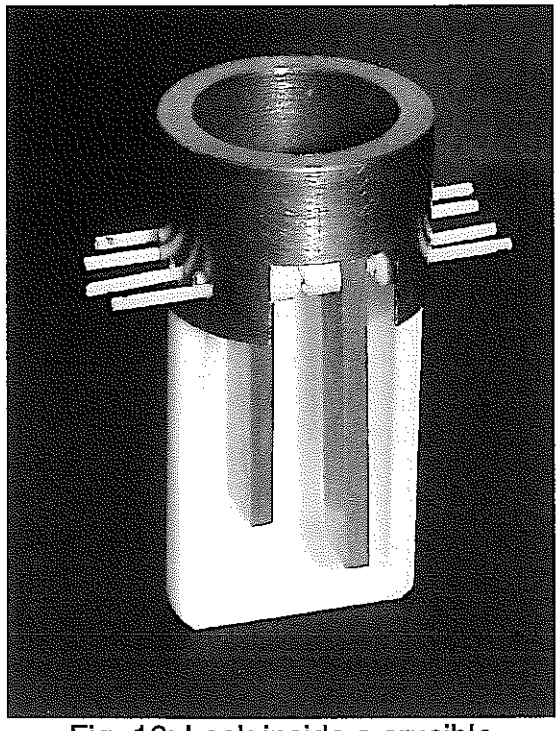

Fig. 16: Look inside a crucible

The specimens are fixed each by two ceramic pins which itself are fastened by the holes in the nickel flange sitting on the rim of the crucible. The mass of the flange is calculated to compensate the buoyancy of the specimens in the liquid Pb/Bi. Note, the specimens are displaced sidewards, thus, the surfaces do not see each other which should minimize any interaction. Little distance tubes on the pins ensure the distance between the surfaces is kept.

Before the experiment starts the crucibles in their carriers (6 on one carrier) are filled with Pb/Bi of high purity. The crucibles are heated under flowing purified Ar 5% H_2 gas (O_2, H_2O < 0.01 ppm) to reduce the liquid alloy to an oxygen potential far below that of Fe_3O_4. Then the temperatures of the different furnaces are established while the gas conditioning is changed to like required by the experiment. The required oxygen concentration in this first series of experiments is 10^{-6} wt%. The necessary H_2/H_2O ratios for this condition is already given in Tab. 2. After 3 days allowed for equilibration the crucibles on their carriers are withdrawn from the furnaces into the exchange box to insert the specimens into the liquid metal. This task starts with furnace 1 and after the specimens are back in the furnace it proceeds to furnace 2 and

so on. The oxygen partial pressure and the moisture of the gas are recorded and inspected day by day.

4.5 Examination of test specimens

After each one of the selected test periods the respective samples are taken out of the liquid metal crucible inside the exchange box. They are transferred to the outside through the gas lock.

Two specimens of each steel type are removed from the furnaces. One of those specimens is not washed or treated to prevent changing of the surface structure. The other specimen is immersed into 180 °C hot oil and wiped with a cloth to remove the remaining Pb/Bi from the surface. After this the specimens are cut 6 mm from the lower specimen end perpendicular to the longitudinal direction. The 6 mm pieces are embedded into resin for metallographic preparation of the cut surface.

The specimens with no surface cleaning are examined in the Karlsruhe lab. They are ground and polished for the examination by scanning electron microscopic (SEM) and energy dispersive x-ray (EDX) analysis. The surface structure is examined with a Hitachi S800 and Leitz AMR 1000. The elemental analysis was done by an ECON 3,40 detector attached to the Leitz SEM and a Kevex thin window detector attached to the Hitachi SEM. The Edax DX-4 and a Windiss system are used for the calculation of the concentrations by employing the standardless method.

Specimens with washed surface are used to examine the surface structure by x-ray diffraction (XRD) analysis with a Seiffert XRD 3003 PTS diffractometer device.

5 Results

5.1 Starting materials

5.1.1 P 122 steel

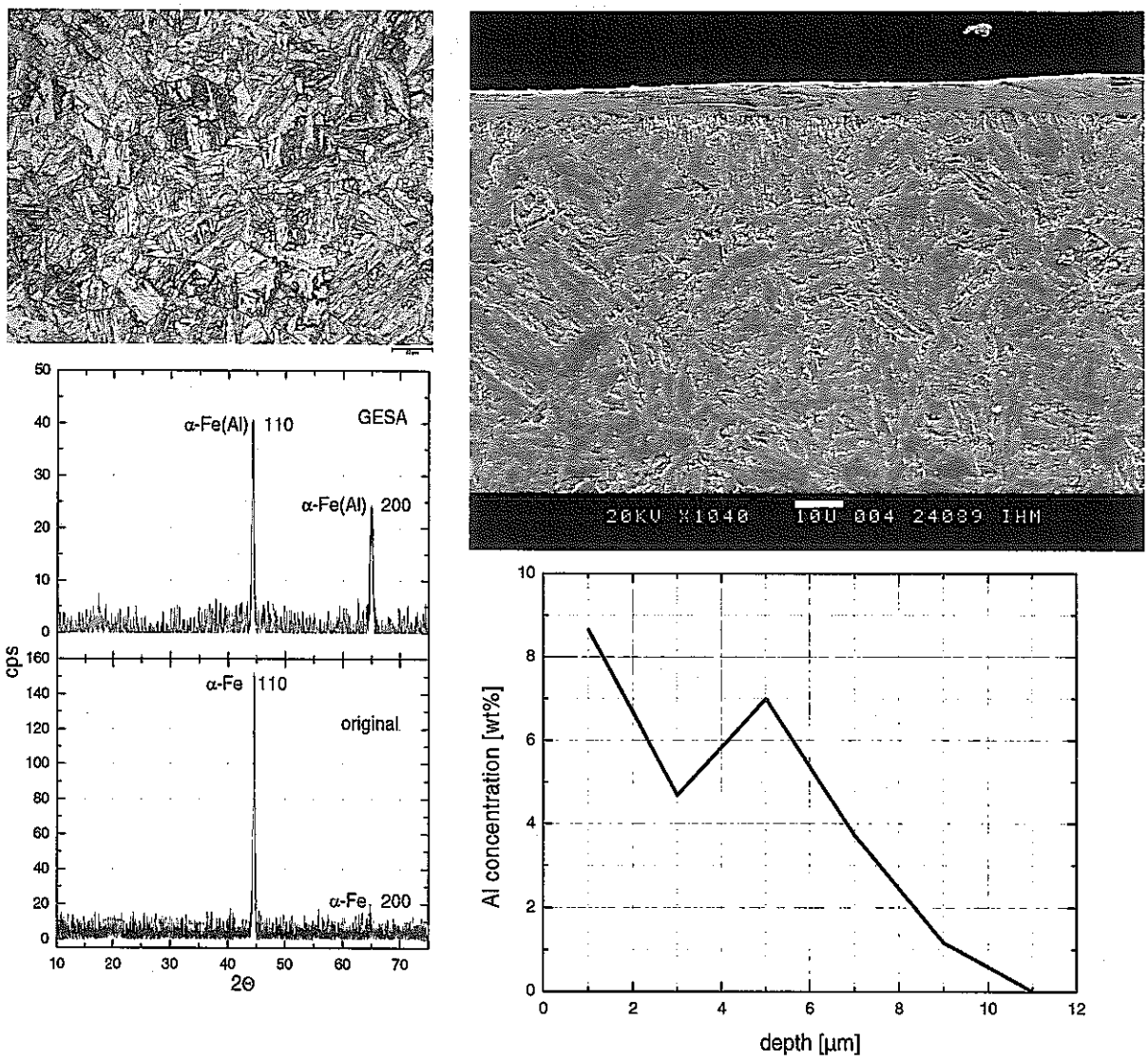

Fig. 17: Cross sections, Al concentration profiles and XRD pattern of the starting P122 material

From the cross sections above we see left the typical structure of martensitic steel. The structure composes of FeCr-carbides having needle like structure. The mean grain size is about 5 – 10 µm. On the right hand side we see the structure after GESA treatment. The melting zone at the surface contains an average of 6 wt% Al on the first six µm of depth. The layered structure results from concentration differences within the molten layer. See the concentration profile to the right.
On the left side the XRD patterns are shown obtained from the surface of both specimens. They show the α-Fe lines before and after alloying Al into the steel surface. The strong increase in intensity of the (200) peak after Al alloying indicates the

preferential direction of crystallization during solidification in the temperature gradient perpendicular to the surface.

5.1.2 ODS steel

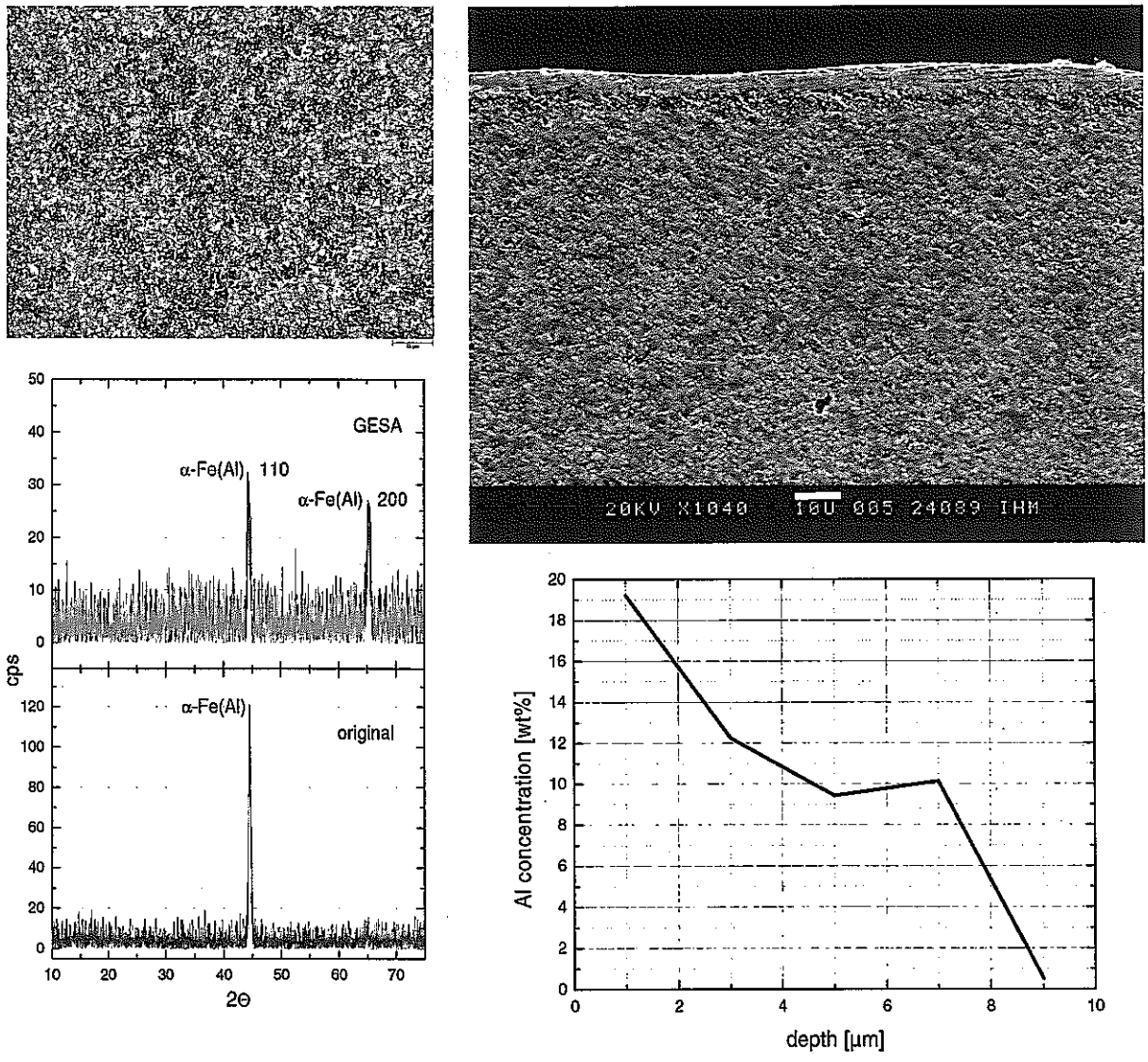

Fig. 18: Cross sections, Al concentration profiles and XRD pattern of the starting ODS material

The cross section of the ODS specimen on the upper left side shows the very fine grain structure (< 4 μm) of the steel. During alloying the same structure changes appear as observed for P122. The only difference is the higher Al concentration at the position of analysis.

5.1.3 316FR

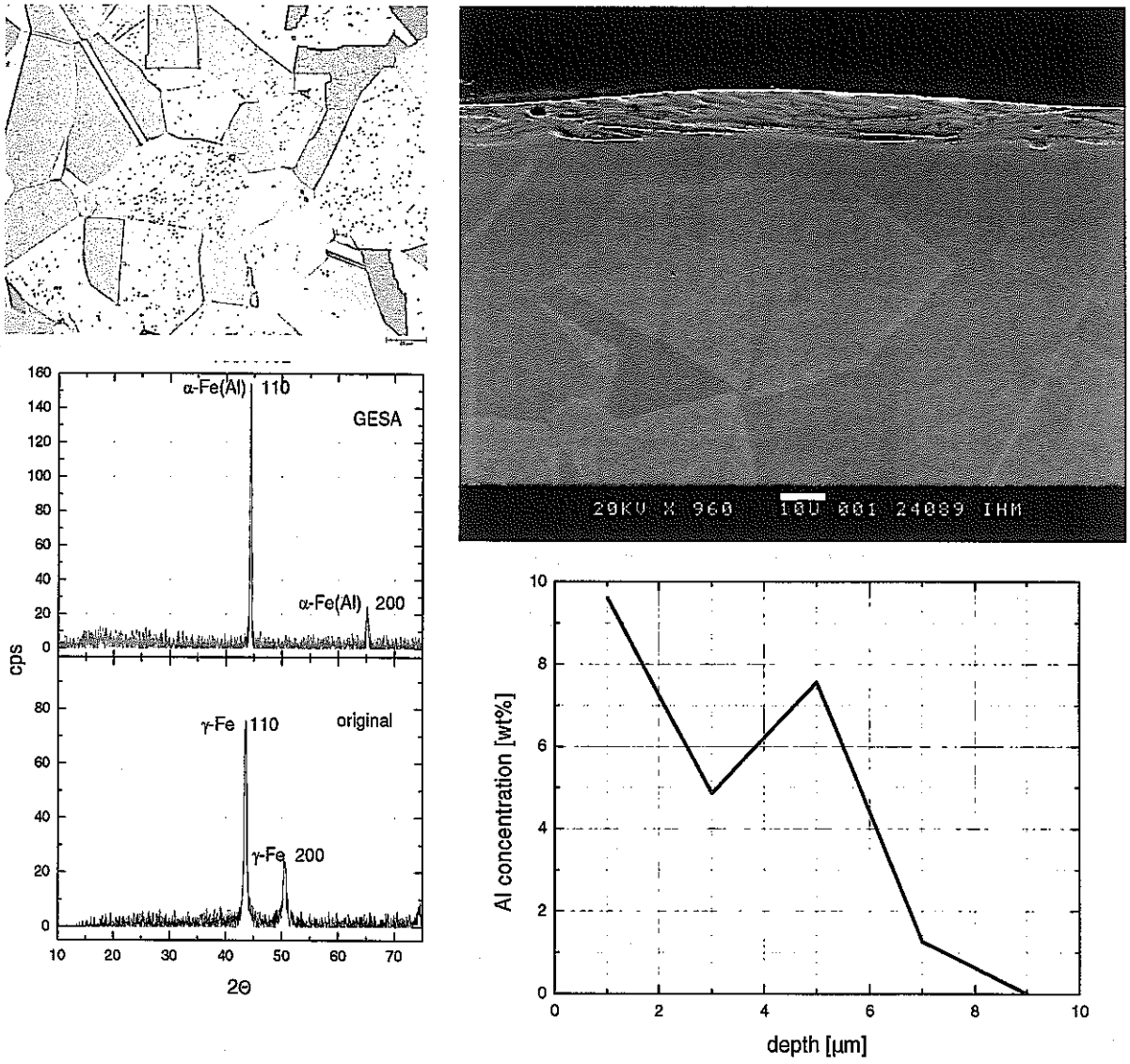

Fig. 19: Cross sections, Al concentration profiles and XRD pattern of the starting 316FR

316FR has a coarse austenitic grain structure (30 – 60 μm, upper left). The structure of the alloyed layer is the same as described in 5.1.1. From the XRD patterns it follows that the original austenitic γ-structure changes into α-Fe(Al).

5.2 Steels in Pb/Bi

5.2.1 316FR

Temperature 500 °C

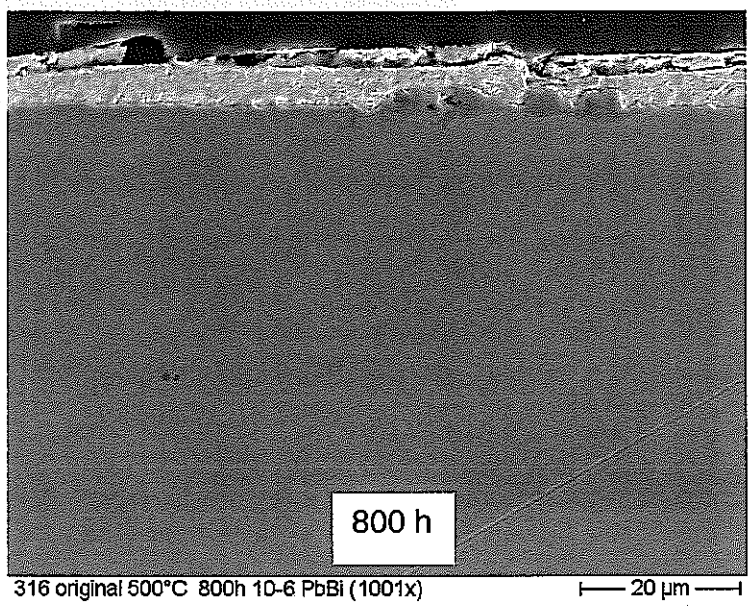

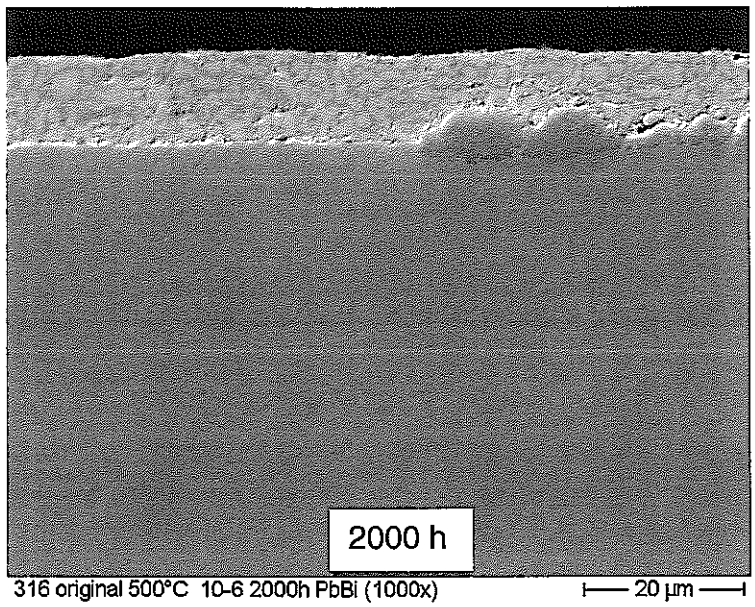

Fig. 20: 316FR after 800 h and 2000 h at 500 °C

A cross section through the surface of the original specimens is shown in the SEM of Fig. 20. After 800 h the steel has a thin protective spinel layer (not visible) with occa-

sional appearance of nodes with a µm thick spinel and magnetite layer caused by structural defects on grain boundaries. After 2000 h this appearance doesn't change. The bright phase on top is Pb/Bi.

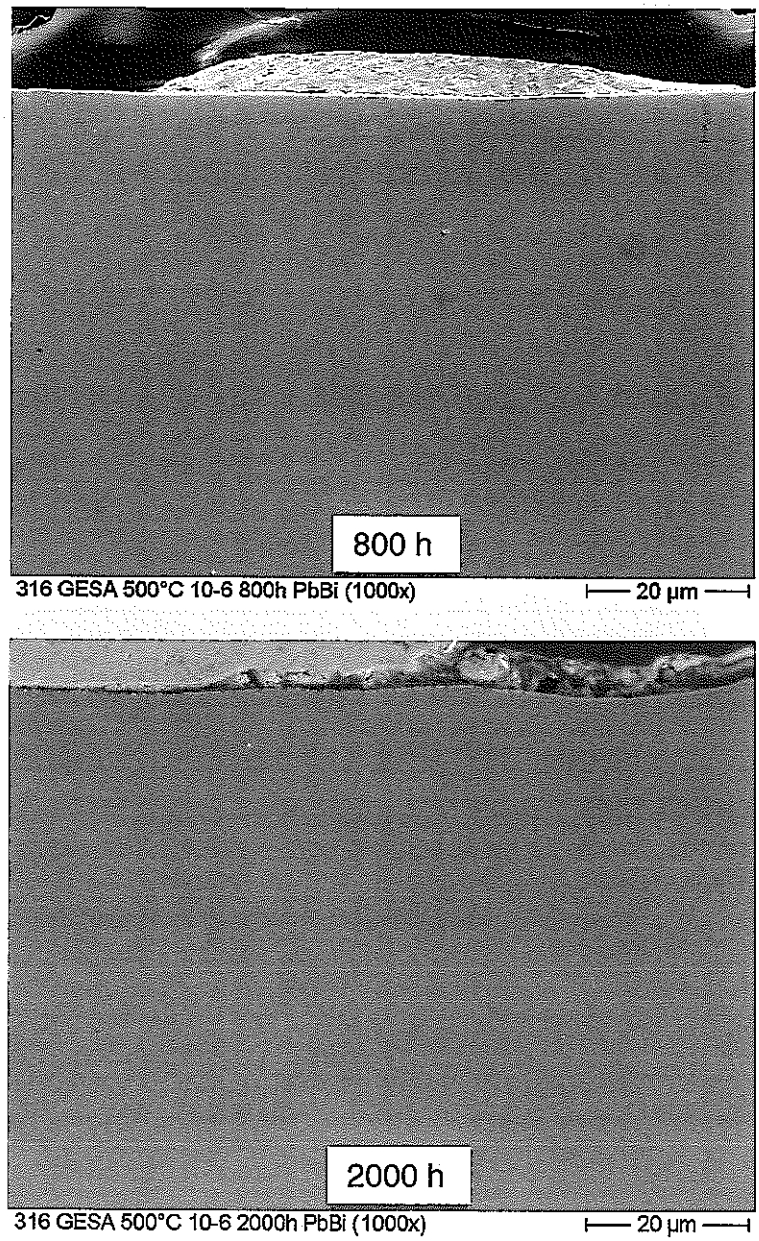

Fig. 21: 316FR GESA alloyed after 800 h and 2000 h at 500 °C

The GESA alloyed specimen did not show any signs of attack after 800 h, Fig. 21. In one position there was a crack in which Cr-Al was oxidized containing Pb/Bi impurities. This situation seems not to be critical. But parameters of GESA and Al-concentration have to be kept at conditions to prevent those cracks. Also after 2000 h of exposure no signs of corrosion or oxidation are visible.

Temperature 550 °C

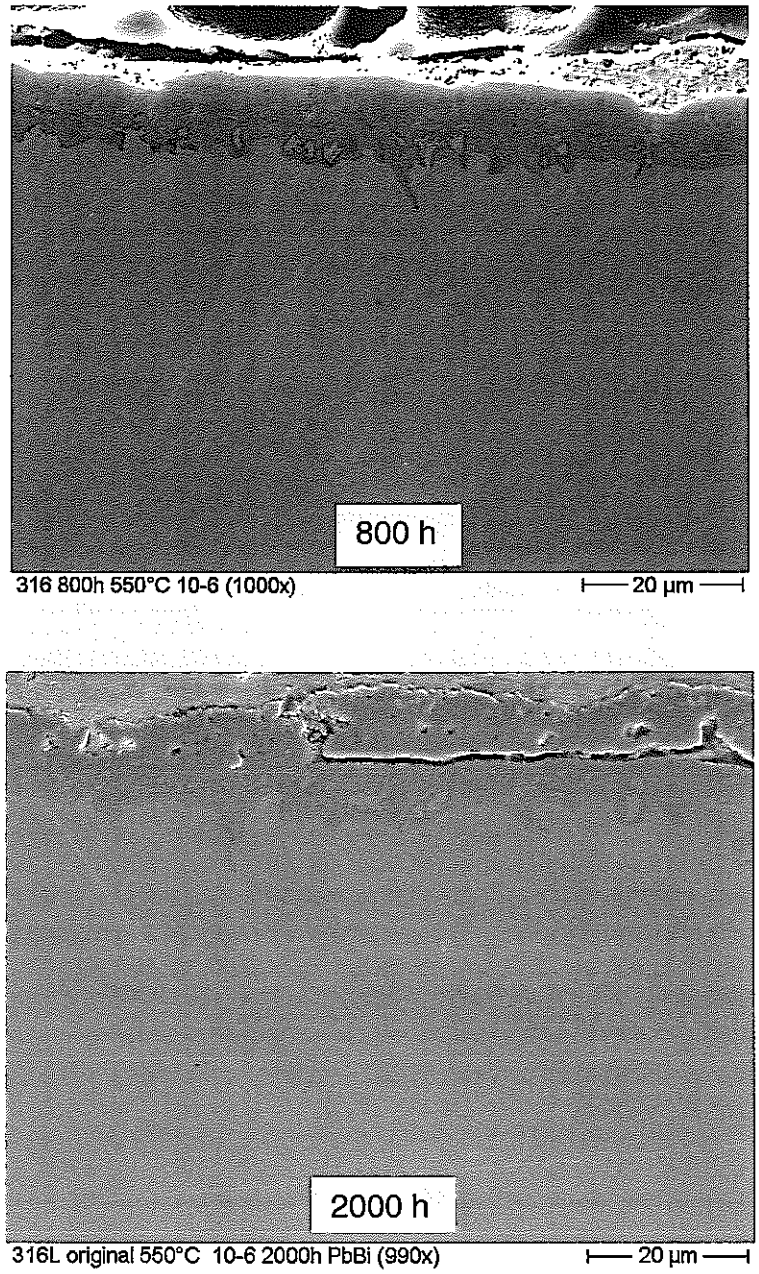

Fig. 22: 316FR after 800 h and 2000 h at 550 °C

After 800 h the original specimen shows a continuous oxide layer of 10 µm thickness with partly 10 µm deep grain boundary penetration of oxygen, Fig. 22. The oxide scale grows by a factor of two after 2000 h. The grain boundary penetration of oxygen is enhanced to about 20 µm. The magnetite layer and a thin part of the spinel layer look like they start spall of partly. This may be as well caused by the preparation process.

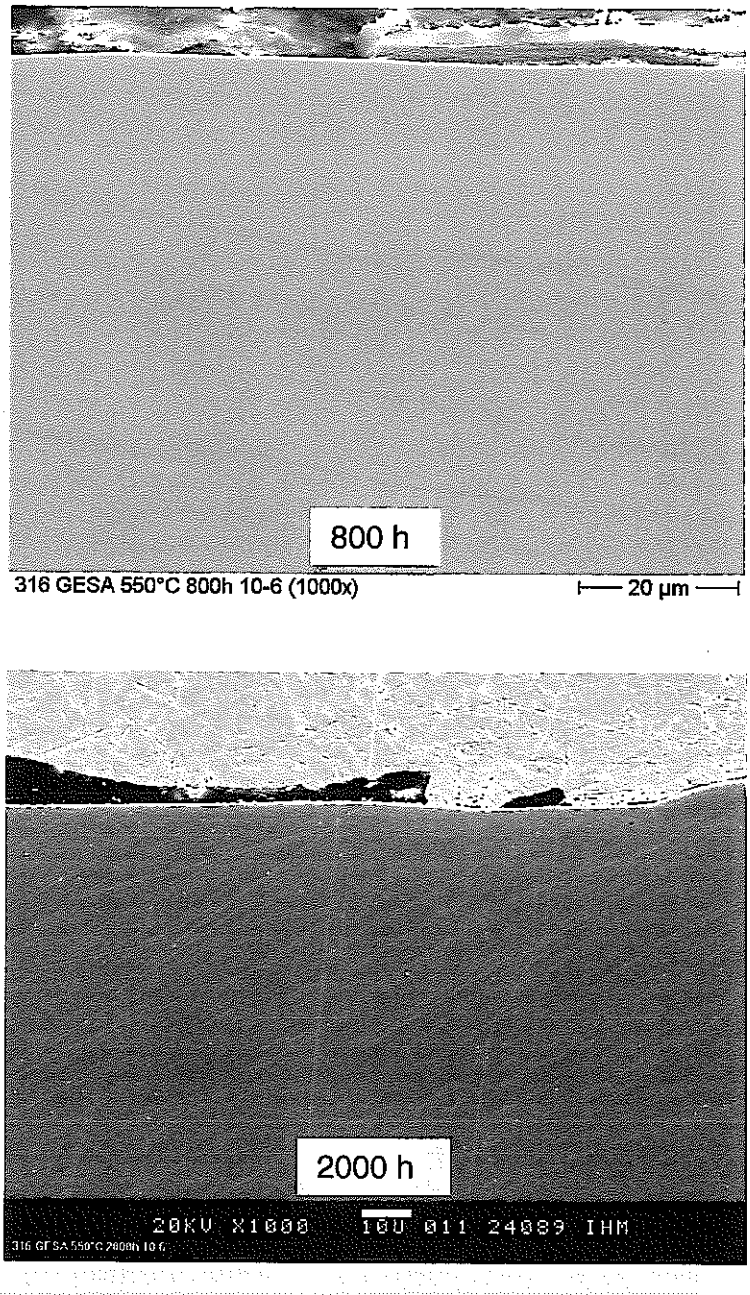

Fig. 23: 316FR GESA alloyed after 800 h and 2000 h at 550 °C

After 800 h and 2000h the GESA alloyed specimen have not any sign of attack, Fig. 23.

Temperature 600 °C

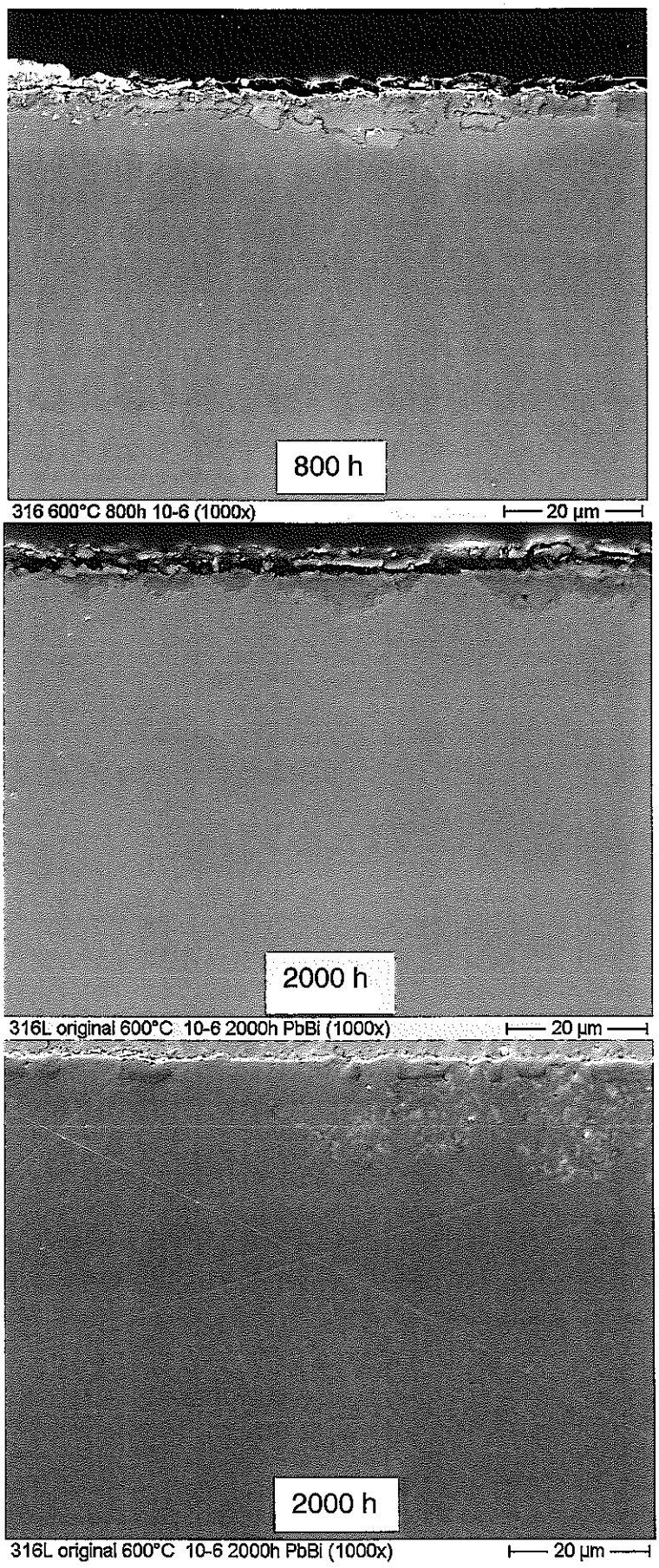

Fig. 24: 316FR original after 800 h and 2000 h at 600 °C

After 800 h at 600 °C the original specimen has no magnetite layer, Fig. 24. Pb/Bi penetrated into the spinel layer by dissolving and extracting Ni and precipitating Cr_2O_3 into a frame around the dissolution zones. Also after 2000 h the specimen has no magnetite layer. At few places corrosion with up to 20 µm deep penetration of Pb/Bi into the steel occurs. Most surface parts of the 2000 h sample look similar to those of the 800 h sample.

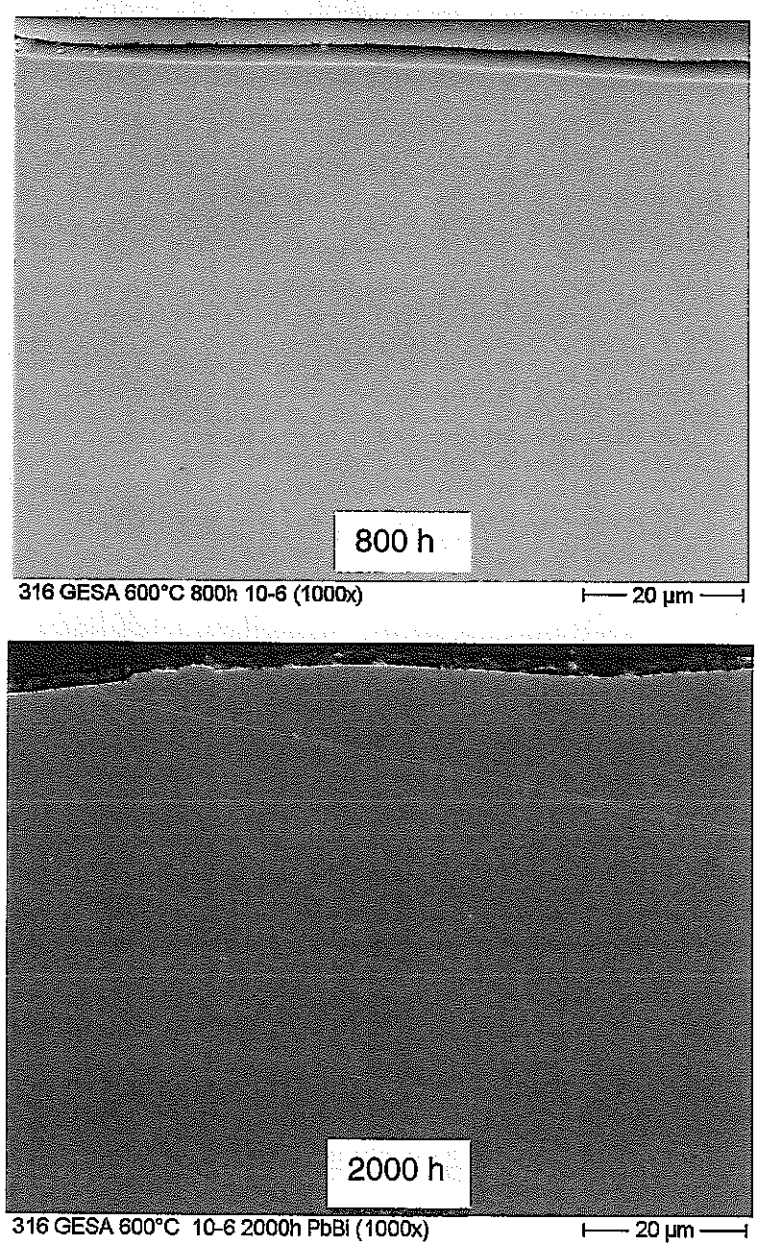

Fig. 25: 316FR GESA alloyed after 800 h and 2000 h at 600 °C

After 800 h and 2000 h the GESA alloyed specimen again shows no sign of reaction, Fig. 25.

Temperature 650 °C

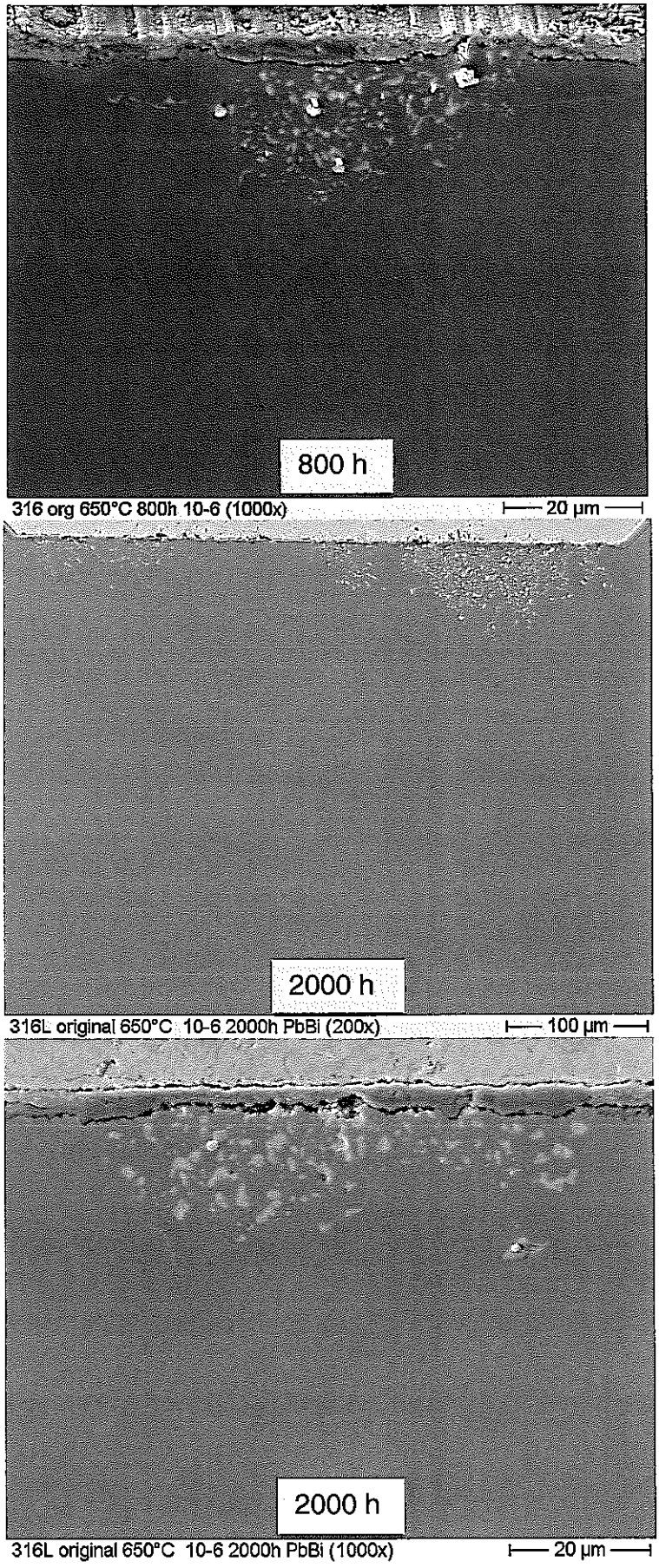

Fig. 26: 316FR original steel specimen after 800 h and 2000 h at 650 °C

The effect of dissolution and Cr_2O_3 precipitation observed for 600 °C after 800 h, Fig. 23, was enhanced at 650 °C after 800 h, Fig. 26. The spinel layer is partly penetrated by Pb/Bi leading to dissolution attack up to 30 µm deep along the grain boundaries. This process is enhanced after 2000 h. Dissolution attack up to 50 µm deep can be observed.

A GESA alloyed specimen was not tested.

5.2.2 ODS steel

Temperature 500 °C

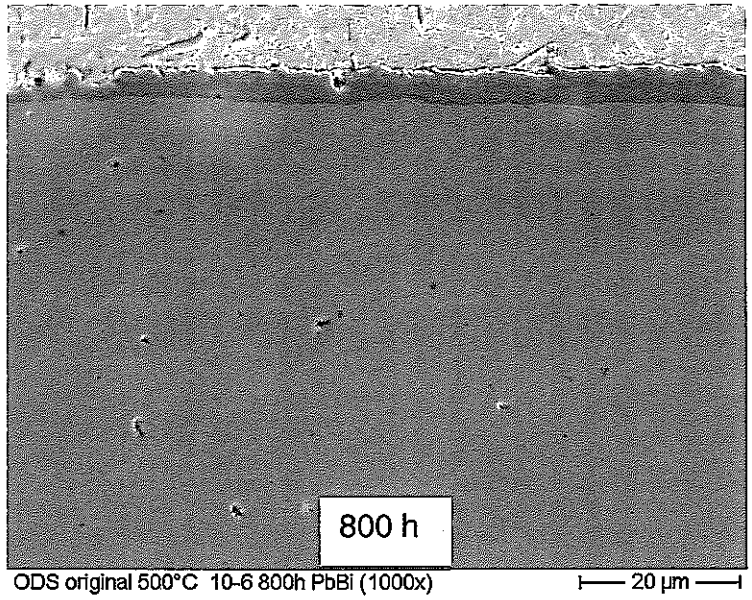

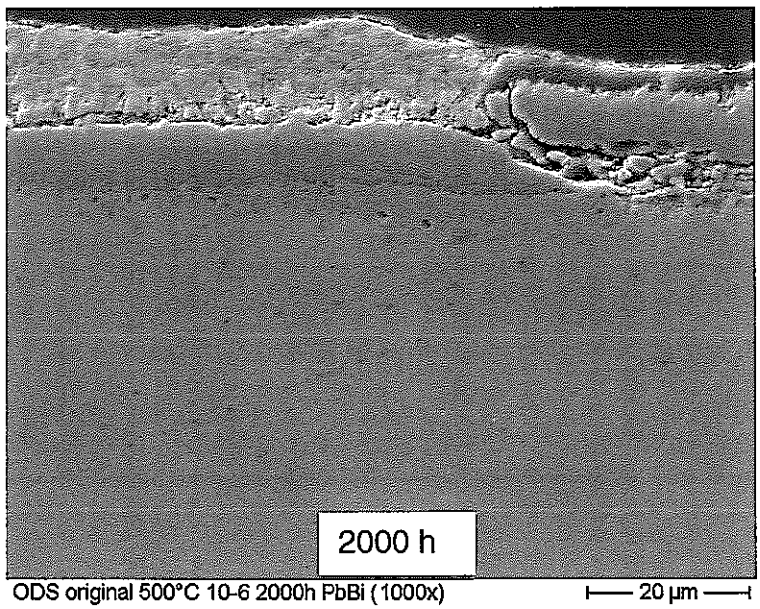

Fig. 27: ODS original steel specimen after 800 h and 2000 h at 500 °C

After 800 h the original specimen shows an oxide layer of 6-7 µm, typical for martensitic steels, Fig. 27. It has a magnetite on top of the spinel layer. At higher magnification one can see a diffusion layer below the spinel with oxygen penetration along the grain boundaries up to a depth of 2-3 µm. After 2000 h the oxide scale grows to about 15 µm having the same structure. The diffusion zone below the oxide scale

grows from 2-3 µm to 5 µm. The oxide scale seems again to spall of at about 1/3 of the specimen surface.

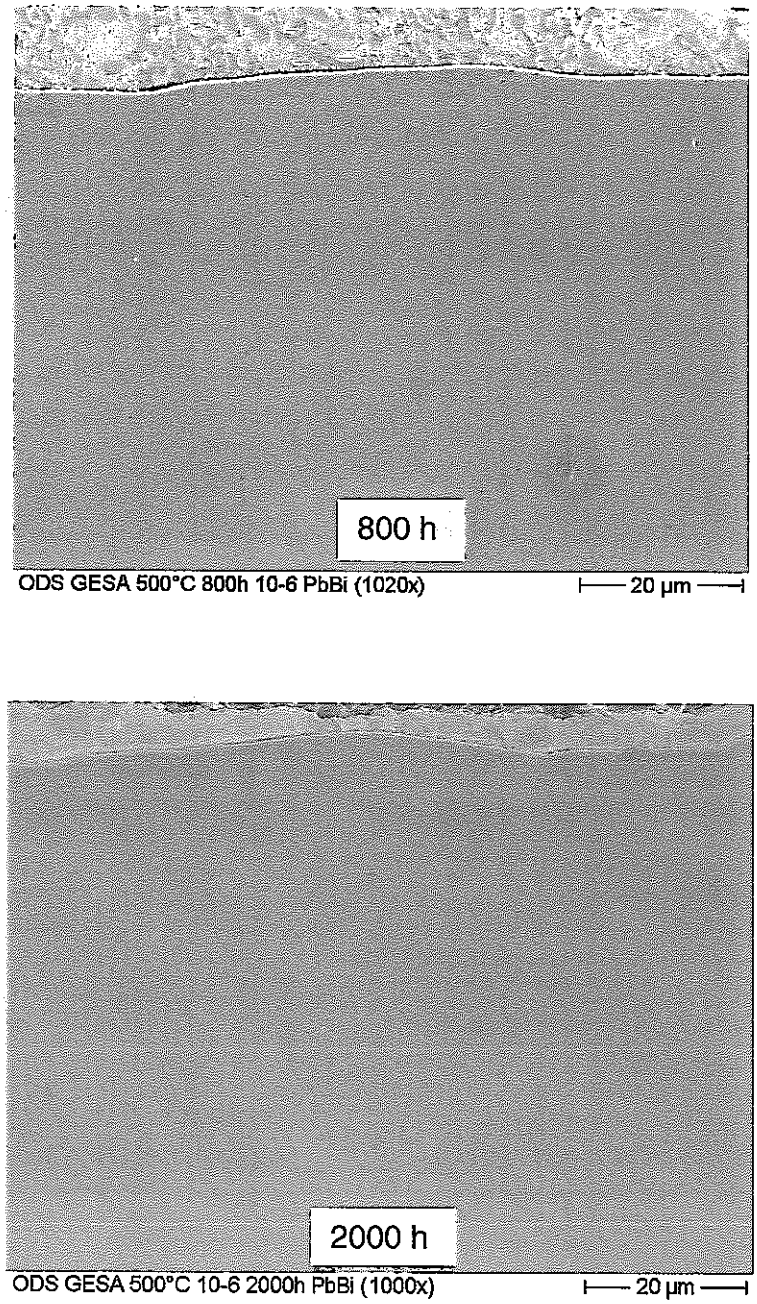

Fig. 28: ODS steel specimen GESA alloyed after 800 h and 2000 h at 500 °C.

The GESA alloyed specimen shows no sign of attack after 800 h and 2000 h, Fig. 28, right.

Temperature 550 °C

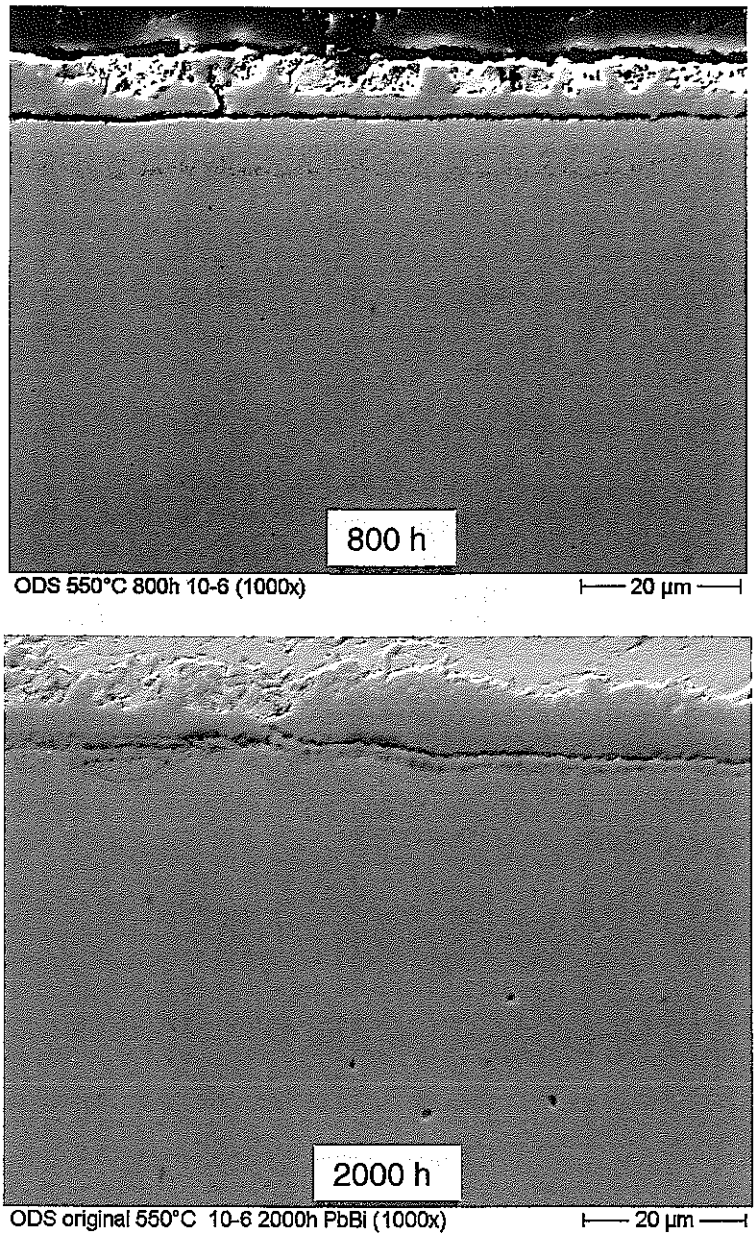

Fig. 29: ODS original steel specimen after 800 h and 2000 h at 550 °C

After 800 h the oxide layer of the original specimen has grown to 12 µm thickness, Fig. 29. Partly spallation of the magnetite layer is observed. The spinel layer is detached from the metal surface probably because of the preparation process on the whole surface indicated by a gap between the layer and base material. Oxygen penetrates the base material along grain boundaries down to a depth of 10 µm.
After 2000h growth of the oxide scale and penetration of oxygen along the grain boundaries, continues. Still no liquid metal corrosion can be observed.

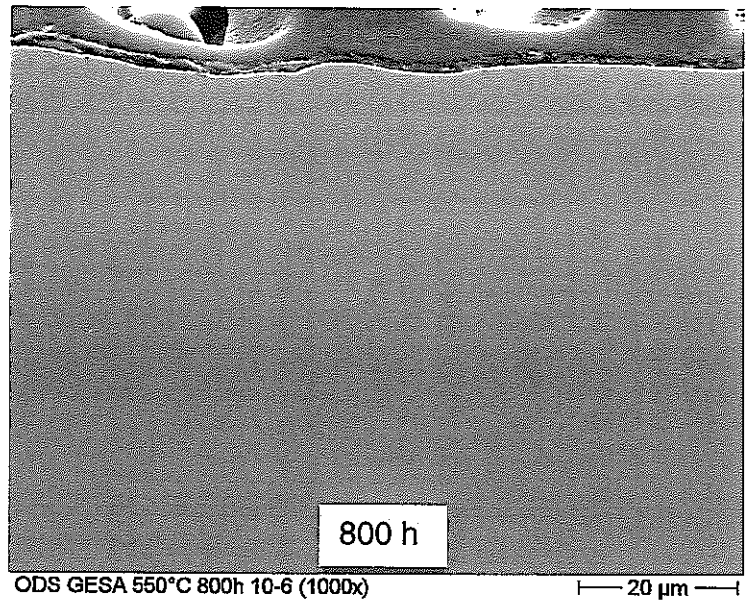

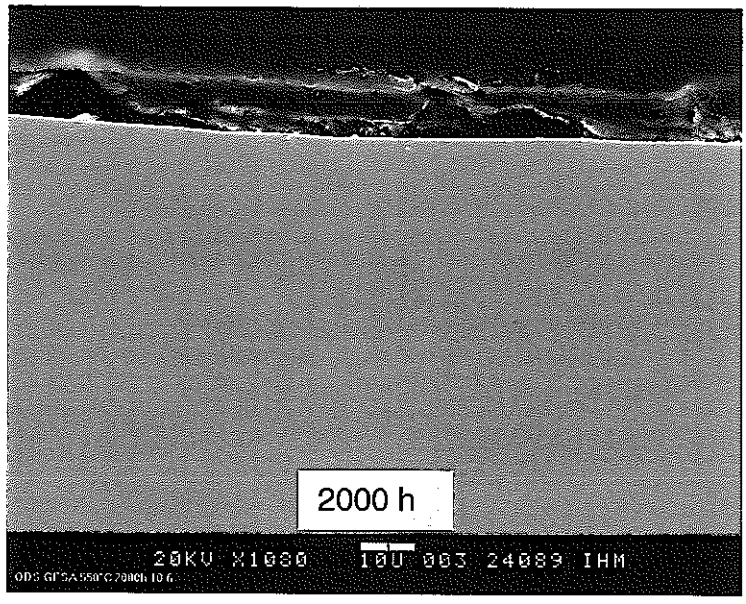

Fig. 30: ODS steel specimen GESA alloyed after 800 h and 2000 h at 550 °C

The GESA alloyed specimen shows no sign of attack after 800h and 2000 h, Fig. 30.

Temperature 600 °C

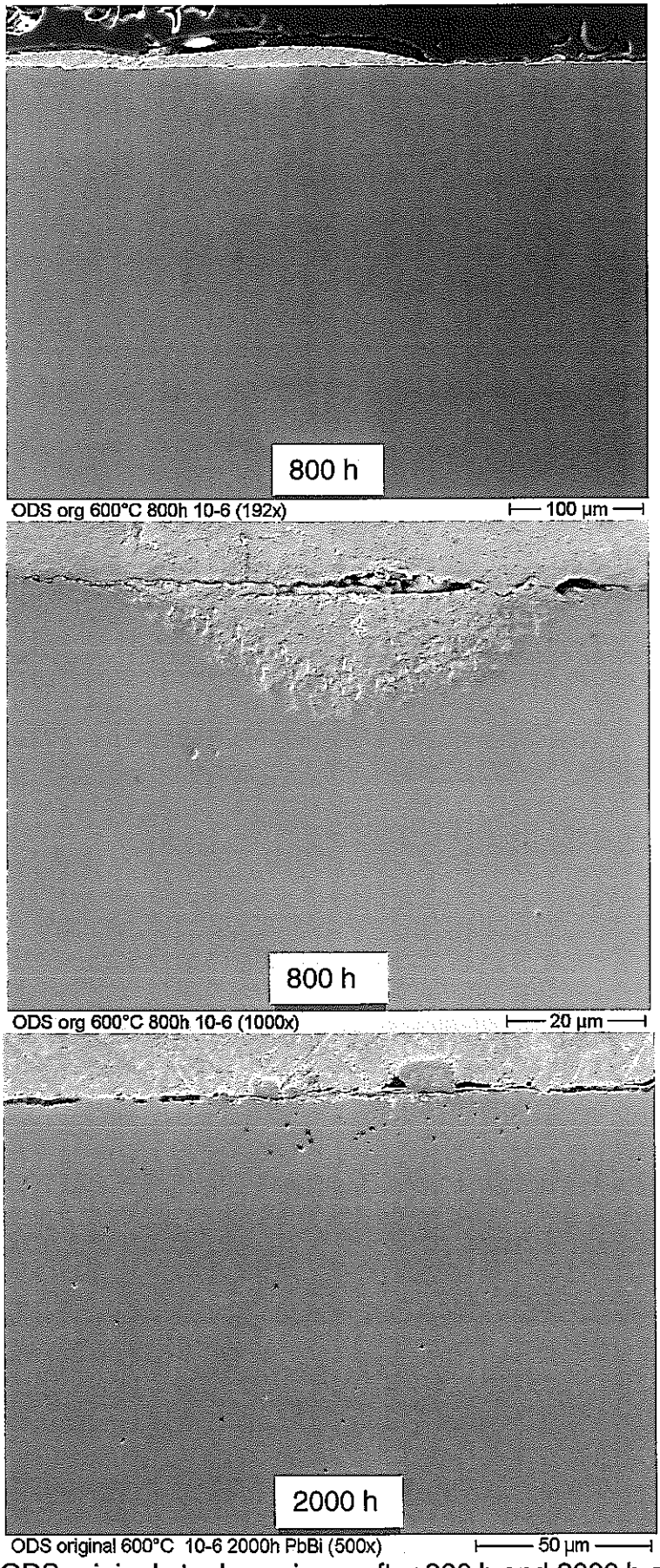

Fig. 31: ODS original steel specimen after 800 h and 2000 h at 600 °C

At 600 °C the oxidation behaviour changes dramatically. After 800 h the original specimen shows only at few singular spots a 20-30 µm deep dissolution attack, Fig. 31. The other part of the surface is protected by a thin spinel layer, which may have been weakened at the places of observed attack. This occurrence doesn't change after 2000 h. Below the attacked spots S und C containing precipitations can be seen.

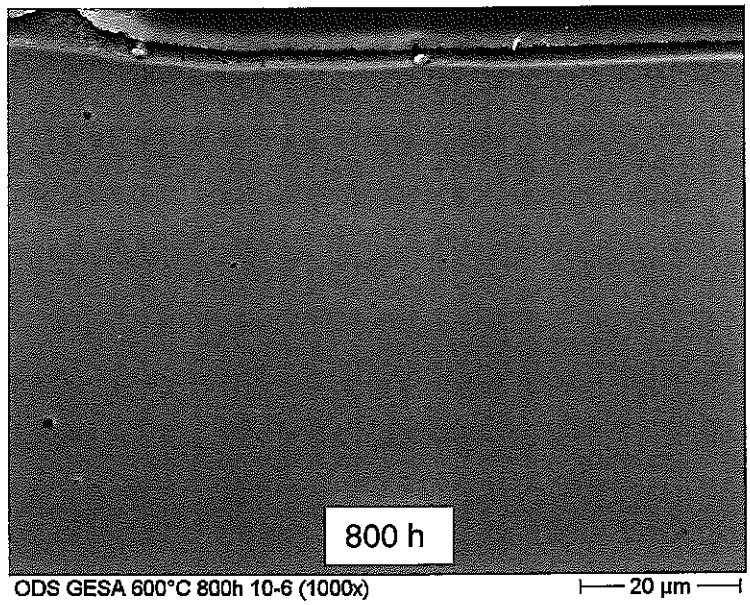

ODS GESA 600°C 800h 10-6 (1000x) — 20 µm — 32a

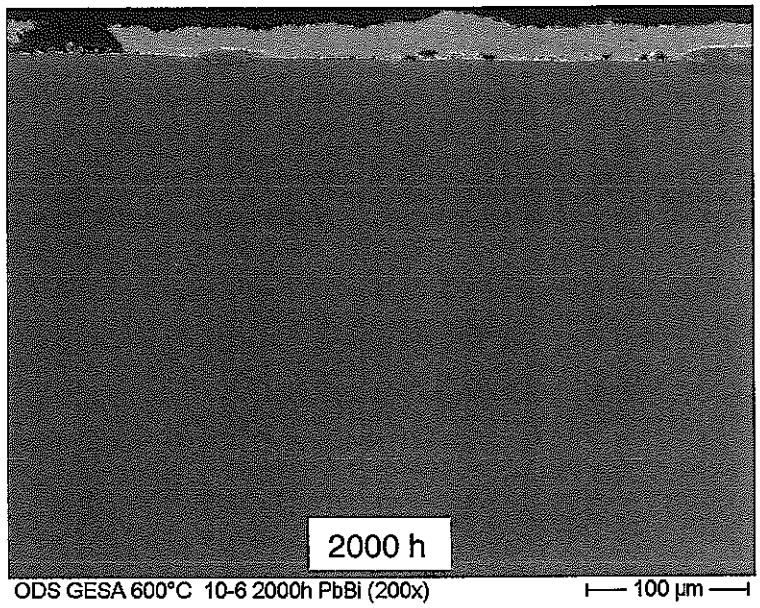

ODS GESA 600°C 10-6 2000h PbBi (200x) — 100 µm — 32b

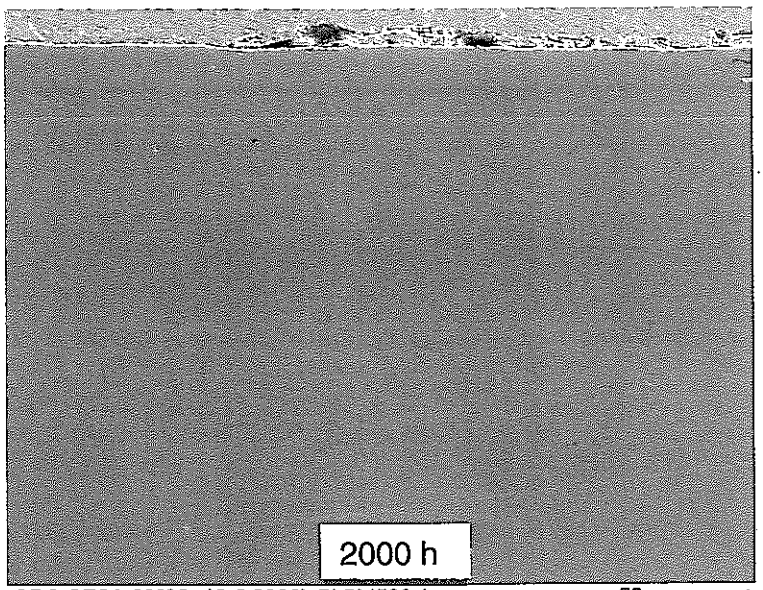

ODS GESA 600°C 10-6 2000h PbBi (500x) — 50 µm — 32c

Fig. 32: ODS steel specimen GESA alloyed after 800 h and 2000 h at 600 °C

The GESA alloyed specimen shows no sign of attack after 800 h, Fig. 32a. The 2000 h specimen shows same areas with 10 – 20 µm thick oxide scales, Fig. 32b. At this place the Al content in the surface layer is not sufficient to form alumina scales. Nevertheless most parts of the surface show no sign of corrosion and oxidation, Fig. 32c.

Temperature 650 °C

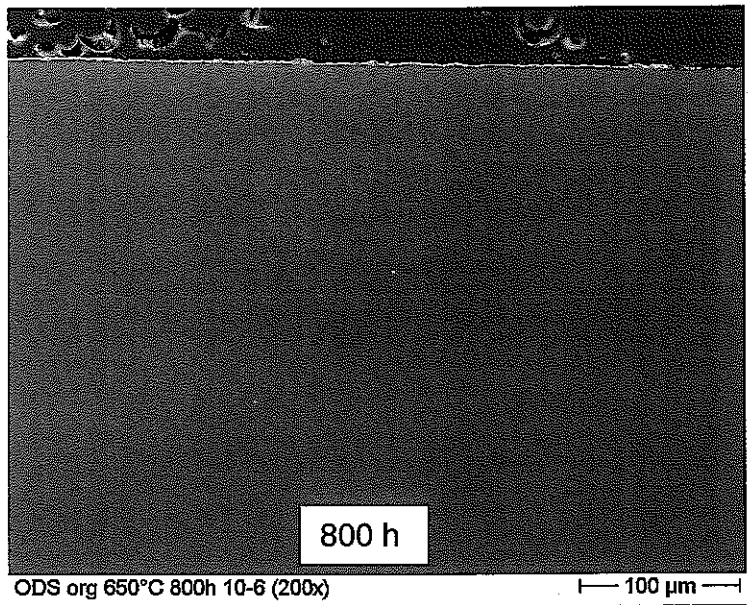

33a

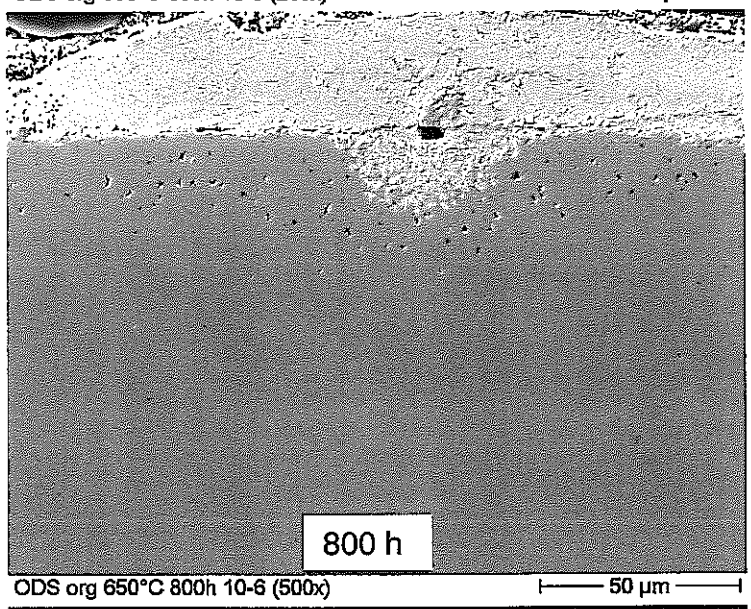

33b

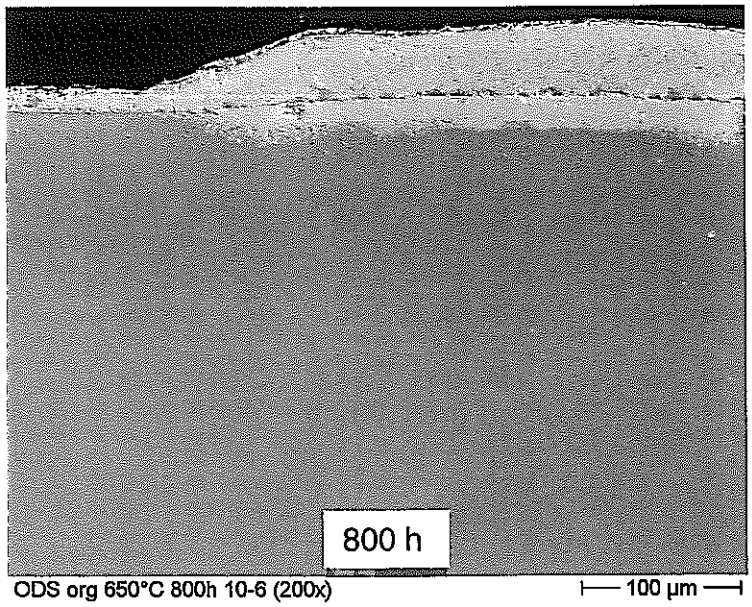

33c

Fig. 33a-c: ODS original steel after 800 h at 650 °C

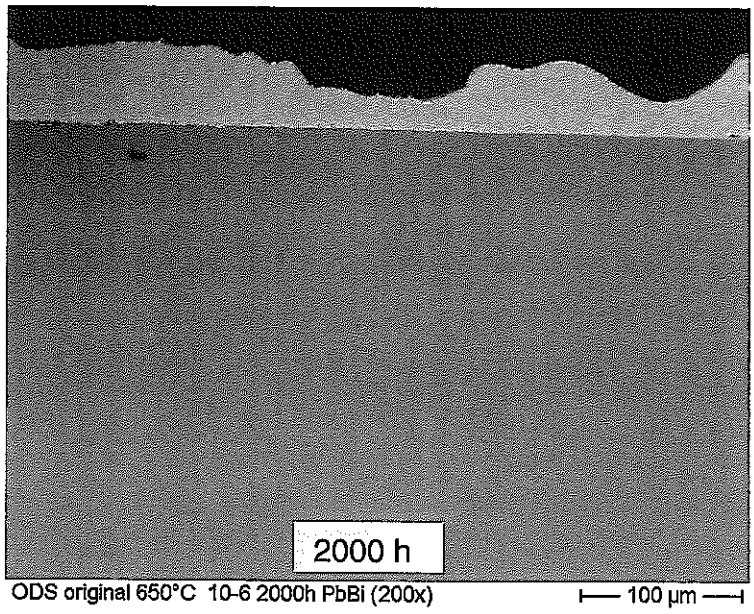

Fig. 33d

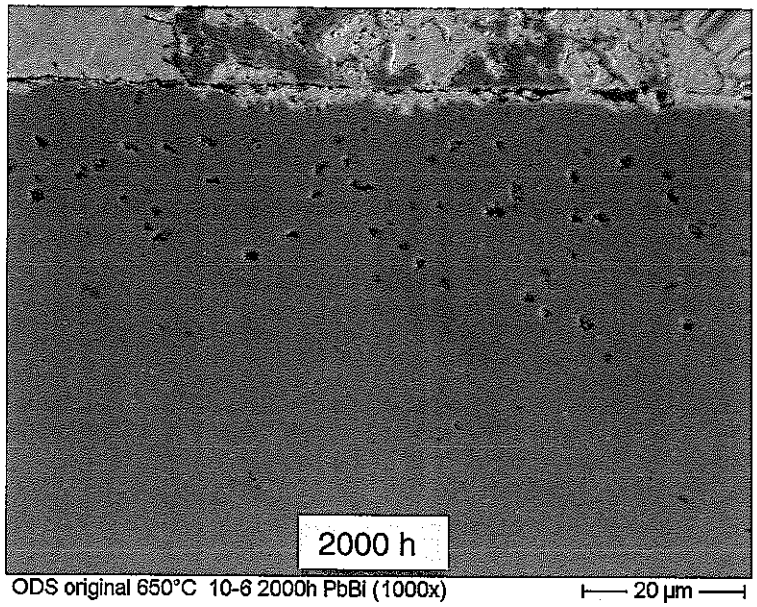

Fig. 33e

Fig. 33d-e: ODS original steel specimen after 2000 h at 650 °C

After 800 h and 2000h most of the surface of the original specimen is protected by a thin spinel layer and therefore shows no attack, Fig. 33a, d. At singular points there appears a dissolution attack, Fig. 33b, 33c, 33e. Above the dissolution zone there is a thin layer with Cr_2O_3 precipitations. The reason for destruction of the protective spinel layer is the presence of sulfur impurities (dark inclusions below the dissolution zone) which attract Cr and therefore weaken the self-healing function of the spinel layer (Sulfur impurities in steel have to be avoided!).

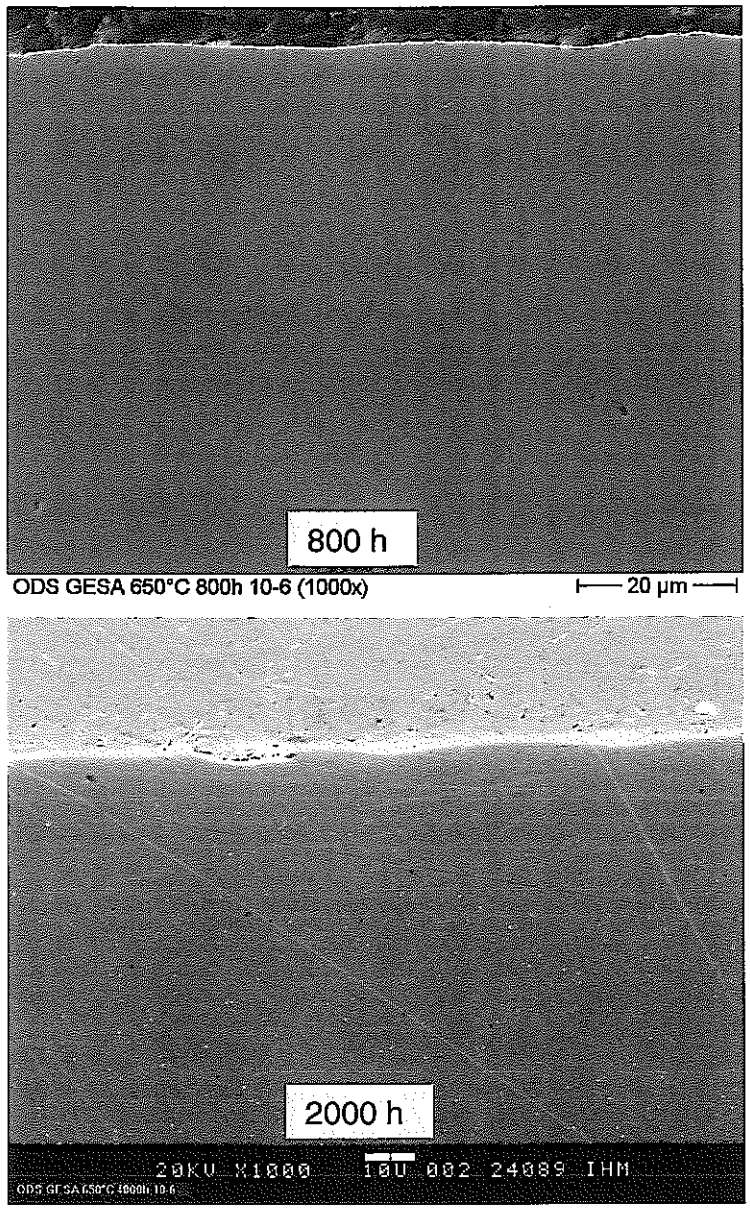

Fig. 34: ODS steel specimen GESA alloyed after 800 h and 2000 h at 650 °C

The GESA alloyed specimen shows no signs of attack after 800 h and 2000 h, Fig 34.

5.2.3 P122 steel

Temperature 500 °C

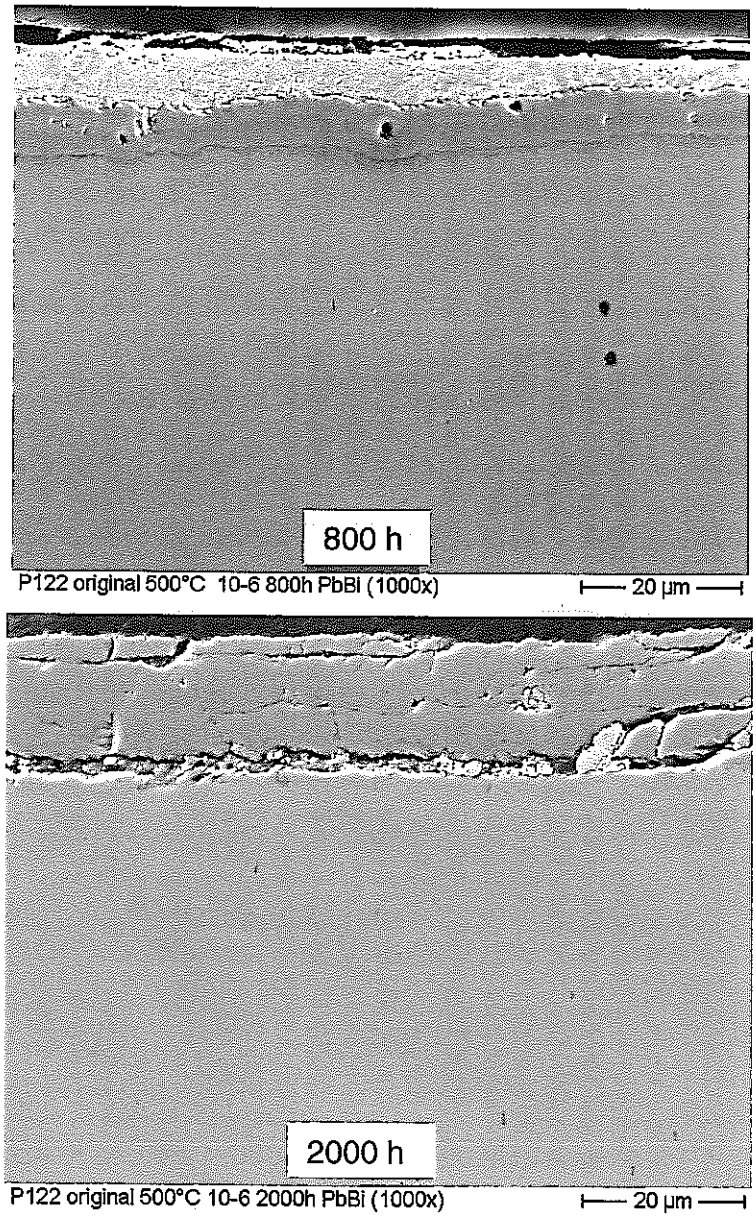

Fig. 35: P122 steel original after 800 h and 2000 h at 500 °C

The behavior of the original specimen is comparable with that of the ODS steel. After 800 h the magnetite + spinel layer is 8 µm thick. The only difference is an enrichment of Cr together with Cu (2 wt%) at the interface between spinel and base material. It is represented by the small band darker than the surrounding in Fig. 35. After 2000h the oxide scale grows to 15 µm thickness and detaches possibly during preparation spalls at most parts of the specimen.

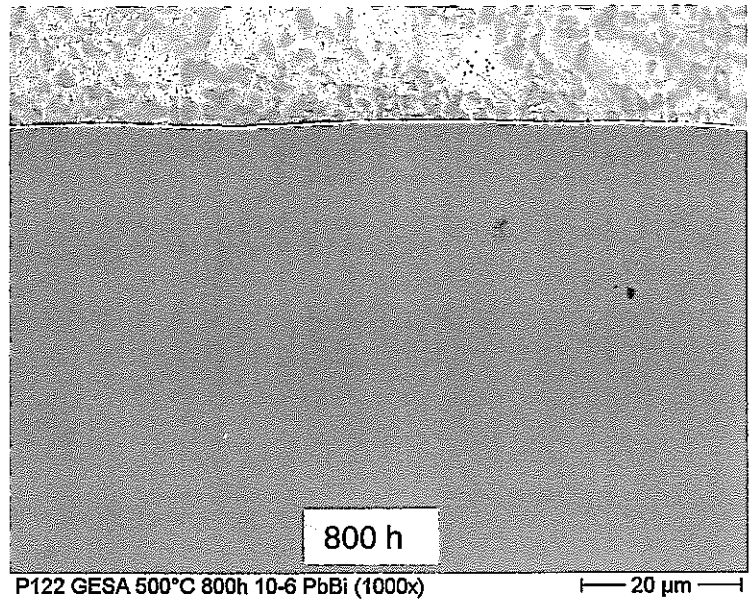

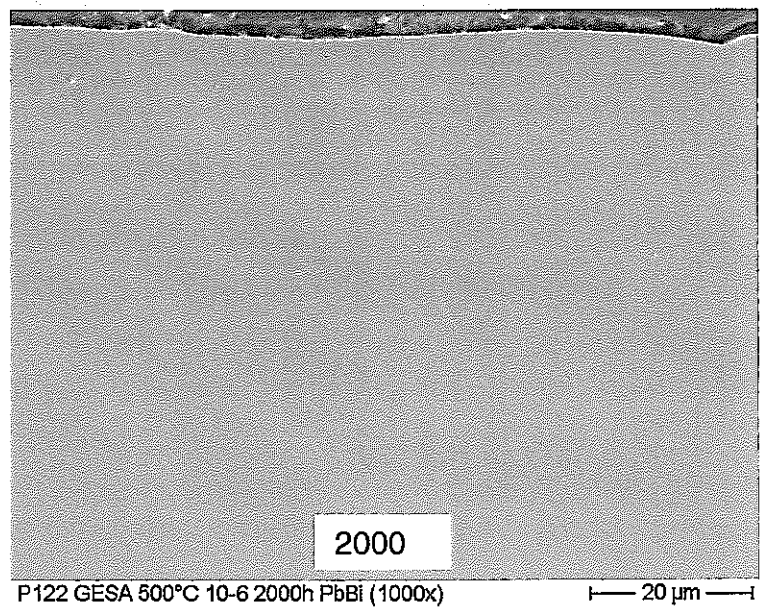

Fig. 36: P122 steel GESA alloyed after 800 h and 2000 h at 500 °C

The GESA alloyed specimen was not attacked after 800 h and 2000 h , Fig. 36.

Temperature 550 °C

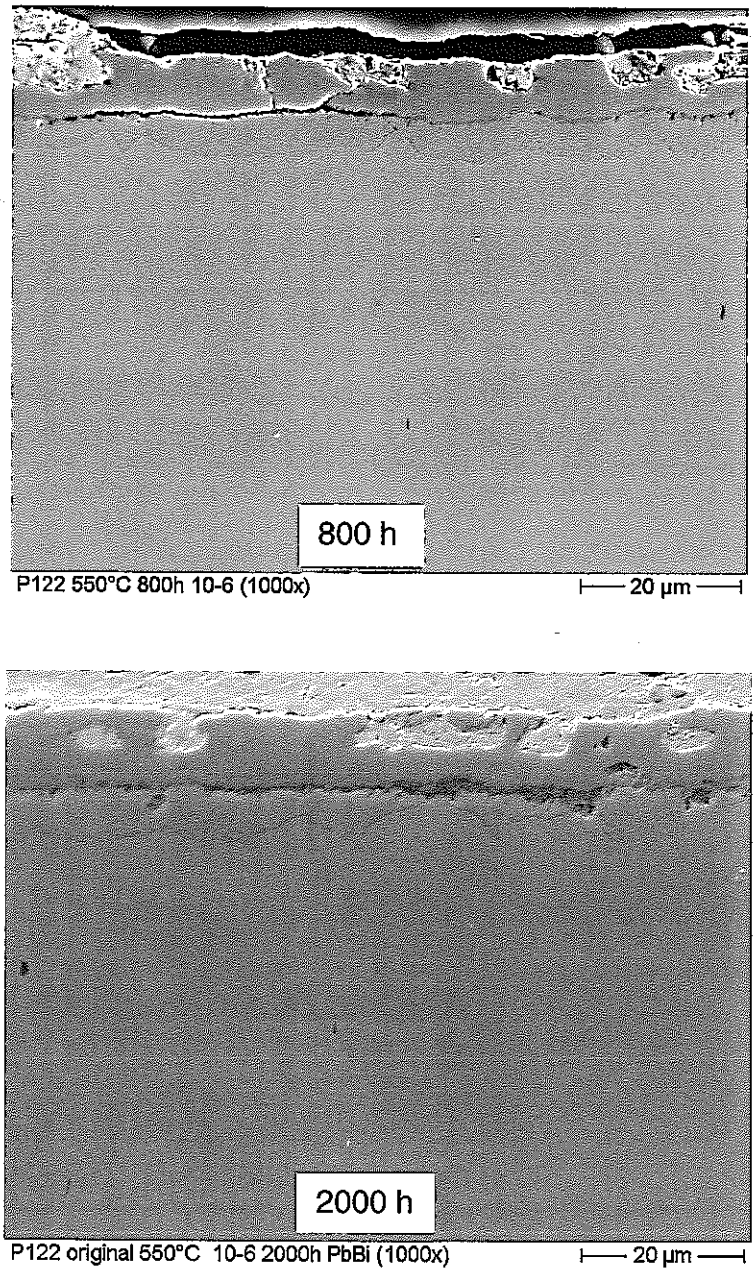

Fig. 37: P122 steel original after 800 h and 2000 h at 550 °C

After 800 h the oxide layer has the same appearance like that at 500 °C with a thickness of about 10 µm, Fig. 37. The diffusion zone below the scale grows to about 8 µm. After 2000 h the structure of the oxide layer is the same like after 800 h, just thicker.

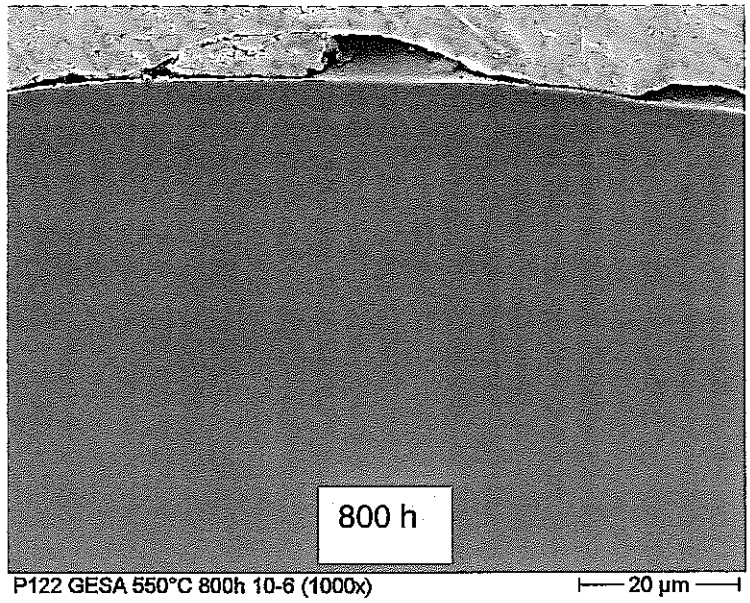

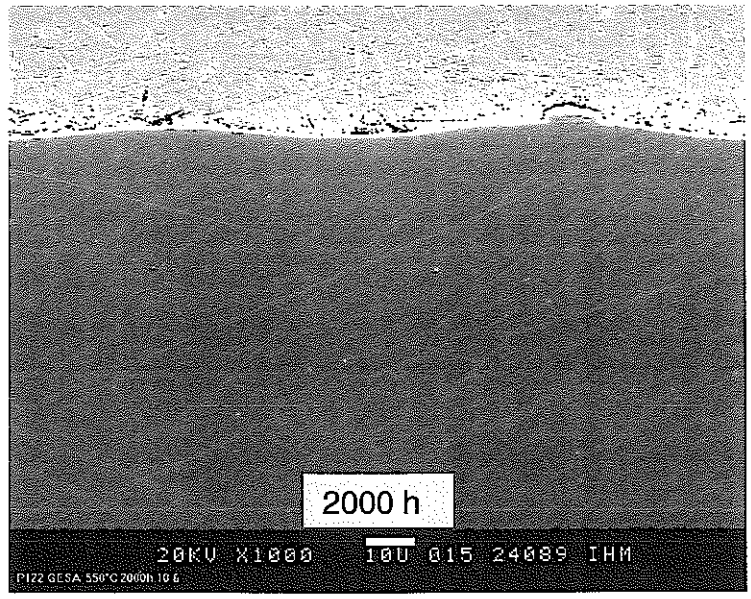

Fig. 38: P122 steel GESA alloyed after 800 h and 2000 h at 550 °C

The GESA alloyed specimen was not attacked after 800 h and 2000 h , Fig. 38.

Temperature 600 °C

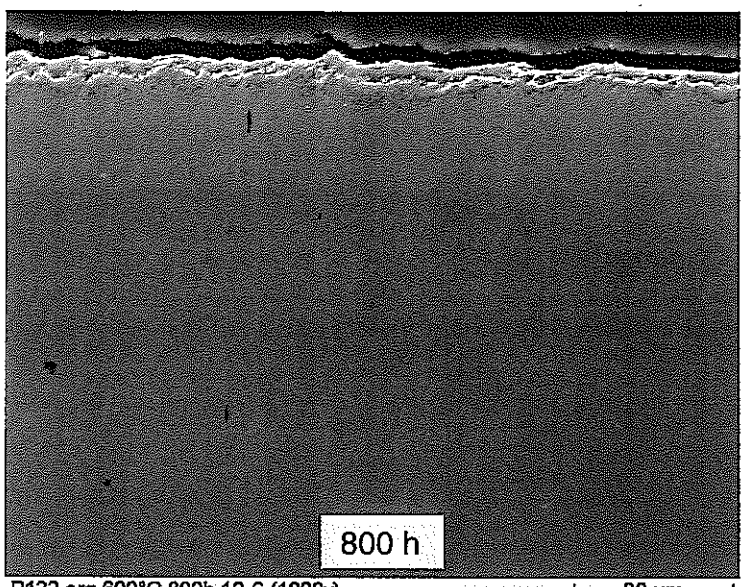

Fig. 39a

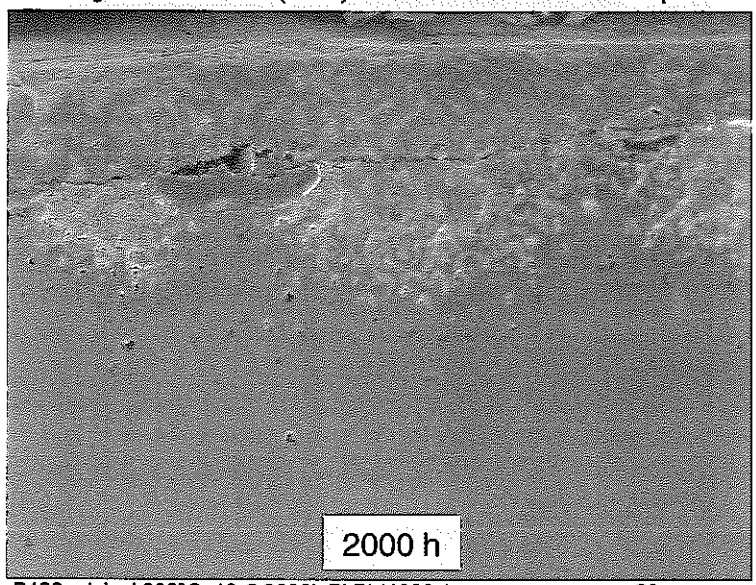

Fig. 39b

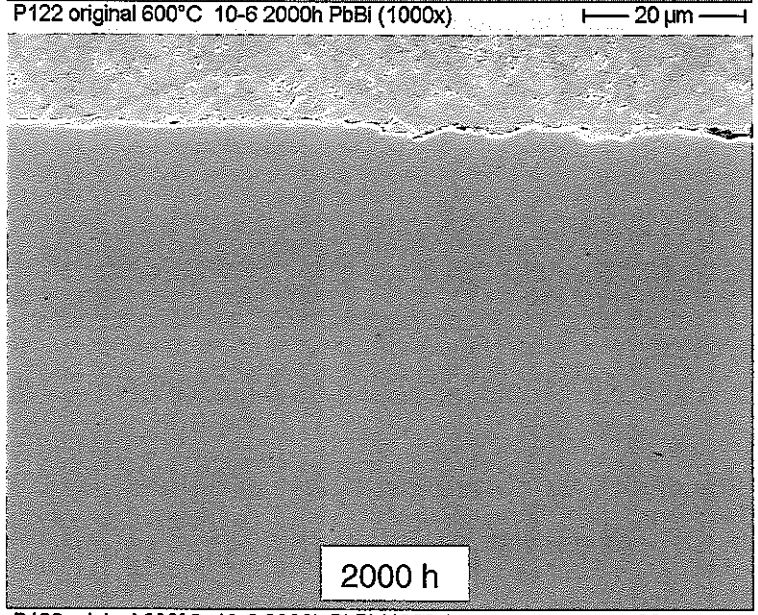

Fig. 39c

Fig. 39: P122 steel original after 800 h and 2000 h at 600 °C

As opposed to lower temperatures no magnetite layer could be observed after 800 h at 600 °C on the original specimen, Fig. 39. Furthermore, the spinel layer is much richer in Cr with a Cr/Fe ratio of 1. After 2000 h the dissolution attack starts at few spots, Fig. 39b. Below these spots S und C containing precipitations can be seen. 20 µm deep penetration of Pb/Bi can be observed. Most parts of the sample surface are still protected by the spinel layer, Fig. 39c.

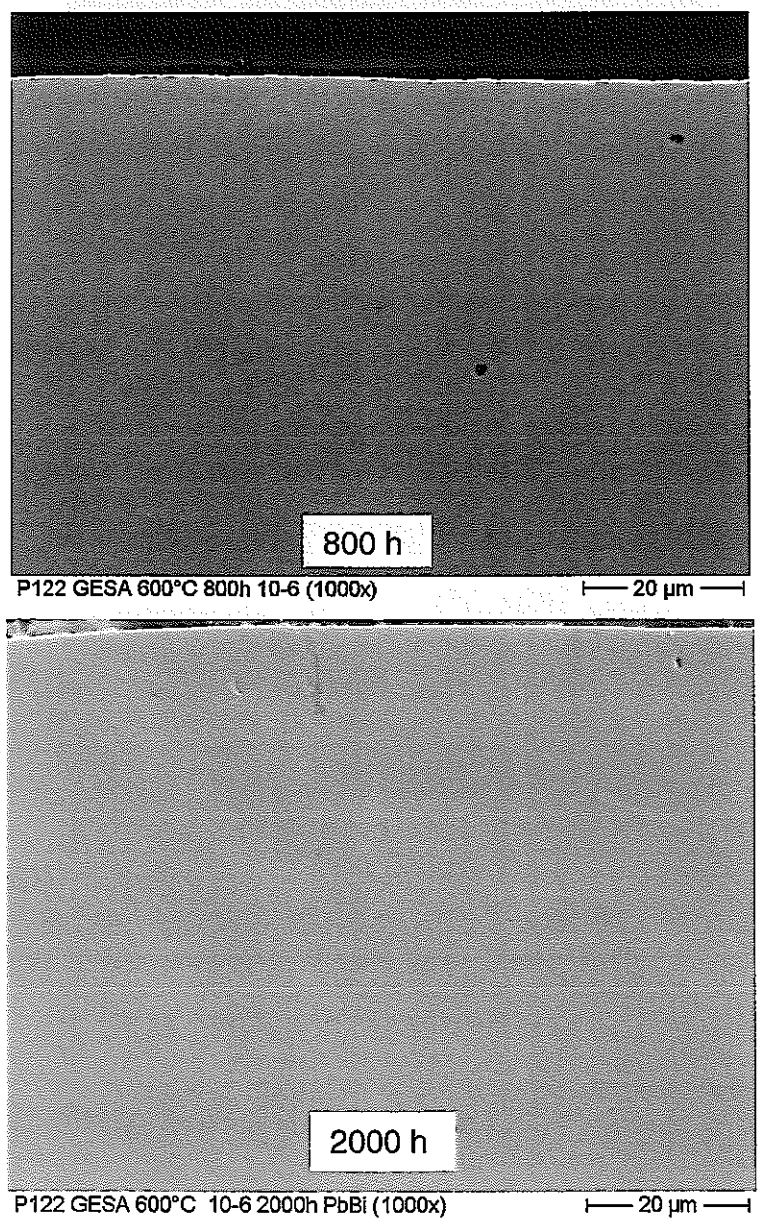

Fig. 40: P122 steel GESA alloyed after 800 h and 2000 h at 600 °C

The GESA alloyed specimen was not attacked after 800 h and 2000 h. Only a few microcracks filled with Cr-Al oxides can be detected.

Temperature 650 °C

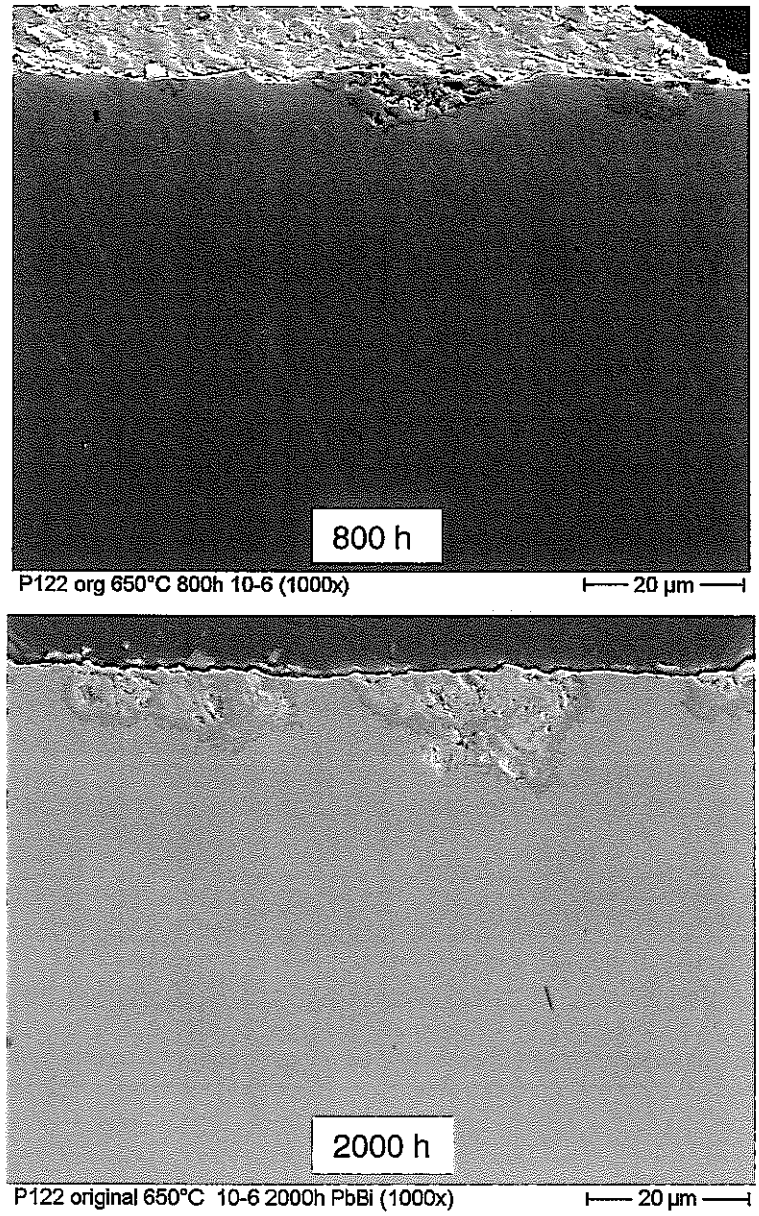

Fig. 41: P122 steel original after 800 h and 2000 h at 650 °C

After 800 h most of the surface is covered by a thin protective spinel layer which is not visible at Fig. 41. There are, however, some spinel nests (see Fig. 41) into which Pb/Bi penetrates and dissolves Cr. They are, therefore, depleted in Cr, which may expected to lead to dissolution of steel components later on. After 2000 h the spinel nests grow by a factor 2. Pb/Bi penetrates into these nests to a depth of 15 µm.
No GESA alloyed P122 specimen was tested at 650 °C.

5.3 X-ray diffractometry of samples exposed to liquid Pb/Bi

5.3.1 316FR

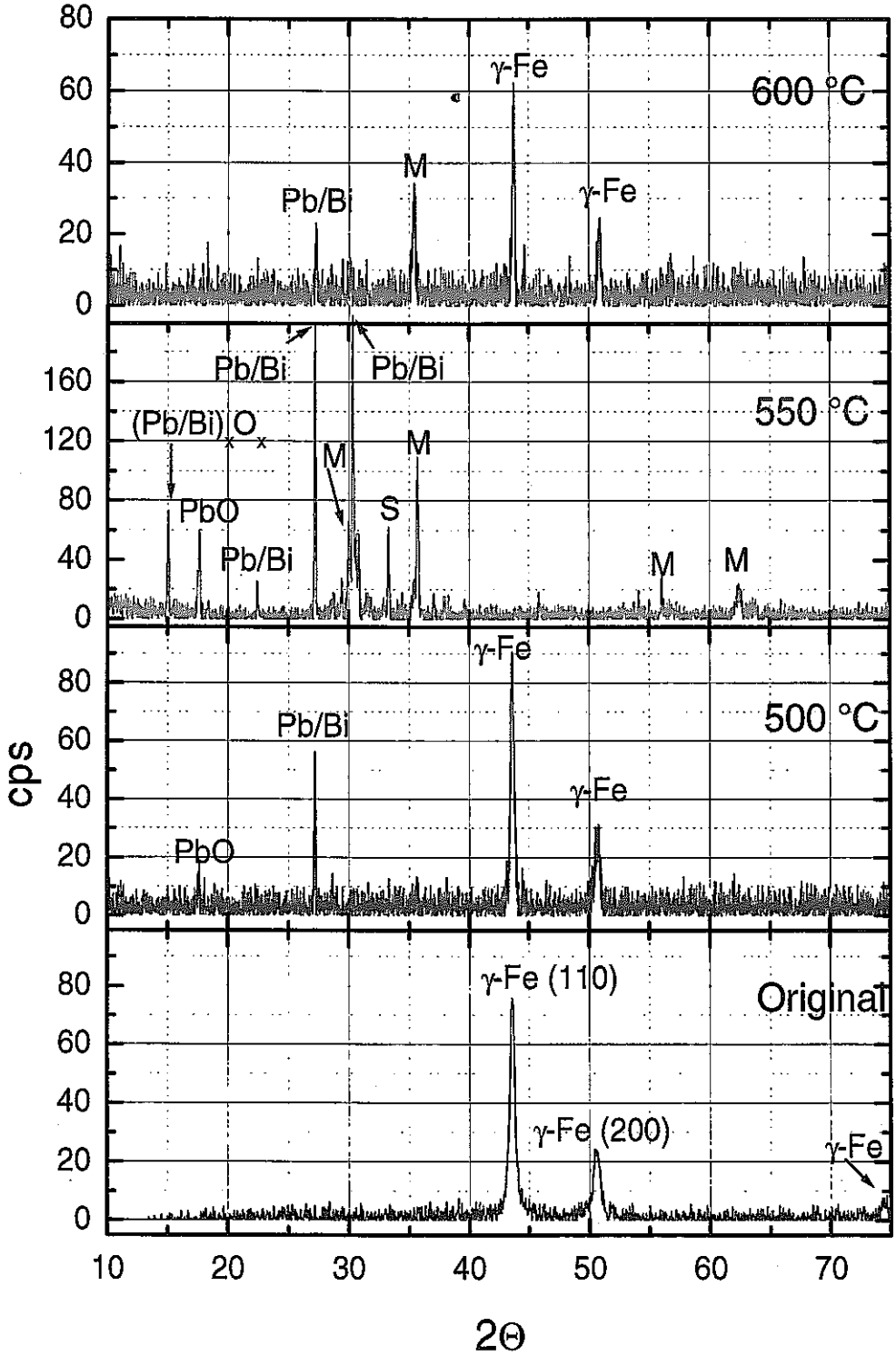

Fig. 42: XRD pattern of 316FR after 800 h

In Fig. 42 we see the XRD pattern for 316FR in original state and after exposure to Pb/Bi at 500, 550 and 600 °C for 800 h. At 500 °C no oxide peaks are detectable with

the exception of PbO. There is some Pb/B remaining on the surface after the cleaning process. Small part of it is oxidized. The γ-Fe peaks of steel are still present of the same magnitude as in starting material.
At 550 °C the steel peaks disappear entirely. Dominating peaks are those of magnetite (M) and spinel (S), $(Fe_{0.6}\ Cr_{0.4})_2O_3$. Again peaks of remaining Pb/B, PbO appear.
At 600 °C behaviour changes again. The γ-Fe peaks of steel are present. Only small amount of magnetite appears and again small Pb/Bi impurities.
The absence of oxide peaks at 500 and 600 °C indicates that there is a very thin protective oxide scale at the surface which protected the steel from dissolution attack (see cross section in 5.2.1).

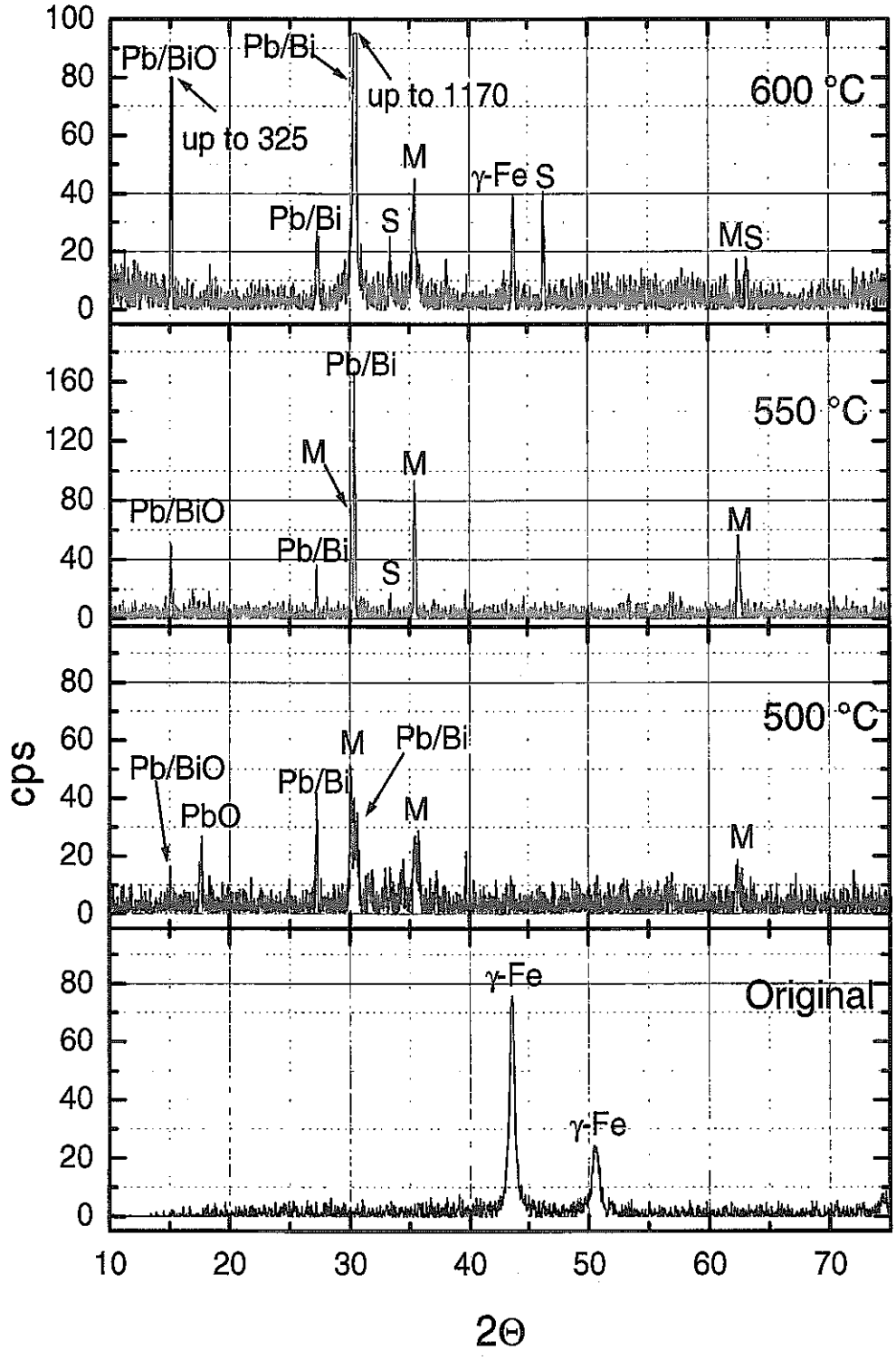

Fig. 43: XRD pattern of 316FR after 2000 h

Fig. 43 shows the XRD patterns after 2000 h. After this time the γ-Fe peaks disappear already at 500 °C. Only magnetite is detectable on the surface and some impurities of Pb/Bi and its oxides.
At 550 °C again only magnetite is visible besides small indications of spinel and some Pb/Bi impurities.
At 600 °C spinel is visible together with γ-Fe and minor magnetite peaks and Pb/Bi and its oxides.

5.3.2 ODS

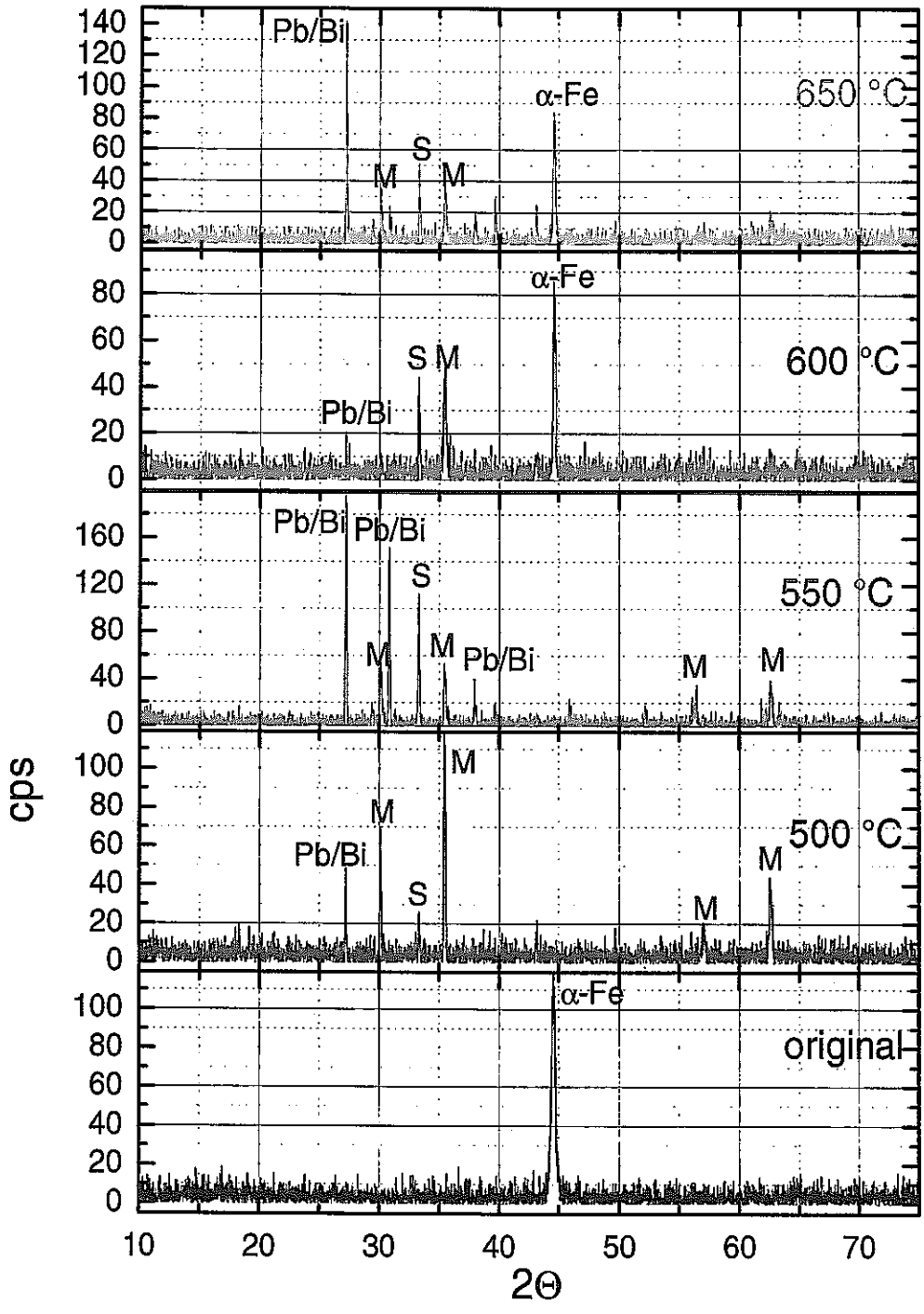

Fig. 44: XRD pattern of ODS after 800 h

Already at 500 °C, Fig. 44, the metal peaks disappear completely. The peaks of magnetite dominating.
At 550 °C the spinel peak dominates the smaller magnetite peaks.
At 600 and 650 °C the α-Fe peaks appear again and only small peaks of spinel and magnetite are visible.

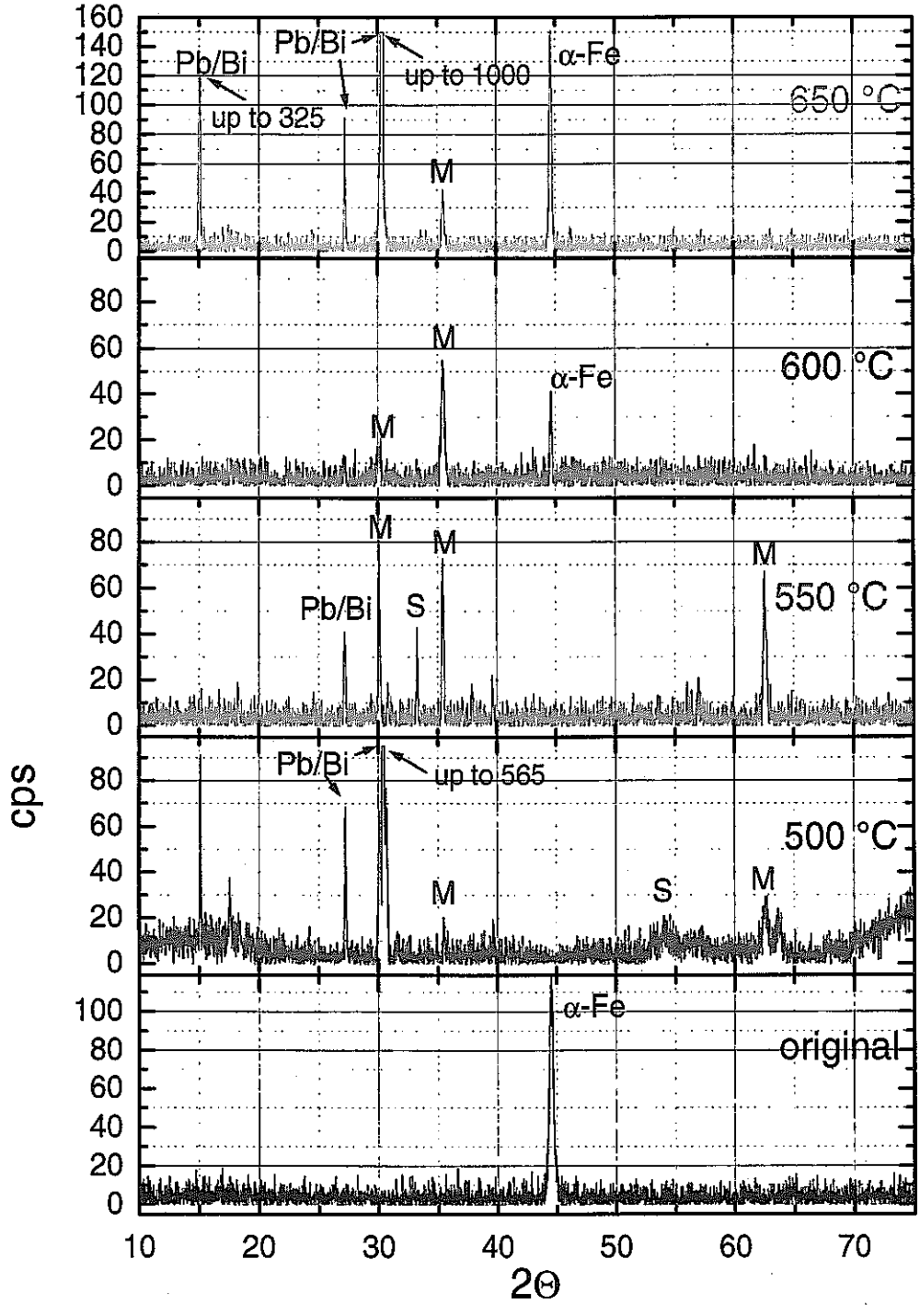

Fig. 45: XRD pattern of ODS after 2000 h

After 2000 h nothing changed as compared to 800 h.

5.3.3 P 122

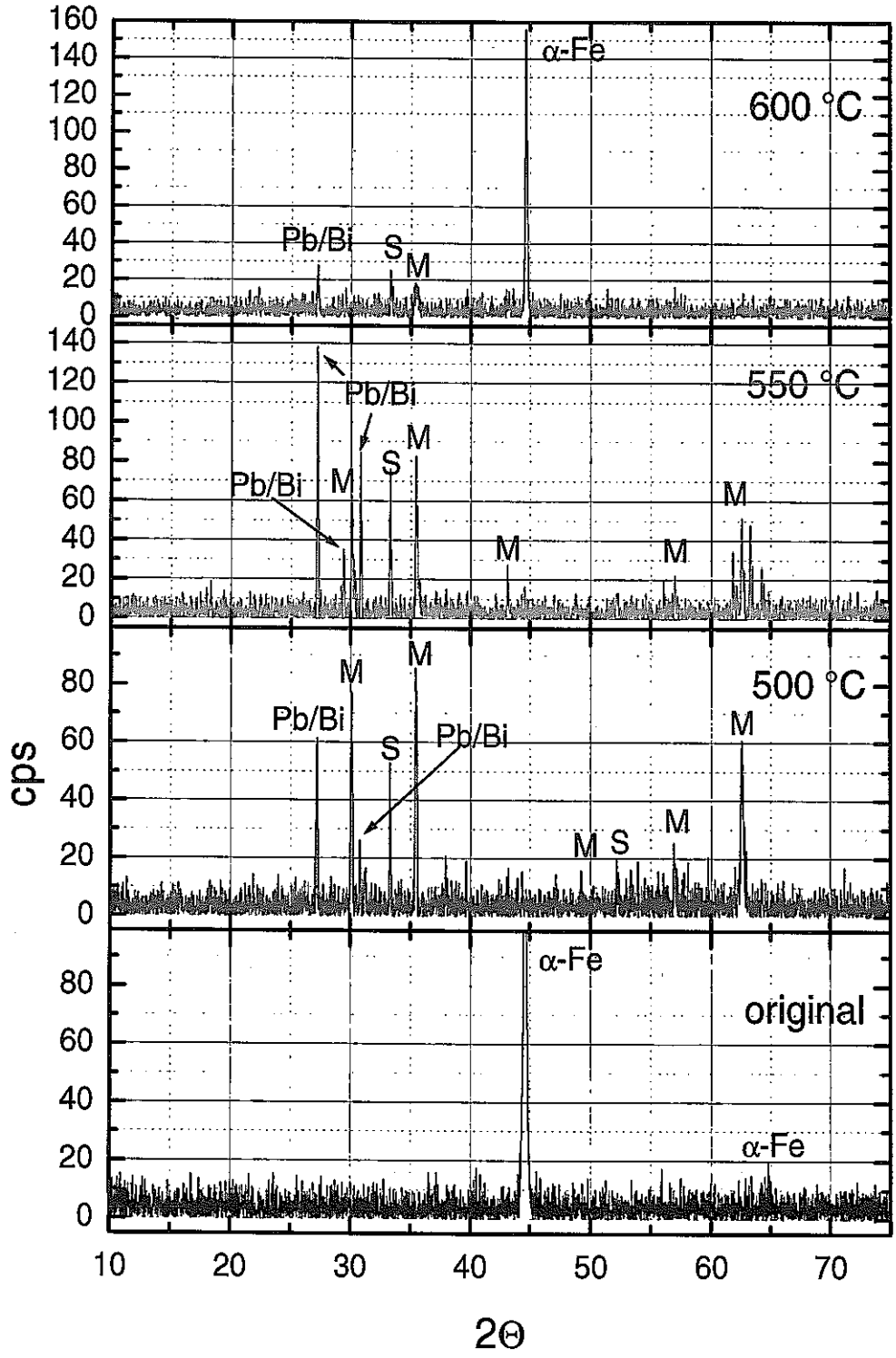

Fig. 46: XRD pattern of P122 after 800 h

At the lower temperatures, 500 and 550 °C, the metal peaks disappeared, Fig. 46, and only spinel and magnetite peaks are present. At 600 °C the oxide peaks are diminished and α-Fe peaks dominate.

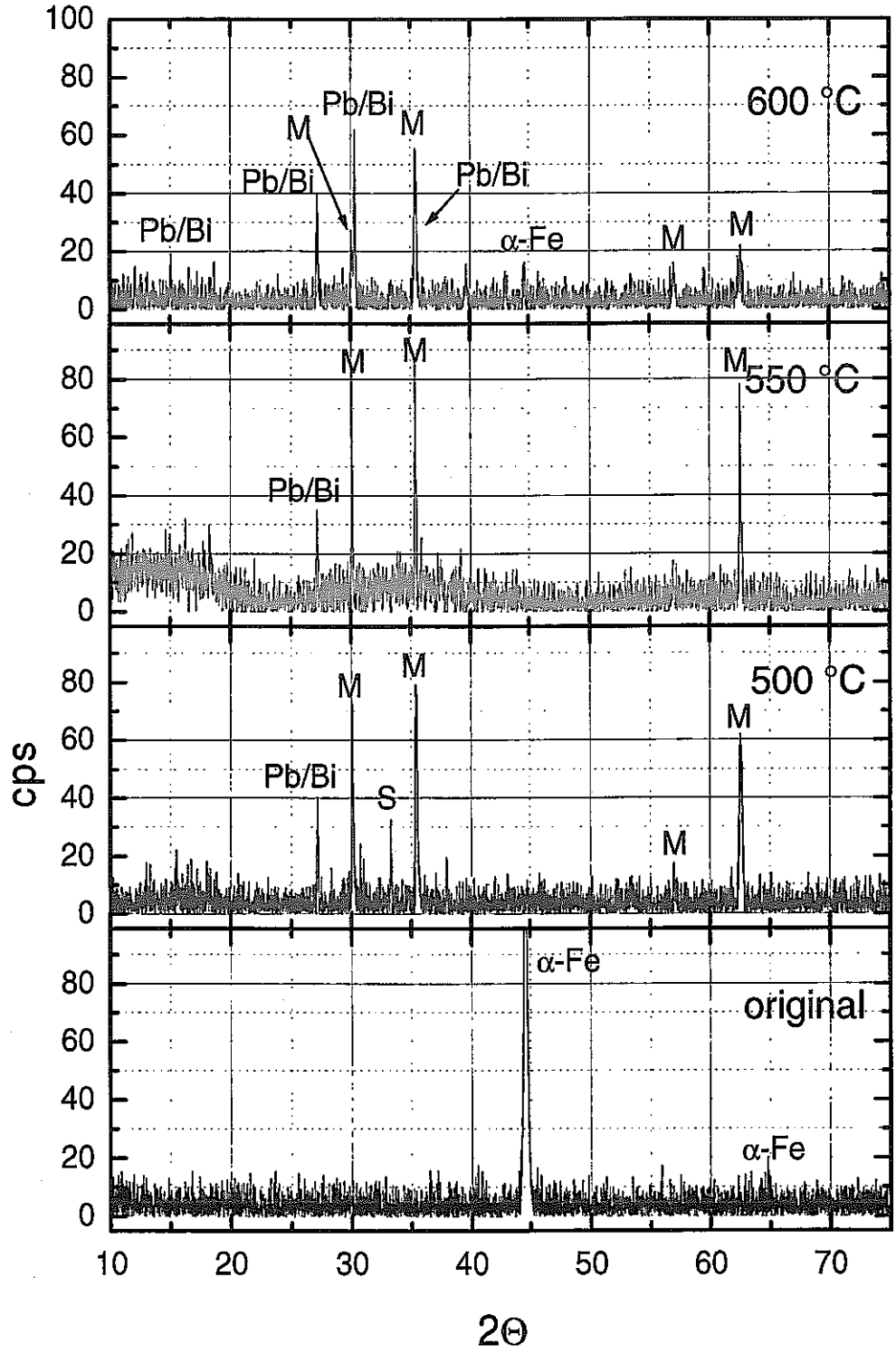

Fig. 47: XRD pattern of P122 after 2000 h

After 2000 h, Fig. 47, the oxide layer of magnetite appears to be thick with diminishing spinel part. At 600 °C small magnetite peaks are visible without spinel. The α-Fe peak is only marginal. This, however, does not agree with the observations obtained from the cross sections.

5.4 Steels in gas atmosphere of the COSTA facilities after 800 h

5.4.1 316FR

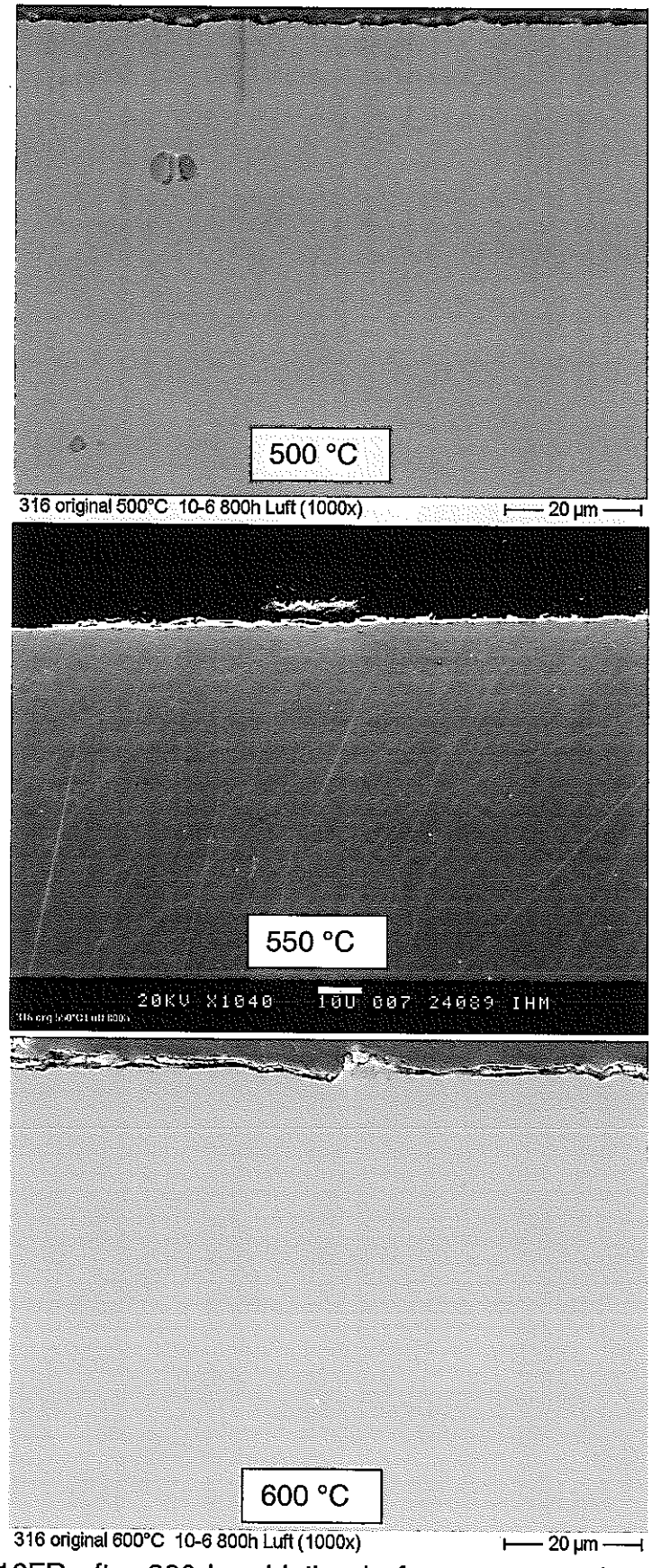

Fig. 48a-c: 316FR after 800 h oxidation in furnace atmosphere at 500 (a), 550(b) and 600 °C(c).

No oxide scales are visible in the cross sections at 500, 550 and 600 °C. They must be very thin.

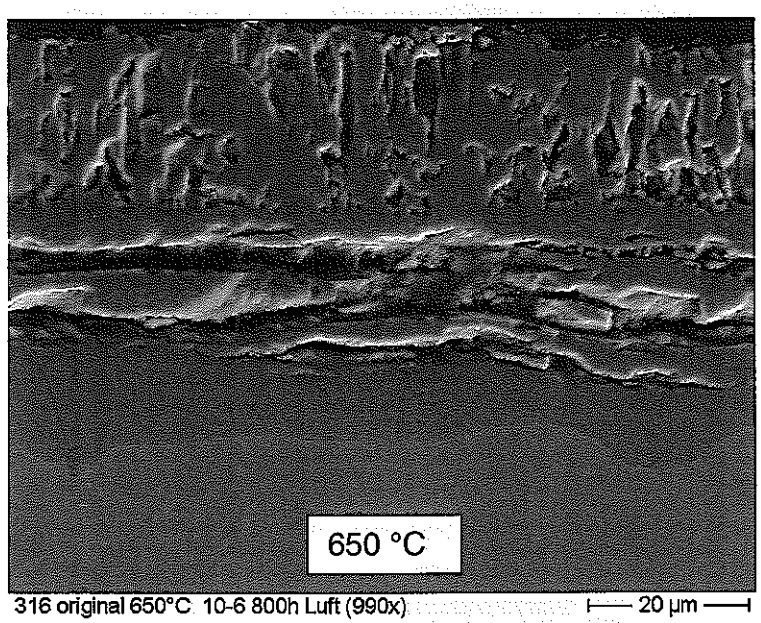

Fig. 49: 316FR after 800 h oxidation in furnace atmosphere at 650 °C

At 650 °C after 800 h in the furnace atmosphere thick magnetite and spinel layers appear

5.4.2 ODS steel in furnace atmosphere

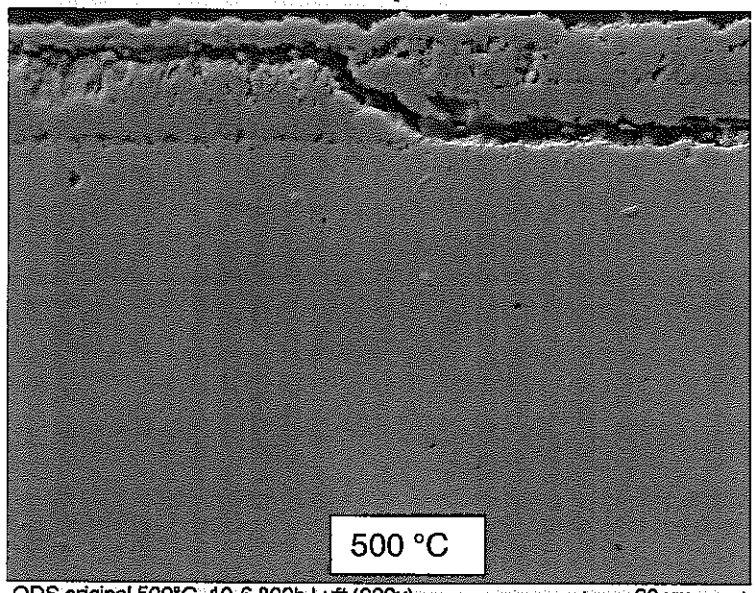

50a

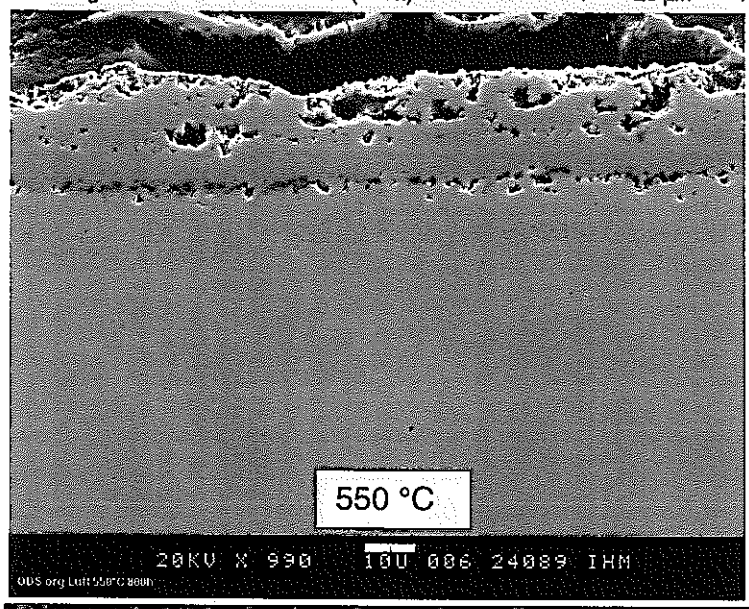

50b

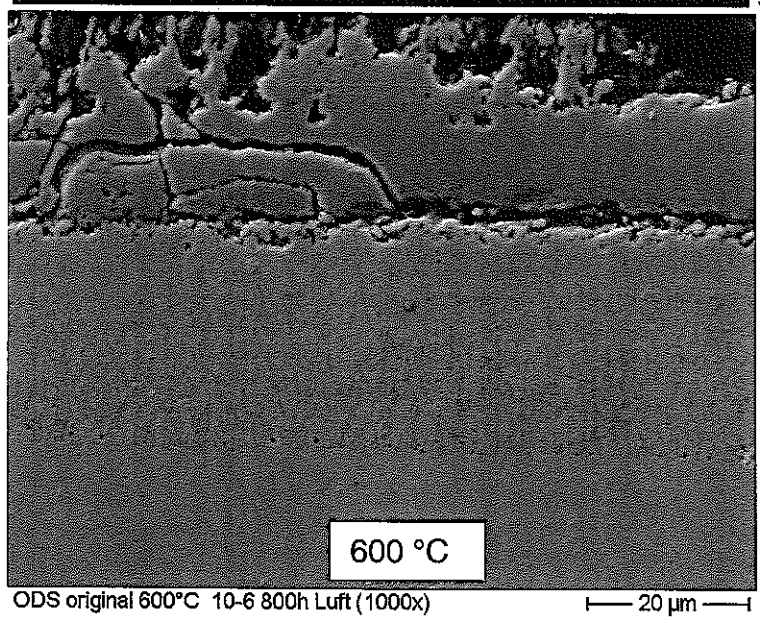

50c

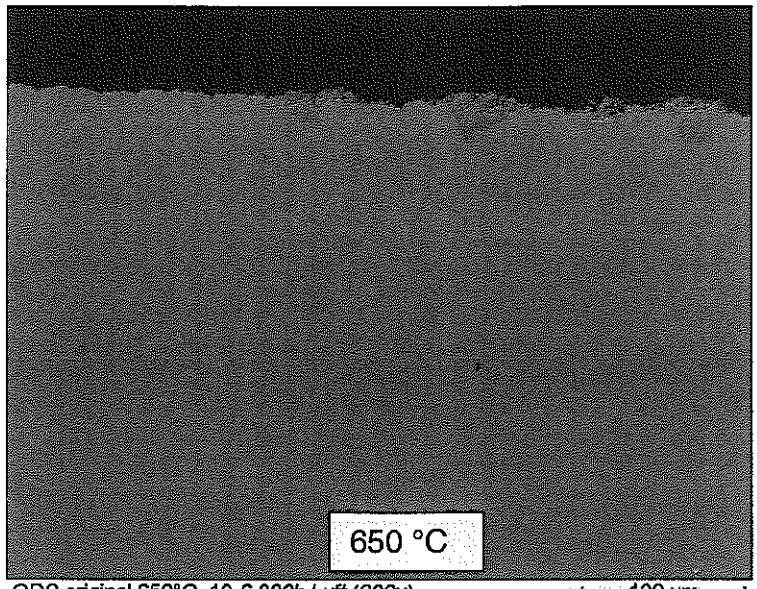

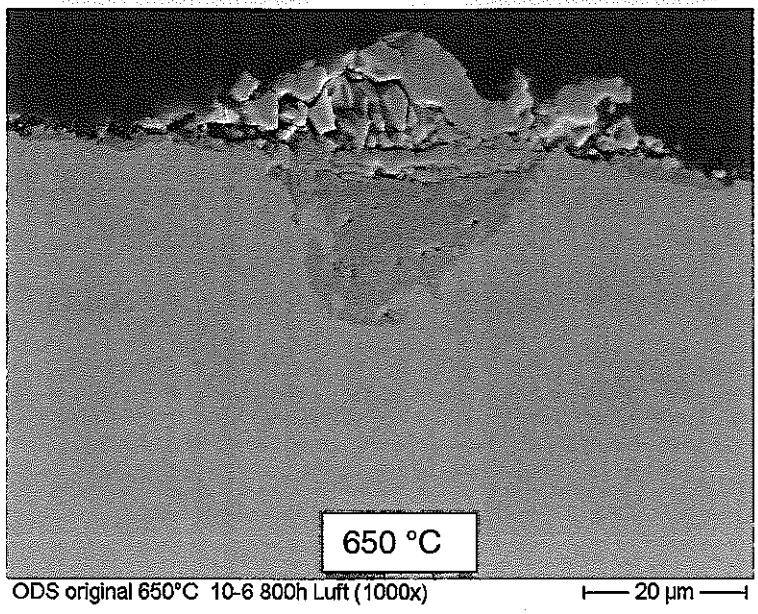

Fig. 50: ODS steel after 800 h oxidation in furnace atmosphere at 500(a), 550(b), 600(c) and 650 °C (d,e)

On ODS steel after 800 h the oxide scale grows with temperature from 500 to 600 °C. However, the scale is porous and subjected to spallation. Therefore, especially at 650 °C it is not visible on the cross section.

5.4.3 P122 steel in furnace atmosphere

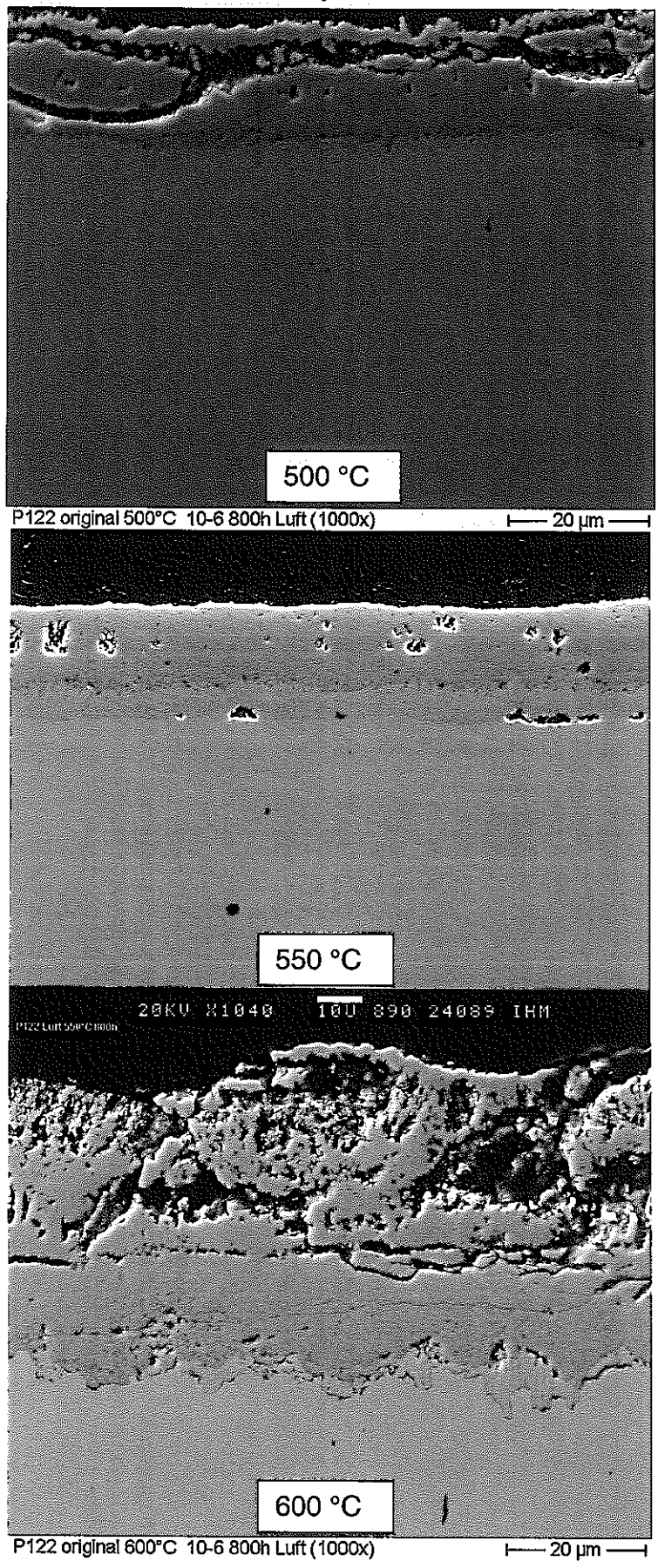

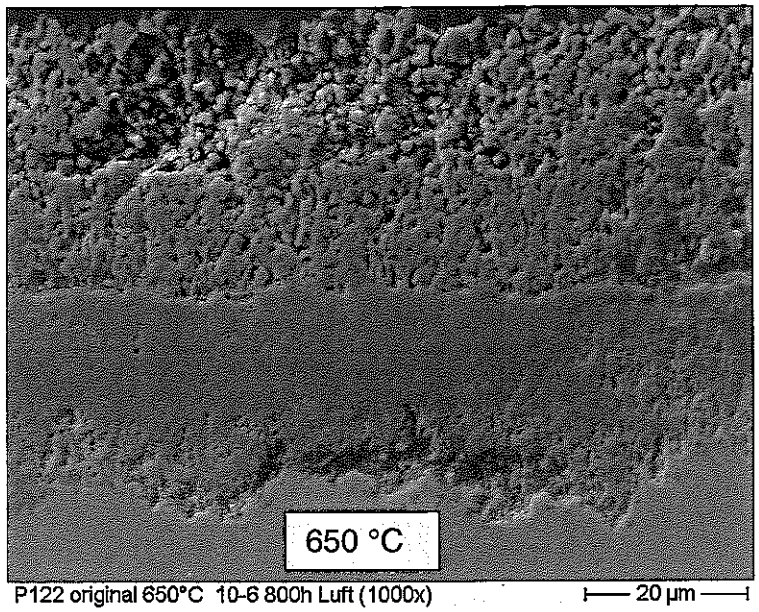

Fig. 51: P122 steel after 800 h oxidation in furnace atmosphere at 500(a), 550(b), 600(c) and 650 °C (d)

On P122 steel after 800 h the oxide scale grows continuously with temperature from 15 up to 60 µm. The magnetite layer gets very porous at high temperatures. Partially spallation is observed of the magnetite layer.

5.5 X-ray diffractometry of specimens exposed to furnace atmosphere

5.5.1 316FR

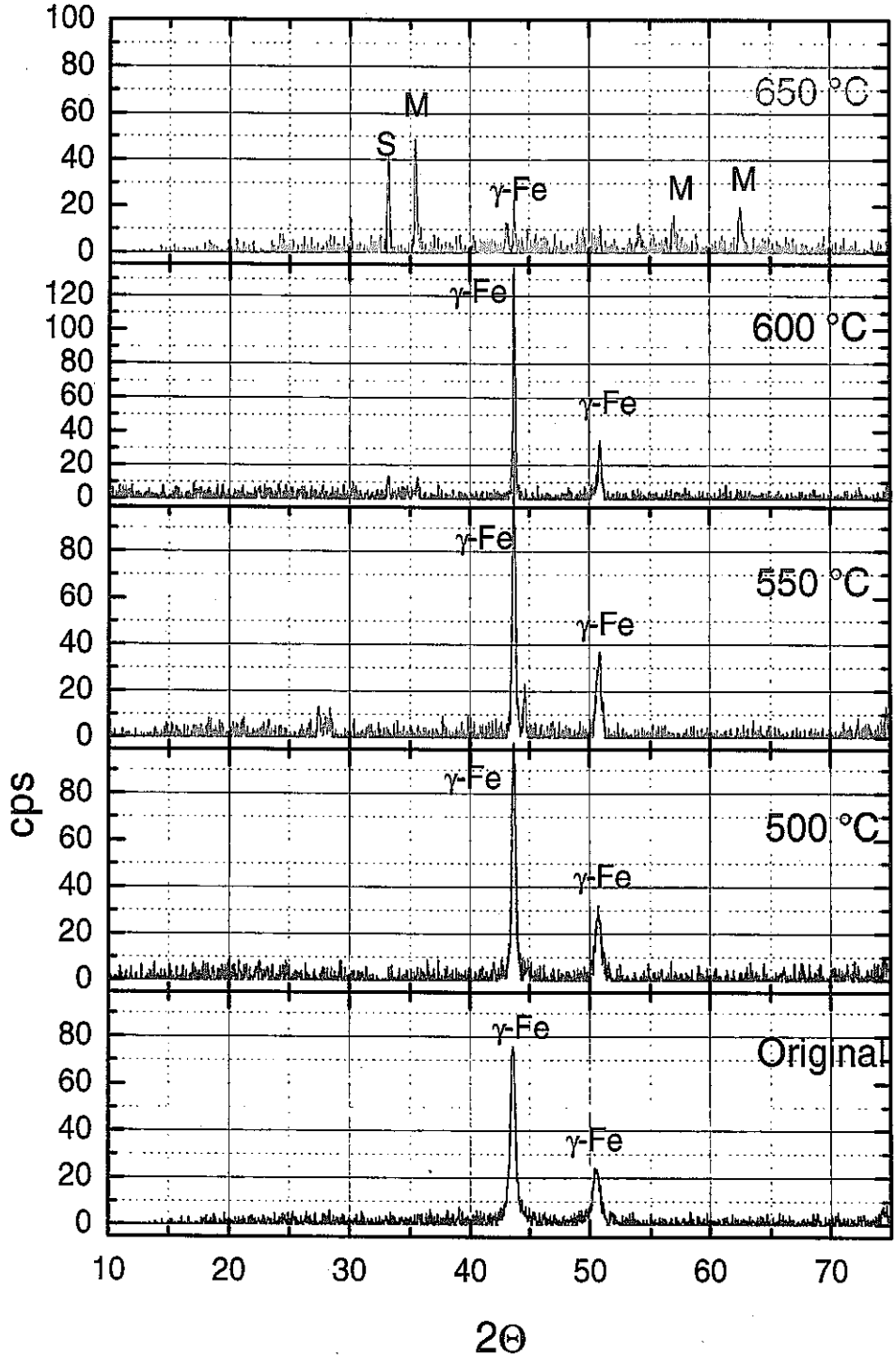

Fig. 52: XRD pattern of 316FR exposed 800 h to furnace atmosphere

Up to 600 °C γ-Fe peaks can be observed only. At 650 °C magnetite and spinel peaks appear and a small γ-Fe peak.

5.5.2 ODS

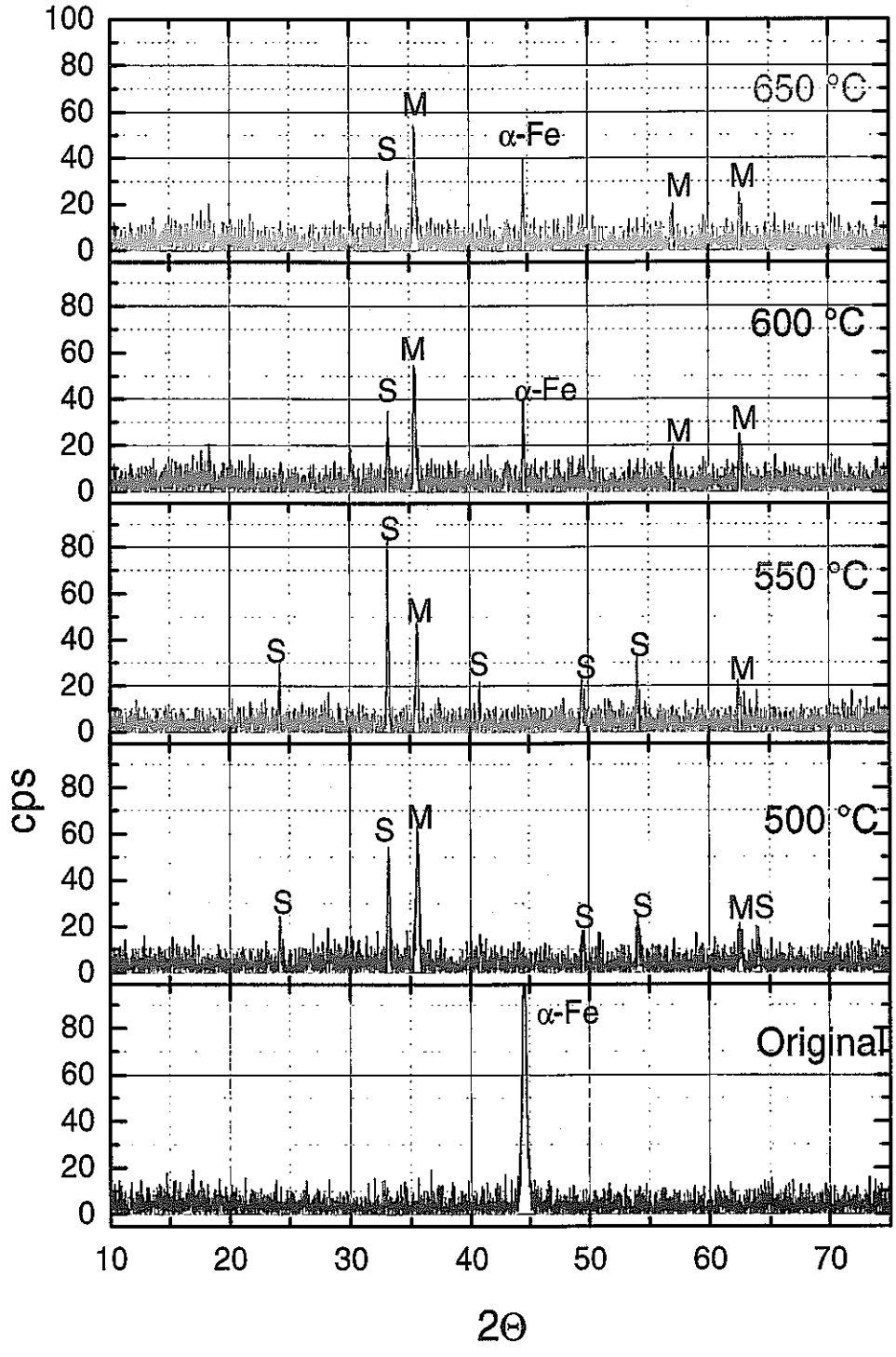

Fig. 53: XRD pattern of ODS steel exposed 800 h to furnace atmosphere

At 500 and 550 °C no metal peaks are visible any more but only magnetite and spinel peaks. The fact that large spinel peaks appear besides magnetite indicates that large parts of the magnetite top layer is spalled off. The presence of α-Fe peaks at 600 and 650 °C shows that also a large part of spinel is spalled off at these temperatures.

5.5.1 P 122

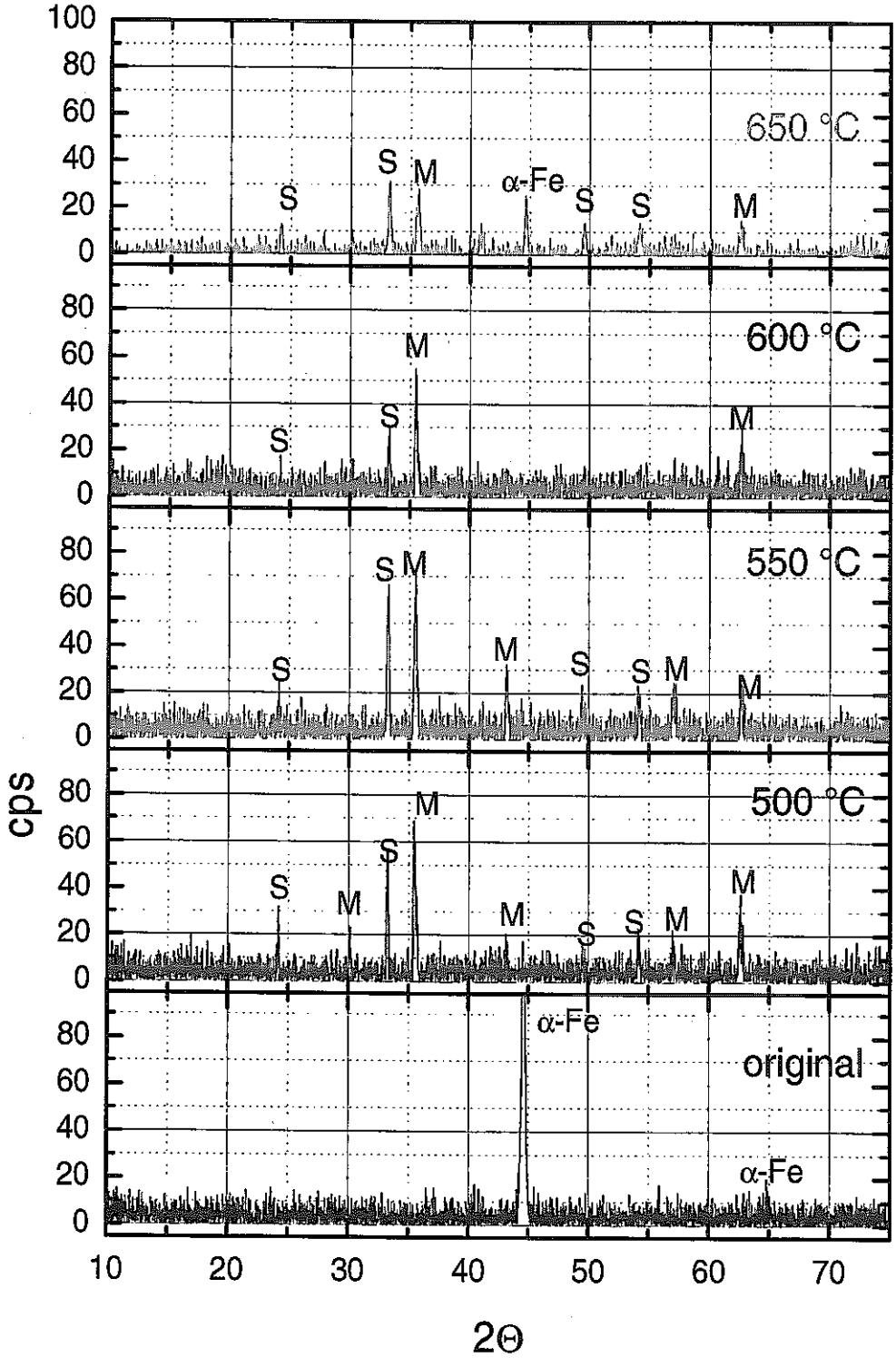

Fig. 54: XRD pattern of P122 steel exposed 800 h to furnace atmosphere

Only oxide patterns are observed on P122 after exposure to Pb/Bi at 500 – 600 °C. The spinel peaks indicate partial spallation of the magnetite scale.

6 Summary

6.1 Experiments of 800 h duration

- At 500 °C all 3 steels show satisfying protection behaviour.
- At 550 °C the steels have still a protective oxide layer.
- At 600 °C the oxidation behaviour changes, the oxide scales are very thin. There is attack of Pb/Bi on singular spots at the surface of 316FR and ODS steel. On 316FR Ni dissolves and Pb/Bi penetrates. ODS shows attack at spots that contain sulphur impurities. P122 is not attacked.
- At 650 °C the ODS steel shows some spots at which sulphur impurities lead to a weakening of the very thin protective spinel layer (sulphur reduces locally the amount of Cr in the bulk by forming chromiumsulfide precipitations, so at this places there is not enough Cr to form the protective oxide layer!). P122 also shows in most surface parts a satisfying protective behaviour, which is disturbed only at a few spots. Severe attack is observed at 316FR steel up to 30 µm depth also only at some spots.
- GESA alloyed surfaces performed well without attack at all 3 steel surfaces at all temperatures . There are only few structural defects, which can be avoided by proper selection of the treatment parameters. Nevertheless although at those defect spots (small cracks) no dissolution attack was observed or has to be expected so far. This small cracks were filled with Cr-Al spinel which hinders Pb/Bi to penetrate.

6.2 Experiments of 2000 h duration

- At 500 °C all 3 steels still show satisfying protection behaviour. The oxide layers are thicker than after 800 h.
- At 550 °C the steels have still a protective oxide layer.
- At 600 °C the attack continues on singular spots like observed after 800 °C on ODS and 316FR. Attack at singular spots starts at P122 steel.

- At 650 °C the attack of Pb/Bi on single spots continues and reaches for instance at 316FR a depth of 50 µm.
- The GESA alloyed specimens do not show any attack at all temperatures.

6.3 Experiments in COSTA atmosphere

- Oxidation behaviour in COSTA atmosphere is the same as the one in liquid Pb/Bi containing 10^{-6} wt% oxygen up to temperatures of 550 °C. Only, the oxidation rate is enhanced. Above 550 °C the oxidation behaviour differs from that in the liquid metal. Magnetite layers are still present and of much higher thickness which is not the case in Pb/Bi.

7 References

[1] T.B. Massalski, Editor, Binary Phase Diagrams, 2nd Edition, ASM Int. (1990)

[2] C. Guminski, Z. Metallkd., 81 (1990) 105

[3] R. C. Asher, D. Davies, S. A. Beetham, Corrosion Science, 17 (1977) 545

[4] G. Y. Lai, High Temperature Corrosion of Engineering Alloys, ASM Int. (1990), Materials Park, OH 44073

[5] B. F. Gromov, Yu. I. Orlov, P. N. Martynov, K. D. Ivanov and V. A. Gulevski, in Liquid Metal Systems, Edited by H. U. Borgstedt and G. Frees, Plenum Press (1995) 339

[6] V. Markov, Seminar on the Concept of Lead-Cooled Fast Reactors, Cadarache, September 22-23, 1997 (unpublished)

[7] R. P. Elliott, Constitution of Binary Alloys, First Supplement, New York, 1965

[8] H. U. Borgstedt and H. Glasbrenner, Fusion Eng. Des., 27 (1995) 659

[9] H. Kleykamp and H. Glasbrenner, Z. Metallkd., 88 (1997) 3

[10] G. Müller, G. Schumacher, F. Zimmermann, Journal of Nuclear Materials, 278 (2000) 85

[11] G. Müller et. al., Journal of Nuclear Materials, 301 (2002)40-46

[12] C. B. Griffith, J. Am. Chem. Soc. 1953, 75, p. 1832 ff.

[13] Y. I. Orlov, personal communication at FZK July (1998)

[14] Alcock, Appl. of Dundamental Thermodynamics to Metallurigical Processes Proc., G. R. Fitterer, Gordan and Breach 1967

[15] V. Engelko, B. Yatsenko, G. Mueller, H. Bluhm, Pulsed electron beam facility (GESA) for surface treatment of materials, Vacuum, Vol. 62/2-3, June 2001, pp. 211-216.